Stony Brook University

Roles of the Chaperone/Usher Pathways of *Yersinia pestis* in Interactions with Host Cells and Virulence

A Dissertation Presented

by

Matthew Ryan Hatkoff

to

The Graduate School

in Partial Fulfillment of the

Requirements

for the Degree of

Doctor of Philosophy

in

Molecular Genetics and Microbiology

Stony Brook University

August 2012

Stony Brook University

The Graduate School

Matthew Ryan Hatkoff

We, the dissertation committee for the above candidate for the

Doctor of Philosophy degree,

hereby recommend acceptance of this dissertation.

David G. Thanassi, Ph.D. (Dissertation Advisor), Professor
Department of Molecular Genetics and Microbiology

James B. Bliska, Ph.D. (Chairperson of Defense), Professor
Department of Molecular Genetics and Microbiology

Adrianus W.M. van der Velden, Ph.D., Assistant Professor
Department of Molecular Genetics and Microbiology

Martha B. Furie, Ph.D., Professor
Department of Pathology

Andrew J. Darwin, Ph.D., Associate Professor
Department of Microbiology, NYU

This dissertation is accepted by the Graduate School.

Charles Taber
Interim Dean of the Graduate School

Abstract of the Dissertation

Roles of the Chaperone/Usher Pathways of *Yersinia pestis* in Interactions with Host Cells and Virulence

by

Matthew Ryan Hatkoff

Doctor of Philosophy

in

Molecular Genetics and Microbiology

Stony Brook University

2012

Yersinia pestis, the causative agent of plague, encodes for a large repertoire of pili, which are hair-like fibers that extend out from the bacterial surface. Pili formed by the chaperone/usher pathway are adhesive structures that contribute to virulence in many Gram-negative bacteria. The *Y. pestis* genome contains eleven chaperone/usher operons. I sought to understand what roles these pathways have on the ability of *Y. pestis* to bind to host cells, cause disease, and contribute to virulence. I initially examined a panel of *Y. pestis* mutants containing deletions of the usher genes for six of these chaperone/usher pathways. I found that at least three of the pathways aided in adhesion to mammalian cells. When ushers *y0350* or *y1858* were deleted, there was a decrease in adhesion to all host cell types examined compared to the wild-type *Y. pestis* strain. When usher *y1871* was deleted, there was a decrease in adhesion to macrophages. In addition, when mice

were infected intranasally with the KIM5+ deletion strains, there was a significant attenuation in virulence of the mutants lacking the three previously mentioned ushers.

To completely investigate the chaperone/usher pathways of *Y. pestis*, I constructed a new panel of mutants containing full deletions of each of the nine uncharacterized chaperone/usher pathways. Adhesion studies were repeated and in agreement with the previous work, when pathways *y0348-y0352* or *y1858-y1862* were knocked out, there was a significant decrease in binding to all cell types, and when pathway *y1869-y1873* was knocked out, there was a significant decrease in binding to macrophages. In addition, a new pathway, *y4060-y4063*, was identified as important for binding a number of cell types. Finally, I examined whether these pathways facilitate the delivery of virulence factors, termed Yops, to host cells. These studies revealed that *Y. pestis* mutants containing deletions of pathways that are important for adhesion to host cells are also impaired in Yop delivery. Together, these studies showed that at least four of the chaperone/usher pathways of *Y. pestis* aid in binding and delivery of Yops to a variety of host cells, and they contribute to the virulence of *Y. pestis* via the pneumonic route.

Table of Contents

List of Tables

List of Figures

Acknowledgments

This work would not have been possible without the help and support from a whole host of people. First of all, I would like to thank my advisor, Dr. David G. Thanassi. Without his constant support, I would not be the scientist I am today. Through his guidance and teachings I have truly learned what it means to be an independent researcher and scientist. I truthfully enjoyed my time here at Stony Brook and in David's lab, I can surely say there was never a dull moment!

The Center for Infectious Diseases, under the guidance of Dr. Jorge Benach, has been a wonderful environment to work in. The atmosphere of open-mindedness and collaboration makes this place one of a kind. I would like to thank him for not only taking the CID under his care but for giving me guidance throughout my career. I would also like to thank all the members of the CID, past and present, for helping me during my entire graduate career. I would be remiss if I did not especially thank the members of my dissertation committee: Dr. James Bliska, Dr. Ando van der Velden, Dr. Martha Furie, and Dr. Andrew Darwin, for their continued guidance both with my research and my professional development. I would also like to thank the entire faculty of the Microbiology program for always being willing to lend a listening ear for science or otherwise.

I can indubitably say that I would not have made it through my five years here without my friends and family. The new friends I made here at Stony Brook helped me both with my science and my extracurricular activities. I would like to especially thank Chris Doyle, Joe Catanzaro, Jameson Crowley, Devin Camenares, and Lawton Chung for allowing me to bounce ideas off of them throughout my years here, as well as reminding

me when it was time to relax and have fun. Every one of my Microbiology and Genetic colleagues made my five years here unforgettable and each of them deserves a very special thank you. I also need to thank my friends from afar who have supported me since I was a youth. I want to thank Paul Gulyas, Kevin McCarthy, and Patrick Beck who for the past twenty-three years have accepted me for being the scientist that I have always been. I would not be here if not for them and all the wonderful friends I have throughout the country.

Last, but certainly not least, I need to thank my family and loved ones who are an endless supply of inspiration and joy. My girlfriend Eve Klajbor has supported me for my last year here at Stony Brook and kept me grounded and sane when I needed it most. She has helped me through some of the most stressful times during my career in graduate school. My sister Kate Hatkoff has been a constant source of happiness throughout my life, both before and during graduate school, and I am sure will continue to be during the next phases of both our lives. Finally, I need to thank two of the most important people in my life, my mother and father, Anne and Andy Hatkoff. They have never once doubted my ability as a scientist, even if I did from time to time. They have been a constant source of support, joy, and guidance in my life and I would not be the person I am today if not for them. I am incredibly proud to have a family as wonderful and supportive as the one I have. Lastly, I would like to dedicate the pages of this dissertation to my mother, who is the single most courageous person I know.

Roles of the Chaperone/Usher Pathways of *Yersinia pestis* in Interactions with Host Cells and Virulence

A Dissertation Presented

by

Matthew Ryan Hatkoff

to

The Graduate School

in Partial Fulfillment of the

Requirements

for the Degree of

Doctor of Philosophy

in

Molecular Genetics and Microbiology

Stony Brook University

August 2012

Stony Brook University

The Graduate School

Matthew Ryan Hatkoff

We, the dissertation committee for the above candidate for the

Doctor of Philosophy degree,

hereby recommend acceptance of this dissertation.

David G. Thanassi, Ph.D. (Dissertation Advisor), Professor
Department of Molecular Genetics and Microbiology

James B. Bliska, Ph.D. (Chairperson of Defense), Professor
Department of Molecular Genetics and Microbiology

Adrianus W.M. van der Velden, Ph.D., Assistant Professor
Department of Molecular Genetics and Microbiology

Martha B. Furie, Ph.D., Professor
Department of Pathology

Andrew J. Darwin, Ph.D., Associate Professor
Department of Microbiology, NYU

This dissertation is accepted by the Graduate School.

Dean of the Graduate School

Abstract of the Dissertation

Roles of the Chaperone/Usher Pathways of *Yersinia pestis* in Interactions with Host Cells and Virulence

by

Matthew Ryan Hatkoff

Doctor of Philosophy

in

Molecular Genetics and Microbiology

Stony Brook University

2012

Yersinia pestis, the causative agent of plague, encodes for a large repertoire of pili, which are hair-like fibers that extend out from the bacterial surface. Pili formed by the chaperone/usher pathway are adhesive structures that contribute to virulence in many Gram-negative bacteria. The *Y. pestis* genome contains eleven chaperone/usher operons. I sought to understand what roles these pathways have on the ability of *Y. pestis* to bind to host cells, cause disease, and contribute to virulence. I initially examined a panel of *Y. pestis* mutants containing deletions of the usher genes for six of these chaperone/usher pathways. I found that at least three of the pathways aided in adhesion to mammalian cells. When ushers *y0350* or *y1858* were deleted, there was a decrease in adhesion to all host cell types examined compared to the wild-type *Y. pestis* strain. When usher *y1871* was deleted, there was a decrease in adhesion to macrophages. In addition, when mice

were infected intranasally with the KIM5+ deletion strains, there was a significant attenuation in virulence of the mutants lacking the three previously mentioned ushers.

To completely investigate the chaperone/usher pathways of *Y. pestis*, I constructed a new panel of mutants containing full deletions of each of the nine uncharacterized chaperone/usher pathways. Adhesion studies were repeated and in agreement with the previous work, when pathways *y0348-y0352* or *y1858-y1862* were knocked out, there was a significant decrease in binding to all cell types, and when pathway *y1869-y1873* was knocked out, there was a significant decrease in binding to macrophages. In addition, a new pathway, *y4060-y4063*, was identified as important for binding a number of cell types. Finally, I examined whether these pathways facilitate the delivery of virulence factors, termed Yops, to host cells. These studies revealed that *Y. pestis* mutants containing deletions of pathways that are important for adhesion to host cells are also impaired in Yop delivery. Together, these studies showed that at least four of the chaperone/usher pathways of *Y. pestis* aid in binding and delivery of Yops to a variety of host cells, and they contribute to the virulence of *Y. pestis* via the pneumonic route.

Table of Contents

List of Tables

List of Figures

Acknowledgments

This work would not have been possible without the help and support from a whole host of people. First of all, I would like to thank my advisor, Dr. David G. Thanassi. Without his constant support, I would not be the scientist I am today. Through his guidance and teachings I have truly learned what it means to be an independent researcher and scientist. I truthfully enjoyed my time here at Stony Brook and in David's lab, I can surely say there was never a dull moment!

The Center for Infectious Diseases, under the guidance of Dr. Jorge Benach, has been a wonderful environment to work in. The atmosphere of open-mindedness and collaboration makes this place one of a kind. I would like to thank him for not only taking the CID under his care but for giving me guidance throughout my career. I would also like to thank all the members of the CID, past and present, for helping me during my entire graduate career. I would be remiss if I did not especially thank the members of my dissertation committee: Dr. James Bliska, Dr. Ando van der Velden, Dr. Martha Furie, and Dr. Andrew Darwin, for their continued guidance both with my research and my professional development. I would also like to thank the entire faculty of the Microbiology program for always being willing to lend a listening ear for science or otherwise.

I can indubitably say that I would not have made it through my five years here without my friends and family. The new friends I made here at Stony Brook helped me both with my science and my extracurricular activities. I would like to especially thank Chris Doyle, Joe Catanzaro, Jameson Crowley, Devin Camenares, and Lawton Chung for allowing me to bounce ideas off of them throughout my years here, as well as reminding

me when it was time to relax and have fun. Every one of my Microbiology and Genetic colleagues made my five years here unforgettable and each of them deserves a very special thank you. I also need to thank my friends from afar who have supported me since I was a youth. I want to thank Paul Gulyas, Kevin McCarthy, and Patrick Beck who for the past twenty-three years have accepted me for being the scientist that I have always been. I would not be here if not for them and all the wonderful friends I have throughout the country.

Last, but certainly not least, I need to thank my family and loved ones who are an endless supply of inspiration and joy. My girlfriend Eve Klajbor has supported me for my last year here at Stony Brook and kept me grounded and sane when I needed it most. She has helped me through some of the most stressful times during my career in graduate school. My sister Kate Hatkoff has been a constant source of happiness throughout my life, both before and during graduate school, and I am sure will continue to be during the next phases of both our lives. Finally, I need to thank two of the most important people in my life, my mother and father, Anne and Andy Hatkoff. They have never once doubted my ability as a scientist, even if I did from time to time. They have been a constant source of support, joy, and guidance in my life and I would not be the person I am today if not for them. I am incredibly proud to have a family as wonderful and supportive as the one I have. Lastly, I would like to dedicate the pages of this dissertation to my mother, who is the single most courageous person I know.

Chapter 1: Introduction

Pathogenesis of *Yersinia pestis*

The background of Yersinia spp.

The *Yersinia* genus, in the family *Enterobacteriaceae,* is comprised of 11 members, all of which are Gram-negative, non-motile, facultative intracellular coccobacilli. Three of these species, *Y. enterocolitica, Y. pseudotuberculosis,* and *Y. pestis,* are human pathogens. The former two are enteric pathogens that generally cause a self-limiting gastroenteritis that can be contracted from contaminated food or water [1, 2]. *Y. pestis* is a vector-borne pathogen that can be contracted via the bite of an infected flea, such as the rat flea (*Xenopyslla cheopis),* or from respiratory droplets expelled from an infected individual [3-5]. *Y. pestis,* which shares at least a 90%-90% DNA homology with *Y. pseudotuberculosis,* is a clone that divergently evolved in the last 1,500-20,000 years [6]. *Y. pestis* has acquired new virulence factors since its split from *Y. pseudotuberculosis* that allow it to cause a drastically different spectrum of diseases, known collectively as the plague. In the time since *Y. pestis* evolved from *Y. pseudotuberculosis,* it has caused three major pandemics. Each pandemic was caused by one of the three major biovars of *Y. pestis:* Antiqua, Mediaevalis, and Orientalis. Throughout the course of history it is estimated that *Y. pestis* has killed over 200 million people worldwide [4, 7]. Despite much controversy, it was recently proven that it was indeed *Yersinia pestis* that was the cause of the Black Death and presumably the previous and subsequent plagues [8]. Elucidating the mechanisms by which the newly evolved

clone of *Y. pseudotuberculosis* could cause such a devastating and deadly disease has been of interest for many years. In the last decade the genome sequence of two key laboratory strains, KIM and CO92, were determined [9, 10]. The genome includes a 4.6 Mb circular chromosome, as well as three plasmids, pCD1 (pYV), pPCP1 (pPla, pPst), and pMT1 (pFra). The virulence factors acquired by the addition of the two plasmids that *Y. pseudotuberculosis* lacks, pPCP1 and pMT1, allowed *Y. pestis* to become a vector-borne pathogen. The virulence factors already encoded by the genome and the Low Calcium Response Stimulon (LCRS), encoded by the pCD1 plasmid, also contribute to the severity of the disease caused by *Y. pestis* [11]. The genome of *Y. pestis* also includes 11 gene clusters belonging to the chaperone/usher pathways that assemble pili. These chaperone/usher pathways will be the focus of this dissertation.

Virulence factors and characteristics of Yersinia pestis

The pCD1 plasmid (~70 kb), which encodes the LCRS, is the only plasmid shared amongst all three human pathogenic *Yersinia* species. The LCRS is a group of genes that comprise the type three secretion system (T3SS) and the Yersinia outer proteins (Yops) [4]. The T3SS, which has been termed a molecular syringe, is a secretion system that exports the anti-host proteins, Yops, directly into host cells. The LCRS is primarily active at 37^{o}C with low concentrations of calcium or nucleotides [11-15]. Once the Yops are in the host cells they have many effects, including dampening the host immune response by preventing or counteracting cytokine production, preventing phagocytosis by disrupting the actin cytoskeleton, and causing host cell death [12, 16-19]. The LCRS and thus the pCD1 plasmid is absolutely required for full virulence of *Yersinia pestis,* as a pCD1

cured strain is attenuated 100,000-fold in the mouse model of infection [20, 21]. The KIM6+ strain, which is used in the majority of this dissertation, lacks the pCD1 plasmid and thus is suitable to use under BSL-2 conditions allowing for easy manipulation and *in vitro* assays.

Yersinia pestis contains two other plasmids, pMT1 and pPCP1, which are not present in the two other human pathogenic *Yersinia*. The pPCP1 plasmid, the smallest of the plasmids at 9.5 kb, encodes the protease Pla, which is also a putative adhesin and invasin [4]. Pla is a plasminogen activating protease that can break down fibrin clots, endowing the bacteria with the ability to disseminate easily [7, 22]. Pla has been shown to aid in adhesion to many cell types, as well as aid in the invasion of these cells [23, 24]. Pla has also been shown to be important for initiating a fulminant pneumonic plague and for dissemination of *Y. pestis* during bubonic plague [25].

Plasmid pMT1, the second unique plasmid, is the largest at 96 kb and encodes a number of critical virulence factors. Plasmid pMT1 encodes phospholipase D also known as Yersinia Murine Toxin (YMT), which is important for survival within the flea midgut, as well as transmission from the flea into a new host [3, 26]. The third virulence factor encoded on the pMT1 plasmid is the Fraction 1 (F1) capsule. The F1 capsule is an amorphous capsule that surrounds the bacterium and is secreted via the chaperone/usher pathway at 37^{o}C [27-29]. The F1 capsule aids in evading phagocytosis by macrophages and neutrophils, and also blocks uptake into epithelial cells [30, 31]. The F1 capsule plays a role in virulence and is one of the two candidate proteins currently used in subunit vaccine trials [32-34]. Currently, in the literature there is a debate on whether the F1 antigen is required for full virulence of *Y. pestis.* Groups have reported that F1 negative

strains can be found in nature and that they have the ability to escape immunity generated by the subunit vaccines. However, other groups have reported that all strains isolated from nature contain an intact and functional F1 capsule [28, 34, 35]. Furthermore, groups have shown that *Y. pestis* strains that do not express the F1 capsule may be attenuated via the subcutaneous route, but may still be fully virulent via the pneumonic route [36, 37]. Clearly more work must be done to understand the role the F1 capsule plays in the natural pathogenesis of *Y. pestis*.

While many of the virulence factors are encoded on the three plasmids of *Y. pestis,* there is also a repertoire of virulence factors within the genome. The pigmentation locus, or *pgm* locus, is a 102 kb region in the genome that encodes a number of well-studied virulence factors, including those for iron acquisition and storage [4]. Also within this virulence island is the *ripA* gene, which is required for intracellular survival of the bacteria in activated macrophages [38]. Outside of the *pgm* locus, another important locus encodes the two component sensing system, Pho P/Q. These proteins allow the bacterium to sense the environment and induce the necessary changes within its gene programs to survive within harsh environments, including phagocytic cells. The Pho P/Q system has been shown to be required for virulence both *in vitro* and *in vivo* [39]. Finally, the unique characteristics of *Y. pestis'* lipopolysaccharide (LPS) also contribute to the bacteria's high virulence. LPS of *Y. pestis* lacks the classic O-antigen that many other Gram-negative bacteria have due to frame shift mutations in the O-antigen gene cluster [40, 41]. *Y. pestis* LPS also lacks the classical highly inflammatory hexa-acylated form of Lipid A, and maintains a tetra-acylated form which causes very little inflammation compared to

standard LPS [42]. This is an important difference from *Y. pseudotuberculosis,* which produces a mixed population of both tetra- and hexa-acylated forms of LPS [42].

Y. pestis has been a highly successful pathogen over the last 1,500 years. It owes its success to two main processes, adhesion and evasion. *Y. pestis* can adhere to many cell types and surfaces through its plethora of adhesins that will be discussed later. However, it must also evade the immune response using the T3SS, *pgm* locus, and Pho P/Q system if it is to cause a successful infection [19, 38, 39, 43, 44]. Therefore it is critical to understand these aspects of the disease caused by *Y. pestis.*

Yersinia pestis pathogenesis

Y. pestis, the causative agent of plague, a disease whose name harkens back to medieval times, still causes fear in people today. Over the course of human history it has been responsible for the deaths of over 200 million people and still infects approximately 3,000 people annually worldwide, with 5-15 cases per year in the United States [4]. *Y. pestis* is a zoonotic, vector-borne disease that is maintained in small mammals such as prairie dogs, rabbits, and most notably rats, and has established foci of infection on every inhabited continent except Australia [4, 45]. Today most people become infected through the bite of a plague-carrying flea [4]. However, in the modern world a second way of becoming infected is also a concern. The intentional release by a rogue person or group of the bacteria in an aerosolized form would lead directly to the pneumonic form of the plague, as opposed to the bubonic or septicemic forms that would occur from a flea bite (Figure 1.1) [46, 47]. Mounting an effective immune response is critical to fighting off

the infection; however, *Y. pestis* seems to have the upper hand when coming into contact with the host immune system.

Upon entering the host, the bacteria will initially encounter either immune cells such as polymorphonuclear (PMN) cells and macrophages or epithelial cells. While many groups have studied the role of various *Y. pestis* adhesins in their ability to contribute to adhesion to epithelial cells in cell culture, and have shown that the bacteria can adhere to these cells very robustly, very little is known about the role interaction with epithelial cells plays *in vivo* [23, 31, 48]. This cell type is most likely one of the first encountered in the host during infection, which indicates it may be critical during infection, however no specific evidence *in vivo* has been presented confirming the importance of *Y. pestis* adhesion to or invasion of these cells [20, 25]. Which immune cell type is encountered first can lead to a very different outcome for the bacteria [49]. The bacteria have a number of genes whose expression is regulated by temperature; for example a number of genes encoding virulence factors which are induced at 37^{o}C but not 28^{o}C. Upon switching hosts from the flea (21^{o}C) to the human (37^{o}C), *Y. pestis* is not expressing the T3SS or F1 capsule and can be engulfed by either PMNs or macrophages. If engulfed by a PMN the bacteria will be killed within the phagolysosome [43]. However, if engulfed by macrophages, the bacteria enter a protective niche and will survive and begin to alter gene expression to upregulate many virulence genes. These genes will not only allow for survival and proliferation within macrophages, but they will also prevent the bacteria from being engulfed by immune cells later during infection [4, 38, 43, 50]. Once *Y. pestis* has survived this initial encounter with the host immune response, and is now expressing its full arsenal of virulence factors, it begins to disseminate throughout the body to distal

organs and lymph nodes, possibly by traveling within the protective niche of the macrophage.

The immune response to *Y. pestis* is a biphasic one, starting off under the radar as a non-inflammatory response followed by a highly inflammatory response which aids in the extreme virulence of this bacterium [17]. During infection bacteria can move into the lymph nodes, where they begin to replicate and kill host cells characteristic of the second phase of the immune response. This response causes massive swelling within the lymph nodes causing them to become tender and enlarged and turning them a black color due to the hemorrhaging and necrosis. These nodes become the characteristic bubo, which lent its name to the Black Death [4]. Bubonic plague is the most common form of plague and generally has a 40% mortality rate if left untreated. From the lymph node the bacteria can spread through the rest of the body via the bloodstream. Septicemic plague has the same characteristics of bubonic plague except that it lacks the enlarged black lymph node. Both types of plague cause a high fever, general malaise, and flu-like symptoms. As the bacteria traverse the body infecting organs such as the liver and spleen, the bacteria may also spread to the lungs causing secondary pneumonic plague, a deadly form of the disease that is easily transmitted. In this case the bacteria spread person-to-person via respiratory droplets. Both primary and secondary pneumonic plague are highly fatal, with 100% mortality if left untreated, and have a very rapid progression, moving into a fulminant disease within 1-3 days [4, 20]. Since the bacteria have such a high mortality and morbidity rate, *Y. pestis* has been targeted for research into its potential use as a bioterrorism weapon by not only our own government but by rogue groups throughout the world.

Yersinia pestis bioterrorism fears and vaccine troubles

In the wake of 9/11 and the anthrax mailings, research into *Y. pestis* has received extra attention due to the damage a terrorist attack could cause [51, 52]. Due to the highly virulent nature of *Y. pestis,* it has been classified as a category A agent of bioterrorism by the Centers for Disease Control and Prevention. Category A agents are characterized by their high mortality and morbidity rate, ease of aerosolization, ability to cause a mass panic, and ease of mass production [167]. The occurrence of naturally multi-drug resistant *Y. pestis*, along with the ease of introducing multi-drug resistance into susceptible strains, would make it difficult to effectively treat an infection with the correct antibiotics [35, 53]. Due to its early non-specific symptoms plague could easily be misdiagnosed, thus shortening the time for effective antibiotic therapy. It has been estimated that 100 kg of aerosolized *Y. pestis,* if released in a highly populated area, could cause around three million deaths due to highly contagious primary pneumonic plague characterized by rapid onset pneumonia and septic shock [54, 55].

The ideal way to prevent such a bioterrorist attack would be a safe and effective vaccine that would provide long lasting protection against both bubonic and pneumonic plague. Numerous vaccines have been attempted, both live attenuated and subunit; however, neither type has provided adequate protection and efficacy across all routes of infection without harmful side effects [47, 56, 57]. The first attempts at vaccination used whole-cell killed or live attenuated strains. It was found that the killed strains were less effective than the live attenuated EV76 strains; however, the EV76 vaccination had harsher side effects, and neither vaccine could provide protection against all routes of infection in all tested animals [58]. Subunit vaccines using the F1 antigen combined with

low calcium response V (LcrV) protein provided some protection against plague [58, 59]. Recent studies have shown that a subunit vaccine comprising F1 and LcrV can protect Cynomolgus macaques from pneumonic plague, but that might not be the case in all animal species, such as African Green monkeys [32, 33, 60]. There have also been attempts at using *Salmonella* expressing the F1 antigen to elicit an immune response against specific proteins that are on the surface of *Y. pestis* [61]. The presence of fully virulent F1 antigen negative strains have provided an unforeseen problem to these studies, as these vaccines are no longer effective against this strain [62]. Generating novel targets for vaccine development would greatly aid in the search for a suitable, safe, highly protective vaccine. If a vaccine of this caliber could be developed, it could alleviate some of the fear of *Y. pestis* being used as a biological weapon. Our hope is that a better understanding of the pili formed via the chaperone/usher pathways of *Y. pestis* could lead to better vaccines and therapeutics.

The Adhesins and Pili of *Yersinia*

Adhesins of Y. pseudotuberculosis and Y. enterocolitica

The two main adhesins of the enteropathogenic *Y. enterocolitica* and *Y. pseudotuberculosis,* YadA and Inv, are not active in *Y. pestis,* opening up speculation that it uses a number of other adhesins to make up for the loss of the these two major proteins [23, 63-66]. Inv is able to mediate binding to host cells directly through β1 integrin; however, YadA binds indirectly through components of the extracellular matrix. Both YadA and Inv increase invasion into host cells through the β1 signaling of Ser/Thr kinases, which can trigger autophagy of host cells but the presence of the T3SS can counter this effect [63, 66-68]. Studies have demonstrated the ability for *E. coli* ectopically expressing either adhesin to take on the phenotypes of the enteropathogenic *Yersinia*, i.e., an ability to adhere to and invade epithelial cells [63]. When either YadA or Inv is knocked out in *Yersinia*, either in combination or alone, the ability of the bacteria to adhere to host cells is decreased dramatically, and the production or proinflammatory cytokines, such as IL-8, is greatly decreased [67, 69]. Another major adhesin of *Y. enterocolitica* and virulence factor of *Y. pseudotuberculosis* is Ail. Ail contributes to adhesion and invasion of host cells as well as confers serum resistance to enteropathogenic *Yersinia* [70-73].

Adhesins of Yersinia pestis

Although neither YadA nor Inv are present in *Y. pestis*, a homolog of Ail is present in the genome along with a plethora of other adhesins that contribute to adhesion

and invasion of host cells [74]. It was shown that Ail could not only play a role in the adhesion of *Y. pestis* to host cells, but also in conferring serum resistance and contributing to biofilm formation much like its homolog in *Y. pseudotuberculosis* [74]. However, the inactivation of Ail in *Y. pestis* does not completely abolish bacterial binding or cause a complete attenuation [75]. Another class of adhesin studied in *Y. pestis* is the autotransporters. *Y. pestis* contains 12 autotransporters, three of which, YapE, YapC and YadBC, have been proven to function in adhesion [76]. When any of the three autotransporters is knocked out, the bacteria still maintain some virulence as well as the ability to bind to host cells [48, 77, 78]. When YapC is knocked out in *Y. pestis,* the bacteria still maintain many of their characteristic phenotypes, such as biofilm formation and autoaggregation [48]. As previously discussed, the Pla protease, which is a *Y. pestis* specific protein, can serve as an adhesin, as well as contribute to bacterial dissemination; however, the bacteria do not lose total virulence nor the ability to bind host cells when Pla is inactivated [23, 25, 79]. Studies of these deletion mutants show that inactivation of a single adhesin in *Y. pestis* may cause a slight to modest decrease in binding to host cells, but it does not attenuate the bacteria to the same level as pCD1 cured strains [20, 21].

Another class of adhesins also exists within the *Y. pestis* genome, the chaperone/usher pathways, which are discussed in detail in the next section [9, 10]. The role that two of these pathways play in host cell adhesion and virulence has been extensively characterized. One of those two well-studied products of the chaperone/usher pathways in *Y. pestis* is the pH 6 antigen encoded by the *psa* operon. The pH 6 antigen has also been found to contribute to adhesion to host cells [31]. Although somewhat

counterintuitive, the pH 6 antigen also acts as an anti-phagocytic outer member structure, as it allows *Y. pestis* to escape phagocytosis by murine macrophages [80]. Depending on the route of infection and type of mice used, the pH 6 antigen may or may not play an important role in virulence [81-83].

The other well-studied member of the chaperone/usher pathway is the F1 antigen, which is encoded by the *caf* operon. The F1 antigen forms an amorphous anti-phagocytic capsule on the outside of *Y. pestis* [29-31]. The bacteria use this capsule, once it is induced at 37^{o}C, to avoid phagocytosis by cells of the immune system [4]. As mentioned before, this protein has been an attractive candidate for subunit vaccines, despite the discovery of F1 negative strains [34]. This underscores the importance of finding critical virulence-associated outer membrane or secreted proteins, possibly members of the chaperone/usher pathway, to develop next generation vaccines.

The Chaperone/Usher Pathway

The unique problem of Gram-negative bacteria

Bacteria need to express proteins on their surface in order to interact with the host and cause disease. Unlike Gram-positive bacteria, Gram-negative bacteria need to export proteins across two membranes, an inner and outer, and the periplasmic space which separates them. Collectively, this 7.5 nm region is termed the cell envelope [84]. Gram-negative bacteria have evolved a variety of secretion pathways in order solve this problem [85]. Proteins initially made in the cytoplasm that are destined for secretion need to contain the proper N or C terminal signals [86]. If secreted first into the periplasm they face a very different environment compared to the cytoplasm. In the periplasm they face an oxidizing environment, with no ATP, and in order to reach the outer membrane they must cross a very thin peptidoglycan layer [87]. Unlike the inner membrane that is mainly a phospholipid bilayer, the outer membrane has an inner leaflet of phospholipids and outer leaflet comprised mainly of lipopolysaccharides (LPS). Proteins to be secreted to the outside of the bacteria must then be translocated across the outer membrane. This is accomplished in a number of different ways depending on the secretion system. I will focus solely on the details of general Sec-dependent secretion across the inner membrane and the chaperone/usher pathway (Figure 1.2).

Assembly of pili via the chaperone/usher pathway

For secretion across the inner membrane by the general Sec pathway, proteins with the correct N-terminal signal sequence will be translocated in an unfolded state

through the SecYEG pore complex. Translocation through SecYEG requires ATP and the cytoplasmic SecA ATPase [84, 85]. The chaperone/usher pathways use this system extensively to move the subunit proteins from the bacterial cytoplasm to the periplasmic space. Once in the periplasm, the signal sequence is cleaved by the signal peptidase, and it is important that the nascent pilus subunit protein is bound by its cognate chaperone; otherwise, the proteins could begin to fold improperly before being degraded by the periplasmic protease, DegP [84, 88] (Figure 1.2). If the proteins aggregate due to misfolding, it could lead to periplasmic stress and decrease bacterial fitness. This highlights the importance of the chaperone and one of its roles in the assembly of pili on the bacterial surface.

The pilus chaperones are a class of proteins that consist of two immunoglobulin (Ig) like domains with an interactive surface between these domains. The chaperone will bind the subunit protein as it enters the periplasm, thus forming the chaperone-subunit complex [89-91] (Figure 1.2). The basis of the chaperone-subunit complex lies in the fact that the chaperone must cap the interactive surface of the subunit protein by a well understood mechanism called donor strand complementation (DSC) [89, 91-96]. The pilus subunit proteins contain an incomplete Ig-like fold, lacking the seventh β-strand that is required for a complete domain, which makes the subunit inherently unstable [91]. However, the chaperone donates one of its strands to complete the incomplete Ig-like fold of the subunit [92]. This serves a dual purpose, allowing proper folding of the nascent subunit in the periplasm and preventing aggregation and improper folding, which as mentioned before could lead to bacterial stress [91, 93].

The next step in the process of assembling pili on the surface of the bacterium occurs at the usher on the outer membrane. Here the chaperone must dissociate from the subunit and allow for subunit-subunit interactions to occur [84, 92, 97, 98] (Figure 1.2). This process is known as donor strand exchange (DSE) [91, 92, 99-101]. In DSE the donated β-strand strand from the chaperone is displaced from the capped subunit by the N-terminal extension (NTE) from the incoming subunit. This NTE strand fills in the hydrophobic cleft in an anti-parallel manner, thus formally completing the Ig-fold of the accepting subunit protein [91] (Figure 1.2). This whole process takes place at the outer membrane on the usher, which serves as a docking station for pilus biogenesis and provides a channel for secretion of the pilus fiber to the cell surface. Without the usher, pili cannot be formed on the outer surface of the bacteria due to a lack of proper docking/nucleation site and pore for pilus biogenesis [88, 97, 102, 103].

The usher is comprised of multiple domains: the 26-strand β-barrel which forms the 2-3 nm pore in the outer membrane, the plug domain which prevents leakage through the pore, and the N and C domains within the periplasm [87, 104-106]. It has been recently determined that the ushers can form a dimer on the outer membrane, which allows for multiple docking sites for the chaperone-subunit complexes [107]. Within the periplasm, the usher's N and C-terminal extensions serve a role in pilus formation. The N-terminal extension serves as the initial docking site for the chaperone-subunit complexes, and the C-terminal domains serve as the pilus assembly site [102, 103, 108-110] (Figure 1.2). The different affinities for various chaperone-subunit complexes allow for an orderly assembly of the pilus at the usher [97, 111]. Since there is no ATP or other energy source within the periplasm, the chaperone/usher pathway uses a creative way to

secrete pili across the outer membrane. The favorable energy generated by the exchange of chaperone-subunit for subunit-subunit interactions drives pilus formation across the usher [88, 92, 98, 100, 103, 105, 112].

Within the chaperone/usher pathway, there are two subtypes, each of which can form a different type of surface structure [84, 95]. The first type, typified in *Y. pestis* by the F1 capsule, forms capsule-like structures on the surface of the bacteria [100]. This subclass is called the FGL class, for F1-G1 long, meaning that the sequence between those two β-strands in the chaperone has a longer loop structure [113]. The second, and more commonly studied, subfamily of the chaperone/usher pathways is the FGS class (F1-G1 short), which is typified by the type 1 and P pili of uropathogenic *E. coli* [113-115]. Most of the molecular mechanisms of the chaperone/usher pathway have been determined using the FGS subfamily [84]. Excluding the two well studied chaperone/usher pathways, F1 and pH 6, the nine remaining chaperone/usher pathways of *Y. pestis* fall into the FGS subfamily, suggesting that they form rigid pili on the bacterial surface [29, 83, 116]. These pathways will be discussed in more detail in the next section.

The chaperone/usher pathways of Yersinia pestis that form pili

Sequencing of both the CO92 and KIM genomes revealed the presence of 9 chaperone/usher pathways in *Y. pestis* in addition to the well-studied *caf* and *psa* systems [9, 10, 29, 116] (Figure 1.3). There have been a few studies on these additional chaperone/usher pathways. Previous work from our laboratory showed that the KIM6+ strain of *Y. pestis* expresses pilus-like fibers at both 28^{o}C and 37^{o}C [29]. Subsequently it was shown that expression of the *Y. pestis* chaperone/usher pathways in *E. coli* results in

the assembly of fibers on the bacterial surface [29, 116]. Groups in collaboration with our own group have begun to explore the roles of these pathways in cell adhesion and virulence.

In support of a role for the *Y. pestis* chaperone/usher pathways as adhesins, expression of locus *y0561-0563* in *E. coli* confers binding to HEp-2 human epithelial and THP-1 human macrophage-like cells, and expression of pathways *y0348-0352*, *y0561-0563*, *y1858-1862* and *y3478-3480* enhances biofilm formation by *E. coli* [83]. However, when deletion mutations of the chaperone/usher pathways are constructed in the *Y. pestis* KIM5 strain, only loss of the *psa* locus, coding for the pH 6 antigen, results in decreased adhesion to host cells and decreased biofilm formation [83]. Finally, Felek and colleagues found that a *Y. pestis* KIM5 strain containing a deletion of chaperone/usher pathway *y1858-1862* is attenuated for virulence in mice via the intravenous route of infection compared to the parental wild-type strain [83]. Taken together, these studies show that the additional *Y. pestis* chaperone/usher pathways are capable of assembling adhesive pili and suggest that these pili may contribute to virulence. However, the functions of the *Y. pestis* chaperone/usher pathways in host-pathogen interactions and in the pathogenesis of plague remain to be established.

Both our group and the Krukonis group undertook qRT-PCR experiments to determine conditions under which the chaperone/usher pathways of *Y. pestis* are expressed. Both groups found that no laboratory condition could significantly induce genes of the chaperone/usher pathway above levels of housekeeping genes [83] (Runco and Thanassi, unpublished data). Lisa Runco, a former graduate student in the Thanassi Laboratory, did find that some genes, especially the chaperone genes, seemed to be

upregulated in rich media, but these findings were inconclusive due to the highly variable nature of her experiments. The most interesting qRT-PCR data came when Felek and colleagues looked at the levels of these genes *in vivo*. Compared to rich media, they saw a 15- to 100-fold up-regulation of genes *y0352, y1860,* and *y1869* in the spleen and liver of mice. In the lungs, *y1869* was the most highly up-regulated gene of the chaperone/usher pathways [83]. These results serve to bolster the results from my studies, because the three pathways they saw expressed *in vivo* are the three pathways found to play a role in our mouse model of infection. This dissertation will describe the functions of the *Y. pestis* chaperone/usher pathways in interactions with host cells and the pathogenesis of bubonic and pneumonic plague.

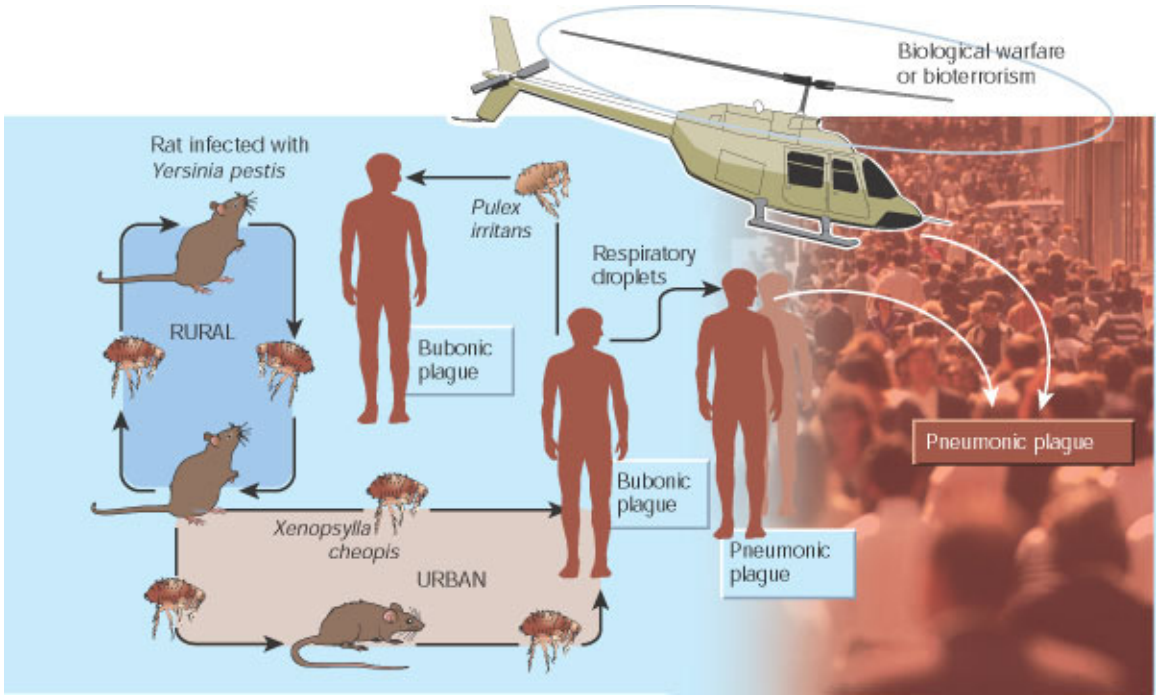

Figure 1.1: Transmission of *Yersinia pestis* in the modern world. Adapted from Cole *et. al.* 2001 with permission [46]. *Y. pestis*, the causative agent of plague, can be transmitted via its natural vector, *Xenopsylla cheopis*, from rat to human causing bubonic or septicemic plague. Bacteria can naturally spread from human to human via respiratory droplets causing pneumonic plague. However, *Y. pestis* can also be intentionally released causing a primary pneumonic plague.

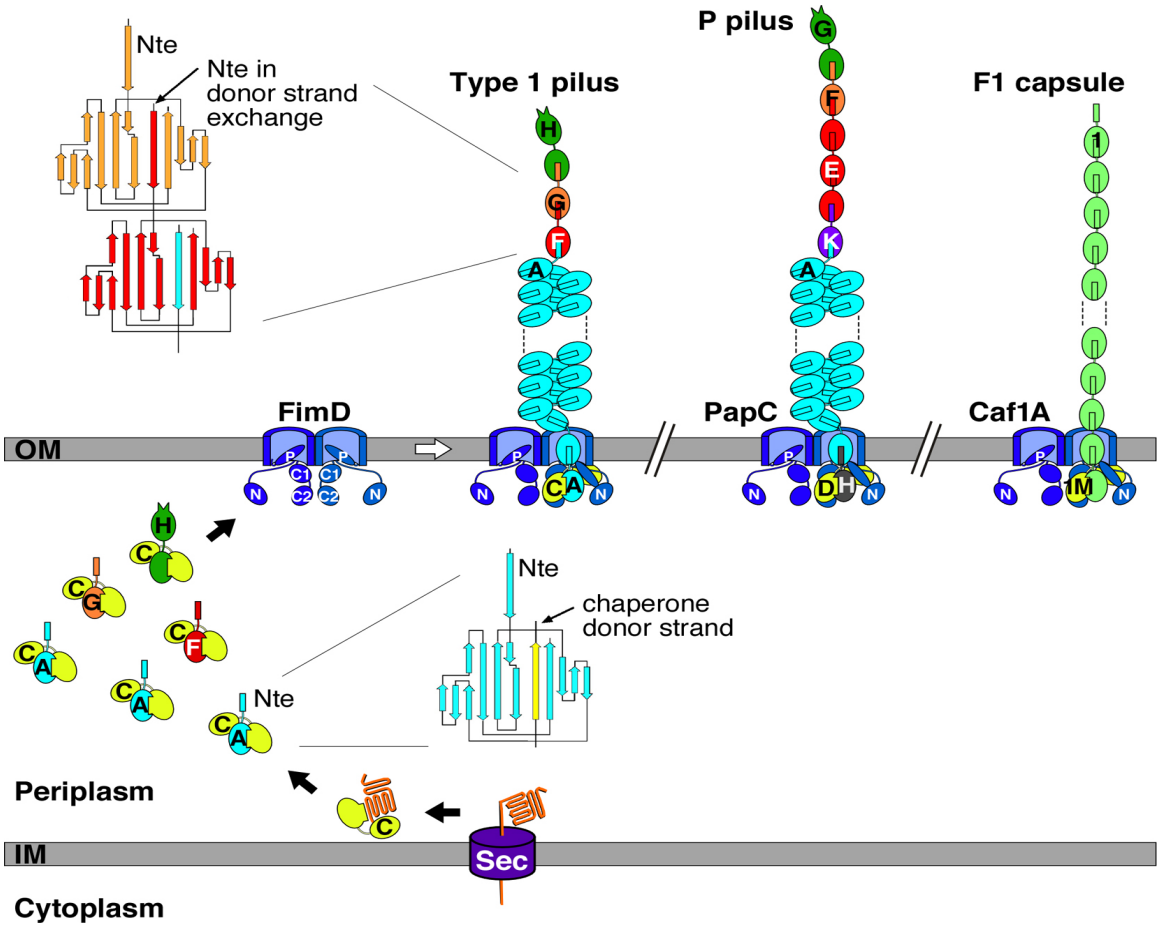

Figure 1.2: Assembly of pili by the chaperone/usher pathway. Adapted from Thanassi *et al*. with permission [117]. Briefly, subunits that form the pili in the chaperone/usher pathways are secreted into the periplasm through the general Sec pathway. In the periplasm they are bound by their cognate chaperone, which promotes proper folding and prevents off pathway interactions. The chaperone-subunit complex then binds the usher, and the chaperone disengages from the subunit protein allowing subunit-subunit interactions to occur. This process secretes the subunits through the pore of the usher and forms the pili on the surface of the bacterium [84].

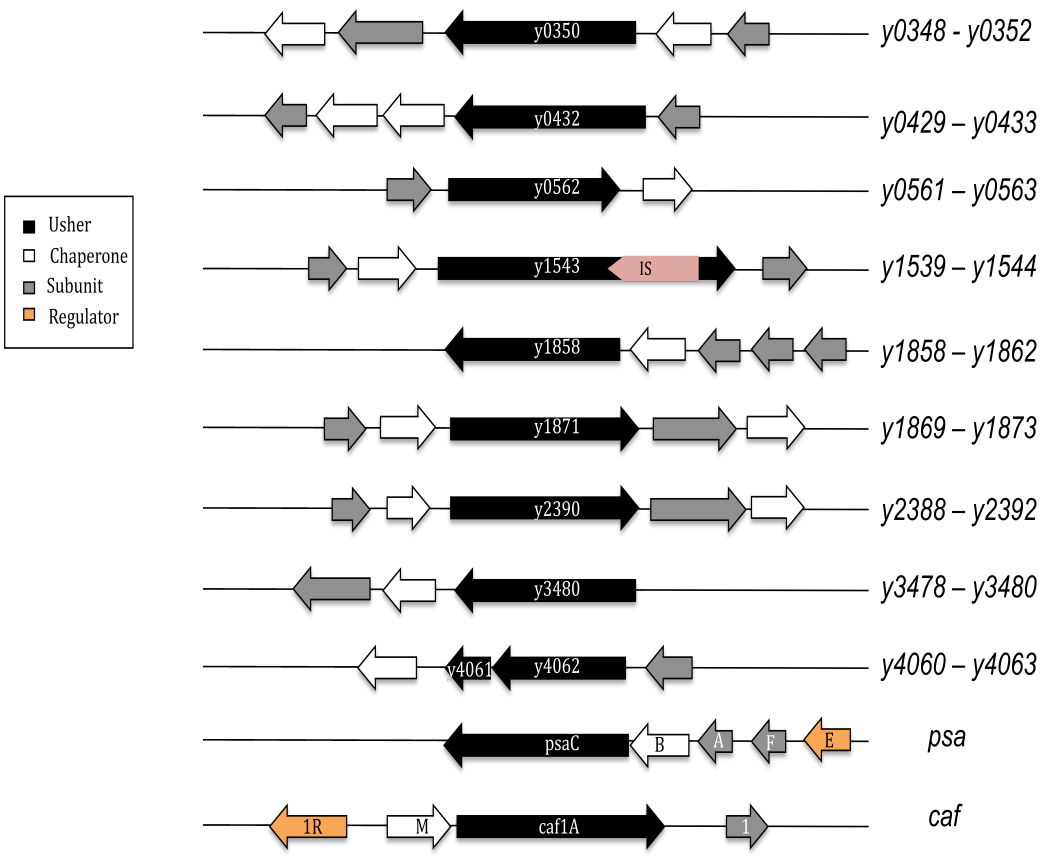

Figure 1.3: Schematic view of the chaperone/usher gene clusters of *Y. pestis*. A schematic view of the pathways studied in this dissertation, including the two well-studied pathways, *caf* and *psa.* Pathway *y1539-y1544* contains an insertion element in the usher, pathway *y4060-y4063* has a premature stop codon in the usher gene, and pathway *y0429-y0433* is a member of the alternate chaperone/usher class.

Chapter 2: Experimental Procedures

Bacterial strains and growth conditions

All bacterial strains and plasmids can be found in Tables 2.1 and 2.2. The *Y. pestis* strains are derived from KIM, a biovar 2.MED strain [118]. *Y. pestis* KIM6+ is an attenuated *pgm* positive strain that lacks the pCD1 virulence plasmid. *Y. pestis* KIM5+Ap is fully virulent and contains both the *pgm* locus and the pCD1 virulence plasmid marked with an ampicillin resistance (Amp^r) gene [119]. *Y. pestis* cultures were streaked out from frozen stocks onto Luria-Bertani (LB) plates and incubated for 48 hours at 28°C. Single colonies were used to inoculate Heart Infusion Broth (HIB) or TMH minimal media at pH 7.4 (when indicated) [14]. Bacterial cultures were then incubated overnight at 28°C with aeration. From these overnight cultures, day cultures were made by diluting the overnight culture 1:20 into fresh HIB and grown at 37°C with aeration for approximately 3-4 hours until an OD_{600} of ~0.7 was reached (log phase), unless otherwise noted. *E. coli* strains were grown in LB medium at 37ºC with aeration. Unless otherwise noted, cultures were supplemented with ampicillin (Amp) at 100 μg/ml, kanamycin (Kan) at 50 μg/ml, or tetracycline (Tet) at 15 μg/ml when necessary. IPTG (isopropyl ß-D-thiogalactoside) was added to 50 μM final concentration to induce expression when necessary.

Construction of chromosomal mutants in Y. pestis

For construction of chromosomal full pathway deletion mutants in *Y. pestis* allelic exchange was performed using a suicide-vector system (Figure 2.1) [120-122]. Briefly,

500-700 bp of both the upstream region (USR) and downstream region (DSR) of each chaperone/usher operon were cloned with primers *y(first gene)* USRForward, USRReverse, and *y(first gene)* DSRForward, DSRReverse (Table 2.3). A linker region consisting of G-C repeats was used to ligate the USR and DSR fragments together with higher efficiency [123]. Fragments were ligated together into a 1000-1200 bp fragment and then cloned into the intermediate vector pGEM T-Easy (Promega). The pGEM with the ligated USR-DSR fragments, termed pGEM *y(first gene)* Ligated, was transformed into DH5α chemically competent cells and was selected for with Amp. Colonies were then screened for the insertion of the ligated fragments, and overnight cultures in LB/Amp were started. Plasmid preparations were performed using the Wizard Plus SV Miniprep DNA Purification System (Promega). The suicide vector pSB890 was purified from S17λpir *E. coli* cells using a Plasmid Midi Kit (Qiagen). Both the pGEM *y(first gene)* Ligated and pSB890 were digested with appropriate restriction enzymes, BamHI or NotI (Roche/ New England Biolabs (NEB)). Plasmid pSB890 was treated with rAPID Phosphatase (NEB) to prevent self ligation. Ligated USR-DSR fragments were gel purified using a Qiagen Gel Extraction Kit (Qiagen). USR-DSR fragments were then ligated into pSB890 and the plasmid was transformed into chemically competent S17λpir cells. Cells were allowed to recover for one hour in LB, plated on LB/Tet, and incubated for 16-24 hours at 37^{o}C. Colonies were again screened for the presence of the correct USR-DSR insert via both PCR and restriction digest pattern.

To create the merodiploid in *Y. pestis,* overnight cultures of the parental KIM6+ and S17λpir pSB(*first gene*) were started. A 25 μL aliquot of the KIM6+ was then mixed with 25 μL of the S17λpir pSB(*first gene*), plated on LB plates, and then incubated at

37°C for 5 hours. Mixed colonies were then plated on Yersinia Selective Media (YSM)/Tet, which only allows the *Y. pestis* that has integrated the suicide vector into the genome to grow. Colonies from the YSM/Tet plate were then restreaked onto YSM/Tet for an additional 48 hours. Overnight cultures of the merodiploid were grown at 28°C with aeration without antibiotic selection. To select for a recombination event, *Y. pestis* from an overnight culture was plated on LB/5% sucrose and incubated at 28°C for 48 hours. Colonies were then plated again on LB/5% sucrose, LB/Tet, or LB alone. Only colonies that were Tet sensitive and sucrose resistant were screened by PCR to confirm the deletion of the genes of interest. To confirm the desired deletion, two PCRs were performed, the first looking for the scar region left by the excision of the operon (the USR-DSR ligated product), and a second looking for the absence of an internal gene using primers found in Table 2.4.

Construction of complementing strains

For construction of complementing plasmids py0350, py1858 and py1871 (Table 2.2), the usher genes were amplified from KIM6+ by PCR using Taq polymerase (Invitrogen) and the primer pairs listed in Table 2.5. The PCR products were ligated into plasmid pGEM-T Easy (Promega), the resulting plasmids were then digested with EcoRI and BamHI or BamHI and SalI (NEB), and the fragments encoding the usher genes were purified using the MinElute PCR Purification Kit (Qiagen). The usher gene fragments were then ligated into plasmid pMMB91 that had been similarly digested and purified. Ligation products were transformed into *E. coli* DH5α for selection of Kan^r colonies. Final plasmids, containing the usher genes downstream of the IPTG-inducible P_{tac}

promoter, were confirmed by sequencing. Purified plasmids were then transformed into their cognate KIM6+ usher deletion strains.

Growth curves

The growth kinetics for each mutant were analyzed at two temperatures, 28°C and 37°C, and compared to the parental strain. An overnight culture of each strain from a single colony was started at 28°C. The culture was then diluted 1:20 at time point 0 and the new cultures were incubated at one of the indicated temperatures. The OD_{600} was read every 1-2 hours for 24 hours.

Transmission electron microscopy

Electron microscopy was performed as previously described [29, 124, 125]. Briefly, overnight cultures of either the parental KIM6+ strain or a mutant strain were grown at 28°C or 37°C in HIB with aeration, harvested by centrifugation, washed and resuspended into PBS, and then adsorbed to polyvinyl formal-carbon-coated grids (E.F. Fullman) for two min. The grids were fixed with 1% glutaraldehyde for one min, washed twice with PBS, washed twice with water, and then negatively stained with 0.5% phosphotungstic acid (Ted Pella) for 35 s. The grids were examined on a TECNAI 12 BioTwin G02 microscope (FEI) at 80 kV accelerating voltage. Digital images were captured with an AMT XR-60 CCD digital camera system (Advanced Microscopy Techniques).

Biofilm formation

The biofilm assay was adapted from O'Toole *et al.* 1999 and Felek *et al.* 2008 [48, 126]. Briefly, overnight cultures of *Y. pestis* were resuspended in HIB to an OD_{600} of approximately 1.0. A 100 µL aliquot of bacterial culture was put into a flat-bottomed 96-well polystyrene culture plate (Falcon) and incubated statically at either 28ºC or 37ºC for 24 h. The OD of the cultures was read in a microplate reader (SpectraMax) at 600 nm. Bacterial cultures were then washed twice with 100 µL PBS, and 0.01% Crystal Violet was added. The bacteria were incubated with the Crystal Violet for 15 min at room temperature. The bacteria were then washed three times with 150 µL distilled water, and the bound Crystal Violet was solubilized with 80% ethanol and 20% acetone. The absorbance of the Crystal Violet was read by the microplate reader at 595 nm. Results were normalized to bacterial culture density.

Autoaggregation assay

Y. pestis strains were grown overnight at either 28ºC or 37ºC in HIB. The overnight cultures were resuspended to an OD_{600} of approximately 1.1-1.6 in 1 mL of HIB in cuvettes. The cultures were then incubated statically at either 28ºC or 37ºC and the OD_{600} was read every 20 min.

Tissue culture

A549 human lung epithelial cells were grown in DMEM (Gibco) containing 10% FBS (HyClone). HEp-2 human epithelial cells were grown in MEM (Gibco) containing 10% FBS. Murine bone marrow-derived macrophages (muBMDM) were obtained as

described previously [38, 127]. Briefly, cells from the femurs of female wild type C57BL/6 mice were grown in Bone Marrow Medium [49% DMEM (Gibco), 30% L-cell supernatant, 20% FBS, and 1% sodium pyruvate (Gibco)]. When muBMDM were seeded for infection, they were grown in Infection Medium [79% DMEM (Gibco), 15% L-cell supernatant, 5% FBS, and 1% sodium pyruvate]. Human monocyte-derived macrophages (huMDM) were isolated as described [128] from healthy human donors and directly seeded at 1.5 x 10^5 cells/well in 24-well plates (Corning) on coverslips. The cells were allowed to differentiate for 5 days in RPMI-1640 medium (Gibco) containing 10% FBS and 10 ng/mL macrophage colony-stimulating factor (Sigma).

Colony forming unit assay

A549 cells were seeded at 1.5 x 10^5 in 24-well tissue culture plates (Falcon) and incubated at 37^{o}C, 5% CO_2. Bacterial cultures were grown as described above until they reached mid-log phase. *Y. pestis* strains were then diluted in DMEM + 10% FBS at a multiplicity of infection (MOI) of 50. After the mammalian cells were washed three times with PBS, 1 mL of bacteria was added to each well, and the plate was centrifuged (50 *g*, room temperature) for 4 minutes to facilitate bacterial contact. Plates were then incubated for two hours at 37^{o}C, 5%CO_2. The cells were then washed rigorously three times with PBS to remove any non-adherent bacteria. Cells were then lysed using 500 μL distilled H_2O + 0.1% Triton-X 100 (BioRad) in dH_2O for 10 minutes at room temperature. Wells were washed one additional time, and the wash was combined with the cell lysate. Lysates were then serially diluted in PBS, plated on LB plates, and incubated at 28^{o}C for 48 hours. Colonies were then enumerated.

Cell culture adhesion/invasion

The adhesion and invasion studies were adapted from a procedure from the Bliska Laboratory [39, 127, 129]. Mammalian cells were seeded on coverslips in a 24-well plate (Corning) at concentrations of 1.5 x 10^5 cells per well and incubated overnight at 37ºC, 5% CO_2 in the growth conditions described above. Overnight cultures of wild type bacteria, deletion mutant *Y. pestis* KIM6+ strains, complemented stains, or the deletion strains containing the pGFP plasmid were diluted 1:20 into fresh HIB and grown at 37ºC with aeration until the OD_{600} was 0.7. *Y. pestis* strains containing the pGFP plasmid (for invasion studies) or deletion strains containing complementation plasmids were induced for expression of the plasmid-encoded genes by addition of 50 μM IPTG at 2 h of growth. For adhesion experiments, the bacteria were resuspended to an MOI of 50 in the appropriate medium for the host cell type used. For invasion experiments, bacteria were resuspended to an MOI of 50 for the epithelial cells or an MOI of 10 for the macrophages. For adhesion experiments, the muBMDM and huMDM were pretreated with 5 μg/mL cytochalasin D for 1 h prior to infection. After the mammalian cells were washed three times with PBS, 1 mL of bacteria was added to each well, and the plate was centrifuged (50 *g*, room temperature) for 4 minutes to facilitate bacterial contact. After 2 h at 37ºC, 5% CO_2 (or 20 min for the macrophage invasion studies), the cells were washed once with PBS and fixed for 30 min in 2.5% paraformaldehyde at room temperature. All subsequent steps were completed at room temperature. The cells were blocked with 3% BSA in PBS for 20 min and then incubated with rabbit anti-*Yersinia* antiserum SB349 [129] diluted 1:1000 in 3% bovine serum albumin in PBS for 30 min. The cells were then washed three times with PBS. Next, a secondary goat anti-rabbit

antibody conjugated to Alexa-594 (Invitrogen) was added at 1:2000 dilution in 3% BSA in PBS and incubated for 30 min. The cells were then washed again three times with PBS. The coverslips were mounted on glass slides using ProLong Gold antifade reagent (Invitrogen), and the slides were examined on a Zeiss Axioplan2 microscope using a 40X objective lens. Images were captured using a Spot camera (Diagnostic Instruments) and processed using Adobe Photoshop. For each experimental replicate, 10 random fields per bacterial strain were photographed. The total numbers of host cells and the total numbers of bacteria bound to the host cells were quantified for each field to calculate the number of bacteria/cell. The values obtained for the ten fields were then averaged to obtain the number of bacteria/cell for the experimental replicate.

Construction of KIM5+ strains

To generate the usher deletion mutations in the fully virulent *Y. pestis* KIM5+ background, plasmid pCD1Ap was introduced by electroporation into the KIM6+ usher deletion or complemented strains under biosafety level 3 (BSL3) conditions. The resultant KIM5+Ap strains were selected by plating onto Yersinia Selective Media (YSM) agar containing 30 μg/mL Amp and 50 μg/mL Kan (for complemented strains only). Colonies were then restreaked on Congo Red/Amp plates to ensure the presence of the *pgm* locus as well as the pCD1Ap plasmid.

Time until death assays

Mouse infections were performed at the University of Medicine and Dentistry of New Jersey Regional Biocontainment Laboratory (Newark, NJ) under BSL3 conditions.

All animal research protocols were approved by the Institutional Animal Care and Use Committees of Stony Brook University and the Regional Biocontainment Lab.

Six-to-eight week old female C57BL/6 mice (Jackson Laboratories) were utilized for the infections. Inoculations via the subcutaneous and intranasal routes were used to mimic bubonic and pneumonic plague, respectively. *Y. pestis* strains were grown overnight at 28ºC in HIB, resuspended in PBS, and diluted in PBS to achieve the desired infectious dose. Groups of five mice were injected subcutaneously with 50 µl containing 200-500 colony forming units (CFU) or inoculated intranasally with 25 µl containing either 2,000-5,000 CFU (approximately 4-to-10 LD_{50} doses for the respective routes). The actual infectious doses were determined by retrospective CFU counts. The mice were observed twice daily and monitored for survival for 21 days.

Construction of KIM5- strains

The transformation of KIM6+ strains into KIM5- required a two-step process in which first the *pgm* locus was recombined out by the flanking IS100 sequences, and then the pCD1 plasmid was electroporated in. Congo Red binding was used to screen for the presence or absence of the *pgm* locus [130, 131]. Overnight cultures of full pathway mutants were serially diluted in PBS five times. A 100 µL aliquot of the last serial dilution (10^{-5}) was plated on Congo Red plates. The plates were then incubated for 48 hours at 28^{o}C. Any white colonies, indicating loss of the *pgm* locus, were then restreaked two more times onto Congo Red plates to ensure pure colonies which lacked the *pgm* locus. PCR was used to confirm the loss of the *pgm* locus by screening for the scar region left by the excision, as well as screening for the absence of the *ripA* gene, a gene that is

contained within the *pgm* locus, using primers found in Table 2.6. Once the deletion of the *pgm* locus was confirmed, stocks of electrocompetent KIM5- bacteria were made for each mutant. Purified pCD1Ap (250-500 ng) was then electroporated into the strains following the protocol as described for construction of the KIM5+ strains.

Yop delivery assay

HEp-2 cells were seeded as described above. KIM5- strains were grown and prepared as described for the adhesion studies with the addition of 100 μg/mL Amp. The bacteria were added to cells at an MOI of 10, and spun down at 50 *g* for 4 minutes at room temperature to ensure contact. The bacteria and cells were co-incubated for two hours at 37^{o}C, 5% CO_2. Cells were gently washed with PBS and fixed with 100% methanol for 30 seconds. The cells were then stained with 0.76 mg/mL Giemsa stain (AppliChem) in dH_2O for 30 minutes at room temperature. To quantitate cytopathic effects of Yop delivery, pictures of cells were taken on an Eclipse E600 microscope (Nikon). Five independent fields of view per strain for each experiment were used to assess the cytopathic effect with approximately 200 cells/field.

Membrane assay for cytokines

Conditioned supernatant was collected from muBMDM infected at an MOI 10 with the parental KIM6+ or full pathway deletion mutants (*y0348-y0352, y1858-y1862,* or *y1869-y1873),* or left uninfected for a total of 24 h. After 2 h of infection with *Y. pestis,* the muBMDM were treated for one hour with 10 μg/mL gentamycin to kill extracellular bacteria. Cells were then washed with PBS, and fresh medium was added to

the cells for an additional 21 h. Conditioned supernatant was then collected, centrifuged at 8,000 rpm at room temperature for five minutes to remove any bacteria or cell fragments, placed in a clean 1.5 mL Eppendorf tube and stored at -80^{o}C until cytokine assays were performed.

RayBio Mouse Cytokine Antibody Array (RayBio) was used to measure the relative levels of 23 cytokines. The manufacturer's protocol was followed and experiments were run in duplicate from two different muBMDM infections. To begin, the membrane was incubated with 2 mL of 1x Blocking Buffer for 30 min at room temperature, followed by a 2 h incubation with 1 mL of the conditioned medium. Membranes were then washed three times with 2 mL of 1x Wash Buffer I for 5 min each at room temperature. Next, the membranes were washed two times with 2 mL of 1x Wash Buffer II for 5 min each at room temperature. Primary biotin-conjugated anti-cytokine antibody was diluted into 2 mL of 1x Blocking Buffer to reach working concentrations. One mL of the diluted anti-cytokine antibody was then added to each membrane and incubated for 2 h at room temperature. Again the membranes were washed as described before. Next, 2 mL of 1,000-fold diluted Horse Radish Peroxidase (HRP)-conjugated strepavidin was incubated with each membrane for 2 h at room temperature and then the wash steps were again repeated. The final step in this process was the detection of positive cytokine spots using chemiluminescence. 1x Detection Buffer C was mixed with 1x Detection Buffer D and incubated with the membranes for 2 min. Membranes were then exposed to X-Ray film (Kodak X-Omat AR film) anywhere from 20 seconds- 2 minutes and run through the SRX-101A Processor (Konica). Levels of the cytokines were then normalized to the positive control spots on each membrane.

Enzyme-linked immunosorbent assay (ELISA) for cytokines

ELISAs for interferon gamma (IFN-γ) (R&D Systems), tumor necrosis factor alpha (TNF-α) (R&D Systems), and interleukin 9 (IL-9) (Biolegend) were run using the conditioned media described above. All ELISAs were run at least in triplicate with three wells per experiment ($N \geq 9$).

For the IL-9 ELISA, the plates were coated with the capture antibody for 18 h at 4°C, and then washed four times with 300 μL Wash Buffer. A 200 μL aliquot of 1x Assay Diluent was added to each well to block non-specific binding and was incubated for 1 h at room temperature with shaking. The standards were prepared following the manufacturer's guidelines. The plate was then washed as described before, 100 μL of the standards or conditioned supernatant were added to each well, and the samples were then incubated at 4°C for 24 h. After the incubation, the plate was again washed as described above, and 100 μL of 1x Detection Antibody Solution was added to each well and allowed to incubate for 1 h at room temperature while shaking. Plates were washed again followed by the addition of 100 μL 1x Avidin-HRP solution to each well for 30 min at room temperature with shaking. The plate was washed five times with Wash Buffer for 30 sec per wash. Finally, 100 μL of Substrate Solution was added to each well, and the plate was incubated in the dark for 15 min to allow for the colorimetric reaction to occur. Adding 100 μL of Stop Solution stopped the reaction. The absorbance of each well was then read on the microplate reader at 450 nm to determine the levels of IL-9 from each sample and then again at 570 nm for a wavelength correction.

The procedures for the ELISAs for IFN-γ and TNF-α are the same with exception of the Assay Diluent (RD1-21 for IFN-γ or RD1W for TNF-α). To begin the procedure,

50 μL of the Assay Diluent was added to each well followed by the addition of 50 μL of the Standard, Control, or conditioned media. The plate was then incubated at room temperature for 2 h. For wash steps, 400 μL of Wash Buffer was added to each well five times. One hundred μL of either IFN-γ or TNF-α conjugate was added to each well, and the plate was again incubated for 2 h at room temperature. The wash step was repeated, followed by the addition of 100 μL of Substrate Solution for 30 min at room temperature in the dark. Addition of 100 μL of Stop Solution stopped the reaction. The absorbance of each well was then read on the microplate reader at 450 nm to determine the levels of IFN-γ or TNF-α from each sample and then again at 570 nm for a wavelength correction.

Table 2.1: Bacterial strains

Strain	Characteristic	Reference
E. coli:		
DH5α	*hsdR recA endA*	[132]
BW25141	oriRγ pir^+	[133]
S17λpir		[134]
Y. pestis:		
KIM6+	*pgm*+ pCD1-	[44]
KIM6+ Δy0350		This study
KIM6+ Δy0562		This study
KIM6+ Δy158		This study
KIM6+ Δy1871		This study
KIM6+ Δy2390		This study
KIM6+ Δy3480		This study
KIM6+ Δy0350 Comp	Kan^r py0350	This study
KIM6+ Δy1858 Comp	Kan^r py1858	This study
KIM6+ Δy1871 Comp	Kan^r py1871	This study
KIM6+ Δy0350 GFP	Amp^r pGFP	This study
KIM6+ Δy0562 GFP	Amp^r pGFP	This study
KIM6+ Δy1858 GFP	Amp^r pGFP	This study
KIM6+ Δy1871 GFP	Amp^r pGFP	This study
KIM6+ Δy2390 GFP	Amp^r pGFP	This study
KIM6+ Δy3480 GFP	Amp^r pGFP	This study
KIM5+ Ap	Amp^r KIM6+/pCD1Ap	[119]
KIM5+ Ap Δy0350	Amp^r	This study
KIM5+ Ap Δy0562	Amp^r	This study
KIM5+ Ap Δy1858	Amp^r	This study
KIM5+ Ap Δy1871	Amp^r	This study
KIM5+ Ap Δy2390	Amp^r	This study
KIM5+ Ap Δy3480	Amp^r	This study
KIM6+ Δy0348-y0352		This study
KIM6+ Δy0429-y0433		This study
KIM6+ Δy0561-y0563		This study
KIM6+ Δy1538-y1544		This study
KIM6+ Δy1858-y1862		Krukonis Lab
KIM6+ Δy1869-y1873		This study
KIM6+ Δy2388-2392		Krukonis Lab
KIM6+ Δy3478-y3480		Krukonis Lab
KIM6+ Δy4060-4063		This study

KIM5-	Amp^r *pgm*-/pCD1+Ap	[50]
KIM5- ΔyopB	Amp^r	[135]
KIM5- Δy0348-y0352	Amp^r	This study
KIM5- Δy1858-y1862	Amp^r	This study
KIM5- Δy1869-y1873	Amp^r	This study
KIM5- Δy4060-y4063	Amp^r	This study

Amp^r = Ampicillin resistance; Kan^r = Kanamycin resistance

Table 2.2: Bacterial plasmids

Plasmid Name	Characteristic	Source
pGEM-T Easy	Amp^r	Promega
pMMB91	vector, IPTG-inducible, Kan^r	[97]
pKD4	FRT sites, Kan^r, Amp^r	[133]
pKOBEG	λ phage *redγβα*, arabinose-inducible, Clm^r	[136, 137]
pFLP2	*sacB FLP-*λp_R Amp^r	[138]
pCD1	*bla* Amp^r cassette	[119]
pGFP	pMMB207gfp3.1, Amp^r Clm^r	[139]
pSB890	Tet^r Suc^s	[140]
pGEM-y0350	Usher gene *y0350* in pGEM-T Easy	This study
pGEM-y1858	Usher gene *y1858* in pGEM-T Easy	This study
pGEM-y1871	Usher gene *y1871* in pGEM-T Easy	This study
py0350	Usher gene *y0350* in pMMB91	This study
py1858	Usher gene *y1858* in pMMB91	This study
py1871	Usher gene *y1871* in pMMB91	This study
pGEM-y0348USR-DSR	*y0348* USR-DSR ligated product in pGEM-T Easy	This study
pGEM-y0429USR-DSR	*y0429* USR-DSR ligated product in pGEM-T Easy	This study
pGEM-y0561USR-DSR	*y0561* USR-DSR ligated product in pGEM-T Easy	This study
pGEM-y1538USR-DSR	*y1538* USR-DSR ligated product in pGEM-T Easy	This study
pGEM-y1869USR-DSR	*y1869* USR-DSR ligated product in pGEM	This study
pGEM-y4060USR-DSR	*y4060* USR-DSR ligated product in pGEM-T Easy	This study
pSB0348	*y0348* USR-DSR ligated product in pSB890	This study
pSB0429	*y0429* USR-DSR ligated product in pSB890	This study
pSB0561	*y0561* USR-DSR ligated product in pSB890	This study

pSB1538	*y1538* USR-DSR ligated product in pSB890	This study
pSB1869	*y1869* USR-DSR ligated product in pSB890	This study
pSB4060	*y4060* USR-DSR ligated product in pSB890	This study

Amp^r = Ampicillin resistance; Kan^r = Kanamycin resistance;
Clm^r = Chloramphenicol resistance; Tet^r = Tetracycline resistance;
Suc^s = Sucrose sensitivity

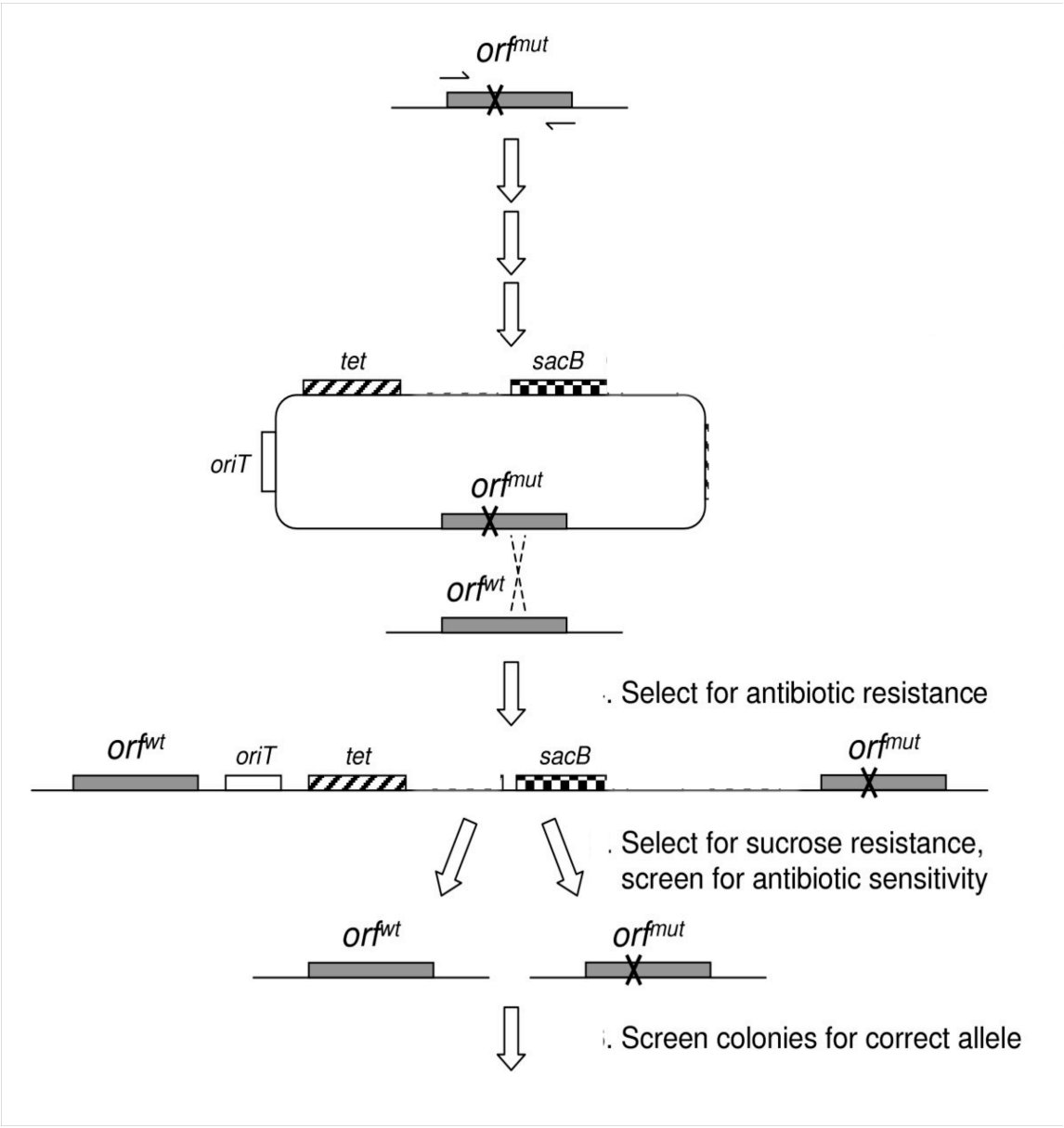

Figure 2.1 Schematic outline of creating knockouts using the suicide vector system. Adapted from Marx 2008 with permission [141].

Table 2.3: Primers used to create *Y. pestis* full pathway deletion mutants

Primer	Sequence
y0348-USRF	ATCGTGGGATCCGCCATTCCCAGCAGCGCACT
y0348-USRR	GGAGGTACGCTCATCATGCTATGCTTAGCCGTATCAACCG
y3480-DSRF	CGGTTGATACGGCTAAGCATAGCATGATGAGCGTACCTTC
y0348-DSRR	GCATTGGGATCCCTATCGCGTTATTCTCGGCA
y0429-USRF	ARCTCGGGATCCCGAATACCAATGTCAGTTGCCC
y0429-USRR	GACAGTAAGACATTGCCCAGAGTGCCCTTCGGGCTAGCCT
y0429-DSRF	AGGCTAGCCCGAAGGGCACTCTGGGAATGTCTTACTGTC
y0429-DSRR	GCAATGGGATCCGCCAAAGAGCCTAATAATGCCG
y0561-USRF	CTTGGGGAAGATAAACGATACGG
y0561-USRR	CCCCCGGGGGCCCCCTAATACAACGGGCGACCACG
y0561-DSRF	GGGGGCCCCCGGGGGAAATGCTGCCGATTGGTGCC
y0561-DSRR	CTGTTCAACCCCTTCAAAAGAGG
y1538-USRF	AACTTCTTATGCTGCTGCTGGCGG
y1538-USRR	CCCCCGGGGGCCCCCTATGCTTTACTGCTGCGGTGACCC
y1538-DSRF	GGGGGCCCCCGGGGGAGTTTCTTCCTATCGGCAC
y1538-DSRR	CTGAACACTATTTTCTCTACCAACG
y1869-USRF	GCGACAATGGGTAATGCCTATG
y1869-USRR	GGGGGCCCCCGGGGGATCACTTCAGCACGAGCCACAGTC
y1869-DSRF	CCCCCGGGGGCCCCCGCAGTTTGGTGTTGAGTGCTACG
y1869-DSRR	CCAGTTTGATAGTGACGCCCTG
y4060-USRF	GCCAGATATCGCTATAATTCGC
y4060-USRR	GGGGGCCCCCGGGGGACAGTGGAATAGCGAAATGAAAGAC
y4060-DSRF	CCCCCGGGGGCCCCCCAAGTAGATAATTCCCCGGAG
y4060-DSRR	TTGTAGCCTGACGGCTCAAG

Table 2.4: Primers used to confirm the deletion of internal genes in knockouts and complement usher deletions

Primer	Sequence
*y0348*TestF	GAATTCATAGACCGCAGTGGTAGACT
*y0348*TestR	GGATCCAAGATGCCGGTAGCTATCGT
*y0429*TestF	GGCCAGTGCTAGCGGTGAGC
*y0429*TestR	ACCCAGCAGTGGTTGGGGGT
*y0561*TestF	TCAGGAAACCTCTGCTTTACGC
*y0561*TestR	ACCCCATCGCCCTTGATAAG
*y1538*TestF	TGCTGCTGCTGGCGGTACTG
*y1538*TestR	CGCTTTGACCTGCCCAGGGG
*y1869*TestF	GGATCCGGCCTCGATATAATGCTTAGTGC
*y1869*TestR	CAGCTGCGCGCAGGTACATGTTGATA
*y4060*TestF	AGTTATTATTCAGCGACACCCCTG
*y4060*TestR	GGTTGATGATTACACCCCTCCG

Table 2.5: Primers used to complement usher deletion mutants

Primer	Sequence
*y0350*ExpF	GAATTCATAGACCGCAGTGGTAGACT
*y0350*ExpR	GGATCCAAGATGCCGGTAGCTATCGT
*y1858*ExpF	GAATTCGACCTACTCTGTTGTTGCCT
*y1858*ExpR	GGATCCCAGTAACTAGCCCATACCAG
*y1871*ExpF	GGATCCGGCCTCGATATAATGCTTAGTGC
*y1871*ExpR	CAGCTGCGCGCAGGTACATGTTGATA

Table 2.6: Primers used to confirm *pgm* deletion

Primer	Sequence
pgm-F1	CCGCAACAACATCATCCGTATTC
pgm-R2	CCCAGAGGCAGACGGACC
ripAF	TATGCCGAAAGTACGGTACTTCATAAA
ripAR	TTAAGGTATTCGTACATTTCTTGTTGC

Chapter 3: The Role of Select Pili Formed by the Chaperone/Usher Pathways of *Yersinia pestis* in Virulence Characteristics, Host Cell Adhesion and Invasion, and Virulence

Abstract

Pili formed via the chaperone/usher pathway have been shown in multiple different bacterial species to contribute to virulence [114, 142]. This led me to hypothesize that these pathways in *Y. pestis* contribute to virulence, most likely by contributing to the adhesion of the bacteria to host cells. To test this hypothesis, an usher deletion library of six of the nine uncharacterized *Y. pestis* chaperone/usher pathways was created (Runco and Thanassi, unpublished data). These mutants were used to test the ability of each of the pathways to contribute to biofilm formation, autoaggregation, adhesion to and invasion of host cells, and virulence in the mouse model of bubonic and pneumonic plague. I found that three of the pathways contributed to the ability of the bacteria to bind host cells and to virulence via the pneumonic route in the mouse model of infection.

Introduction

In many bacteria, such as *E. coli* and *Salmonella,* pili formed via the chaperone/usher pathway contribute to the virulence of the bacteria, and in fact different pathways may contribute in different ways [114, 142, 143]. Runco *et. al*. showed that the KIM6+ strain of *Y. pestis* expresses pilus-like fibers on the surface of the bacteria, and that within the genome there are a number of chaperone/usher pilus operons (Figure 1.3) [9, 10, 29]. Very little work has been done on the pili formed via these pathways in *Y. pestis* despite the fact that many adhesins, such as YadA and Inv, are inactive in this species of *Yersinia* [23, 63, 65]. There are several adhesins in *Y. pestis* that have been shown to be active and contribute not only to host cell binding but virulence in the mouse model of infection. However, loss of any one of these adhesins does not completely abolish virulence or the ability to adhere to host cells [23, 25, 48, 75, 78, 79, 81, 82, 144, 145]. Therefore, it is possible that there are unexplored pathways that also contribute to adhesion and virulence of the plague bacterium. To study the contribution of the chaperone/usher pathways to adhesion and virulence of *Y. pestis*, a panel of six usher deletion mutants was initially created (Runco and Thanassi, unpublished data). The usher is a critical outer membrane component of the chaperone/usher pathway, which serves as the docking and assembly site for the pili on the outer membrane of Gram-negative bacteria (Figure 1.2) [87, 105, 109]. With a specific usher deleted, pili of that pathway are unable to form on the surface of the bacterium. The work done in this chapter is the beginning of exploring the role of the chaperone/usher pathways of *Y. pestis* with respect to biofilm formation, autoaggregation, host cell adhesion and invasion, and virulence *in vivo*.

Results

Visualization of the pili formed by Y. pestis

A previous graduate student in the laboratory, Lisa Runco, constructed a panel of six single usher deletion mutants in *Y. pestis* strain KIM6+. These deletion mutants were constructed by inactivating genes *y0350, y0562, y1858, y1871, y2390,* and *y3480* (Figure 1.3). She first checked each of the six usher deletion mutants for the presence or absence of pilus fibers on the bacterial surface by using transmission electron microscopy of bacteria that were grown in HIB at 37^{o}C. She found that no single usher deletion abolished the formation of pili on the surface on the mutant bacteria (Figure 3.1). This indicated that either multiple pathways are active under the condition examined or a yet unexplored pathway is the source of these fibers.

Contribution of pili to in vitro traits of Yersinia pestis

The ability to autoaggregate in culture media can be indicative of the virulence of *Yersinia spp.* [48, 146-148]. To test the role of the chaperone/usher pathways in this process, I examined the ability of the six usher deletion mutants to autoaggregate in HIB at both 28^{o}C and 37^{o}C, mimicking the temperatures found in insect vectors and the human host, respectively. It has been previously shown that *Y. pestis* will autoaggregate very quickly under static conditions, especially at 28^{o}C [149]. I found rapid autoaggregation, as measured by a decrease in OD_{600}, to occur at 28^{o}C. No single usher deletion mutant appeared to have any effect on autoaggregation at this temperature (Figure 3.2). At 37^{o}C there was very little autoaggregation, in either the KIM6+ wild type

or any usher deletion mutant (Figure 3.3). Comparison of the 140-minute time point for Figures 3.2 and Figure 3.3 highlights this difference between temperatures. The lack of autoaggregation at 37°C has been reported previously and is most likely due to the expression of the F1 capsule at 37°C [149]. From these data I concluded that the pili formed by these six chaperone/usher pathways do not contribute to autoaggregation.

The ability to form a biofilm, most notably at 28°C, a temperature that mimics the flea vector, is another attribute that is linked to the pathogenesis of plague [146, 147]. The ability to form a biofilm in the flea is needed to allow for efficient transmission of the bacteria to the next host [45, 146, 147]. However, the ability to form a biofilm at 37°C is also very important, because this allows a population of bacteria to be resistant to antibiotics and antibacterial factors within the host [150, 151]. Using the commonly established microtiter plate method for studying biofilm formation, I examined the contribution to biofilm formation of each of the chaperone/usher pathways at both 28°C and 37°C. I found that biofilms formed efficiently at both temperatures for the parental KIM6+, as well as the six usher deletion mutants (Figure 3.4 and 3.5). It appeared that the biofilms formed slightly better at 28°C compared to 37°C, although this was a minor difference and might be attributed to the expression of either an adhesin at 28°C or anti-adhesive factor at 37°C, such as the F1 capsule.

The role of pili in adhesion and invasion of host cells

I next assessed the ability of the usher deletion mutants to adhere to a range of host cells. It is well established that pili formed via the chaperone/usher pathway can contribute to the adhesion of pathogenic bacteria to host cells [114, 142, 152]. If a single

pathway contributed in a significant way to the ability of *Y. pestis* to adhere to or invade a specific cell type, I would see a decrease in the total bacteria bound to the cell when the usher, and thus the pili, was not present. By using multiple host cell types, both cell lines and primary cells, I hoped to gain an understanding of how each pathway contributed to the overall picture of plague.

The first study was done using A549 cells, which are immortalized human type II pulmonary epithelial cells, and possibly one of the first cell types encountered in a primary pneumonic plague. I first began my studies into these pathways using a colony forming unit (CFU) assay to determine the ability of the wild type KIM6+ strain or usher deletion mutants to associate with A549 cells. Using the CFU assay, I found that *Y. pestis* associated robustly with this cell line. Two of the usher deletion mutants, Δ*y0350* and Δ*y1858*, associated to a lower level compared to the parental KIM6+ strain (Figure 3.6). However, results from this assay were not statistically significant due to a high level of variability of the CFU counts. Therefore, I decided to move to a more consistent means of measuring both adhesion to and invasion of various cell types.

I next used a microscopy-based assay to compare wild type KIM6+ with the usher deletion mutants for association with different host cells. I first examined interactions of the bacteria with A549 cells. Bacterial binding to the host cells was detected using a polyclonal anti-*Y. pestis* antibody in the absence of permeabilization, so only surface-bound bacteria were visualized. I proceeded with confirming the initial results from the CFU assay, that is to say that usher deletion mutants Δ*y0350* and Δ*y1858* had a defect in binding to the A549 cells. Cells infected with KIM6+ or usher deletions Δ*y0562,* Δ*y1871,* Δ*y2390*, or Δ*y3480* had approximately 2 bacteria bound to every cell after the two-hour

incubation (Figure 3.7). However, cells infected with usher deletion Δ*y0350* had an average of fewer than one bacteria bound to each cell. This difference is highly significant with a P value less than 0.001. Cells infected with usher deletion Δ*y1858* had an average of fewer than 1.25 bacteria per cells, which is also significant with a P value less than 0.05. Similar experiments were performed using *Y. pestis* strains expressing GFP to measure invasion of the host cells. In these assays, intracellular bacteria appeared green due to the GFP, and extracellular bacteria appeared both green from the GFP and red due to antibody labeling. No invasion was seen for the A549 cell line for the wild type bacteria and all six usher deletion mutants. These experiments demonstrated that at least two of the chaperone/usher pathways are important for adhesion to host cells.

The next cell type I used were HEp-2 cells, a human cervical epithelial cell line. HEp-2 cells have been used for studies of both *Y. pestis* and *Y. pseudotuberculosis,* and they have been found to allow not only adhesion but also invasion of *Yersinia* spp. [48, 66, 74, 75, 83]. After a two-hour incubation with either the GFP expressing wild type KIM6+ or any of the six usher deletion mutants, I observed a very low level of invasion of this cell line. On average there were five internalized bacteria per every 100 HEp-2 cells, which with respect to the total amount of bacteria associated with these cells was a small subpopulation (Figure 3.8). There was no difference in invasion among the parental strain or any of the deletion mutants.

I next compared the usher deletion mutants with the wild type KIM6+ for adhesion to HEp-2 cells. The same trend of decreased adhesion for usher mutants Δ*y0350* and Δ*y1858*, as observed for the A549 cells, presented itself with this cell type (Figure 3.9). When usher Δ*y0350* was deleted, on average there was just under 0.25 *Y. pestis* per

HEp-2 cell, which is significantly different from the wild-type, with a P value of less than 0.05. While the difference between the KIM6+ wild type and usher deletion Δ*y1858* was not statistically significant, there was a reduction to just over 0.25 bacteria per HEp-2 cell compared to the 0.5 bacteria per HEp-2 cell for the parental strain. Usher deletion mutants Δ*y0562,* Δ*y1871,* Δ*y2390,* and Δ*y3480* all bound to similar levels as the wild type strain. Interestingly, compared to the A549 cells, there were fewer total bacteria adhered for all strains used (2 KIM6+/cell for A549 cells compared to only 0.5 KIM6+/cell for HEp-2 cells). These studies support the hypothesis that pathways with ushers *y0350* or *y0562* are important for binding to host epithelial cells.

A common mouse strain used for infections with *Y. pestis* is C57BL/6, so I felt it was important to test the ability for the usher deletion mutants to bind to or invade primary macrophages from this strain. To determine if the chaperone/usher pathways played a role in either invading or preventing phagocytosis by the macrophages, the muBMDM were infected at an MOI of 10 for 20 minutes with the GFP expressing bacterial strains. There was approximately one bacterium per cell for all strains tested (Figure 3.10). There was no difference in the level of internalization of bacteria, with 80% of all the associated bacteria being internalized by the macrophages (Figure 3.11). The high rate of invasion/phagocytosis may obscure any adhesion defects that any usher deletion mutant may have.

To determine if there was a difference in adhesion when a single chaperone/usher pathway was not present, I pretreated the muBMDM with 5 μg/mL of cytochalasin D for one hour prior to infection to paralyze the macrophages and inhibit their ability to phagocytose the *Y. pestis.* The muBMDM were infected with an MOI of 50 for two

hours, to more closely mimic the conditions used to test adhesion with the A549 and HEp-2 cell lines. Under these conditions, I found that when ushers *y0350* or *y1858* were deleted, there were significantly fewer bacteria per cell as compared to the wild type (Figure 3.12). Interestingly, a third pathway played a role in adhesion to the muBMDM. When usher *y1871* was deleted, there were also significantly fewer bacteria per cell (Figure 3.12). Mutants in this third pathway did not play a role in adhesion to either A549 cells or the HEp-2 cells. Mutants in all three pathways had approximately 0.5 bacteria per cell, whereas as the KIM6+ parental strain and usher deletion mutants Δ*y0562,* Δ*y2390,* and Δ*y3480* had 1.4 bacteria per cell. This is highly significant, with all three mutants having P values of less than 0.01 when compared to the wild type bacteria. At this point it was unclear whether the pili formed by the pathway with usher *y1871* were binding to a murine specific moiety, since this was the first mouse cell tested (A549 and HEp-2 are both human cell lines), or a macrophage specific element.

The final cell type that I used to evaluate the roles that the pili formed by the chaperone/usher pathways play in adhesion to host cells was human monocyte derived macrophages (huMDM). Using this cell type offers the advantage of being able to answer the question of whether pili from pathway *y1871* play a role in binding a macrophage specific or mouse specific moiety. I pretreated the cells with cytochalasin D to prevent phagocytosis to solely assess adhesion. I found, similar to the muBMDM, that when ushers *y0350, y1858*, or *y1871* were removed there were significantly fewer bacteria per cell as compared to the parental KIM6+ (Figure 3.13). On average, the parental KIM6+ strain and usher deletions Δ*y0562,* Δ*y2390,* and Δ*y3480* had approximately 1.25 bacteria per cell, where as the three deletion mutants which showed a binding defect had on

average 0.5 bacteria per cell. This difference was highly significant, with P values less than 0.001. These data indicate that the chaperone/usher pathway with usher *y1871* is important for adhesion to a macrophage specific moiety, as opposed to a mouse specific moiety.

To complement the adhesion defects and verify the specificity of the usher deletion mutants, I constructed complementing plasmids for usher *y0350, y1858*, and *y1871* in which usher expression was under IPTG control. The usher genes were expressed with the addition of 50 μM IPTG for 2 hours, and then the host cells were infected with the complemented strains. Adhesion to all cell types (A549, HEp-2, and cytochalasin D treated muBMDM and huMDM) was fully complemented and returned to wild type levels (Figures 3.7, 3.9, 3.12, 3.13).

Role of the Y. pestis chaperone/usher pathways in bubonic and pneumonic plague

To analyze the roles of the *Y. pestis* chaperone/usher pathways in the host during infection, we first converted the KIM6+ usher deletion mutants to the fully virulent KIM5+ background by adding in the pCD1Ap virulence plasmid by electroporation. Strains then were shipped to the Public Health Research Institute (PHRI) in New Jersey for the studies to be done under animal BSL-3 conditions. Mice were infected by either the subcutaneous route, to mimic bubonic plague, or the intranasal route, to mimic pneumonic plague. Two doses were used for each route of infection, a high dose of approximately 10 LD_{50}, or a lower dose of approximately 4-to-5 LD_{50}.

Mice infected subcutaneously with 10 LD_{50} (approximately 500 CFU) of the wild type KIM5+ or usher deletion mutants all died between days two and five, which is

typical for a *Y. pestis* infection [49, 59, 153]. Mice infected with usher deletion Δ*y1871*, the macrophage specific pathway, seemed to have a delay in time until death, with mice dying slightly later in the infection (Figure 3.14). However, this difference was not statistically significant. It is possible that the high infectious dose used overwhelmed any attenuation caused by the usher deletion mutants.

For the next round of subcutaneous infections, approximately 4 to 5 LD_{50} (200-250 CFU) of the parental KIM5+ strain or equal doses of the six usher deletion mutants were delivered to mice via injection. No statistically significant differences between the wild type strain and any single usher deletion mutant were observed in the time to death for mice infected by the subcutaneous route (Figure 3.15). However, there was a trend toward increased survival times for the usher deletion mutants compared to wild type KIM5+, with mutants *y0350*, *y0562*, *y1858* and *y1871* having *P* values just above significance (0.052, 0.059, 0.084 and 0.083, respectively). All mice succumbed to infection between days two and seven, with mice infected with the usher deletions having a slight delay. The mean time to death for all groups was approximately three days post infection. Thus, the chaperone/usher pathways tested do not provide critical functions during the murine model of bubonic plague.

I next examined the roles of the chaperone/usher pathways in pneumonic plague, which if the bacteria were to be released intentionally would be the most likely route of infection. Mice infected with fully virulent *Y. pestis* via the intranasal route typically die between days three and five, with the majority of mice dying on or before day three [20, 153, 154]. Mice were first infected intranasally with 10 LD_{50} (approximately 5,000 CFU) of either the KIM5+ wild type or one of the six usher deletion mutants. Mice infected

with either the wild type KIM5+ or any usher deletion mutants died within three to four days (Figure 3.16). All the mice infected with the KIM5+ parental strain died on day three, while a number of mice infected with the usher deletion mutants, most notably usher deletion Δ*y1871*, tended to die on day four. This again suggested that the high infectious dose might be overwhelming any attenuation caused by the usher deletions.

For the intranasal infections at the lower dose of 4 to 5 LD_{50} (2,000-2,500 CFU), three of the single usher deletion mutants had significant shifts in their mouse survival curves compared to the parental KIM5+ strain. Deletion of ushers y*0350* or y*1858* caused small, yet significant ($P = 0.0137$), attenuation in *Y. pestis* virulence, with a higher percentage of mice surviving past day three post infection (Figure 3.17). For the y*1858* usher deletion mutant, 7% (1 out of 15) of the mice survived the entire 21-day course of the infection. Most significantly ($P = 0.0006$), infection with usher deletion mutant *y1871* resulted in 13% (2 out of 15) of the mice surviving the course of the infection and an increase in the mean time of death to four days, as compared to three days for mice infected with wild type KIM5+ (Figure 3.17). Mice infected with the other usher deletion mutants all succumbed to infection with a mean time to death of three days and had survival curves similar to infection with the wild type strain. I conclude from these findings that chaperone/usher pathways with ushers *y0350, y1858*, and *y1871* function within the host and contribute to the virulence of *Y. pestis* during pneumonic plague.

Discussion

Chaperone/usher pathways have been shown to form structures on the surface of Gram-negative bacteria that can contribute to the virulence of many species [87, 155]. In bacteria such as *E. coli* or *Salmonella*, pili formed via the chaperone/usher pathways contribute to adherence to specific cell types, which can aid in the virulence of these bacteria [87, 114, 142, 143]. The *Y. pestis* genome encodes 11 chaperone/usher gene clusters [9, 10]. Two of these pathways, the *caf* and *psa* operons, have been shown to contribute to the ability of *Y. pestis* to escape phagocytosis by immune cells and to bind to host cells in the case of the *psa* operon [29-31, 145]. It was not known what role each of the additional chaperone/usher pathways of *Y. pestis* might play in biofilm formation, autoaggregation, adhesion to or invasion of host cells, or virulence via natural routes of infection.

Using a collection of six usher deletion mutants, I found no evidence for roles of individual chaperone/usher pathways in biofilm formation at either 28^{o}C or 37^{o}C when compared to the parental KIM6+ strain. The Krukonis group showed that expression of pathways *y0348-0352*, *y0561-0563*, *y1858-1862* and *y3478-3480* enhanced biofilm formation by *E. coli*. However, when deletion mutations of the chaperone/usher pathways were constructed in the *Y. pestis* KIM5 strain, only loss of the *psa* locus, coding for the pH 6 antigen, resulted in decreased biofilm formation [83]. This indicates that the chaperone/usher pathways are capable of contributing to biofilm formation but are overshadowed by other factors in *Y. pestis.* The lack of biofilm phenotypes is consistent with the known role of the *hms* system as the major biofilm-forming pathway of *Y. pestis* [147, 156]. It is important to take from these experiments that results gained from

exogenous expression of the chaperone/usher pathways of *Y. pestis* in a non-natural setting, specifically a non-fimbriated *E. coli* strain, may not correlate to loss of function in *Y. pestis.*

Deletion of the ushers from any of the six chaperone/usher pathways did not reduce the ability of *Y. pestis* to autoaggregate at 28^{o}C. Felek *et al.* showed that *pgmA* is a critical gene for autoaggregation at 28^{o}C [149]. None of the strains exhibited autoaggregation when grown at 37^{o}C. Most likely, the lack of autoaggregation at this temperature is due to an anti-adhesive factor, such as the F1 antigen, being expressed at 37^{o}C. The F1 capsule significantly decreases the ability of the bacteria to aggregate, possibly by masking self-adhesive structures. Taken together, these studies indicate that under the conditions tested, none of the six chaperone/usher pathways of *Y. pestis* are required for biofilm formation or autoaggregation.

To explore the role that the six chaperone/usher pathways may play in adhesion to and invasion of host cells, I first studied interactions with immortalized human epithelial cell lines A549 and HEp-2. I felt these cell lines were important because epithelial cells could be one of the first cell types encountered, especially lung epithelial cells, if there was an intentional release of the bacteria. I found that when ushers *y0350* or *y1858* were deleted, there was a 2-3-fold reduction in binding to these epithelial cells compared to the KIM6+ wild type strain. This phenotype was fully complemented upon expression of the deleted usher from a plasmid, proving that the defect in adhesion was specifically due to the loss of the usher. These results identify at least two chaperone/usher pathways of *Y. pestis* that contribute to the ability of the bacteria to adhere to host cells, presumably through the formation of adhesive pili.

I next focused on the interactions of *Y. pestis* with primary macrophages, both muBMDM and huMDM. Macrophages have a naturally high rate of phagocytosis, and after 20 minutes over 80% of the bacteria were internalized. To study only adhesion, cells were pre-treated with cytochalasin D. An interesting finding came out of these studies; not only were there fewer bacteria adhered to host cells when genes encoding ushers *y0350* or *y1858* were deleted, but now when the gene encoding usher *y1871* was deleted there was also a 2-3-fold reduction in the amount of adhered bacteria. This indicated that the pili formed by the chaperone/usher pathway using usher *y1871* bound a macrophage specific protein or carbohydrate moiety that was present on both mouse and human derived macrophages.

In contrast to our results, Felek *et al.* did not detect any loss in binding to host cells for *Y. pestis* KIM5 strains containing deletions of the same chaperone/usher pathways [83]. Although both studies examined binding to HEp-2 epithelial cells and macrophages, the prior study did not examine binding to A549 cells and used macrophage-like cell lines (RAW264.2 and THP-1) rather than primary macrophages. In addition, Felek *et al.* used MOI of 1-3 and measured binding by a CFU plating assay, as opposed to the MOI of 50 and microscopy-based method used here. We have found the microscopy-based assay to be more sensitive and reproducible for detecting differences in bacterial association with host cells, for example, by comparing the results of A549 adhesion using the CFU method vs. direct microscopy. Use of the microscopy method, combined with the higher MOI, may have allowed us to detect the two-to-three-fold changes in binding observed for our *Y. pestis* chaperone/usher pathway mutants. Finally, the KIM5 strain used by Felek *et al.* contains the pCD1 virulence plasmid, and it is

possible that engagement of host cells by the T3SS apparatus may have masked binding defects caused by loss of the chaperone/usher pathways.

Lastly, I wanted to determine what role each of the chaperone/usher pathways might be playing during a natural infection, either via the bubonic or pneumonic route. Analysis of single usher deletion mutants in the fully virulent KIM5+ background identified chaperone/usher pathways with ushers *y0350*, *y1858*, and *y1871* as contributing to the virulence of *Y. pestis* in mice via the intranasal, but not subcutaneous, route of infection. In agreement with my findings, Felek and colleagues previously identified chaperone/usher locus *y1858-1862* as contributing to the virulence of *Y. pestis* in mice infected by the intravenous route [83]. This suggests that pili assembled by pathway *y1858-1862* may be important for host interactions during the systemic phase of infection. However, the Δ*y1858* usher deletion mutant was attenuated by the pneumonic, but not bubonic routes, arguing for another role for pathway *y1858-1862*. Future studies will need to address the specific host receptors recognized by the *y1858-1862* pili, as well as the other *Y. pestis* chaperone/usher pili, and determine at what points in the infectious process these pili function. In contrast to our findings, Felek *et al*. did not identify roles for chaperone/usher pathways y*0348-0352* or y*1869-1873* in virulence [83]. There are several differences between the studies that may explain these results, including that the previous study used the attenuated KIM5 (*pgm*$^{-}$) strain of *Y. pestis* and only examined the intravenous route of infection in Swiss-Weber mice, where my studies used the fully virulent KIM5+ background, and C57BL/6 mice were infected by subcutaneous and intranasal routes that more closely mimicked natural infection.

The overall results from this panel of six single usher deletion mutants begin to shed light on the role that the pili of *Y. pestis* may be playing during pathogenesis. The results suggest that at least three of the *Y. pestis* chaperone/usher pathways, other than the F1 capsule and pH 6 antigen, are virulence factors of *Y. pestis*. Pathways *y0348-y0352*, *y1858-y1862*, and *y1869-y1873* contribute to adhesion to different types of host cells, as well as play roles in virulence via the pneumonic route. The correlation between the chaperone/usher pathways identified as important for binding to host cells and those found to contribute to virulence in mice strongly supports roles for these three chaperone/usher pathways in interactions with host cells during pathogenesis. The decreased binding to host cells for the Δ*y0350*, Δ*y1858* and Δ*y1871* usher deletion mutants compared to WT *Y. pestis* was significant but modest (three-fold at most). The *in vivo* attenuation in virulence for these usher deletion strains was also relatively small; the Δ*y1871* strain had the strongest phenotype, with a one-day increase in mean time to death and 13% of mice surviving the course of the infection. These results likely reflect redundancy among the multiple chaperone/usher pathways and other adhesins expressed by *Y. pestis*. Studies on the functions of multiple chaperone/usher pathways present in the genomes of other bacterial pathogens have also found redundancy and have documented cross-talk among the various pathways, such that loss of one pathway may be compensated for by expression of another [115, 142, 157]. Thus, it may be necessary to delete multiple chaperone/usher pathways to obtain a strong virulence phenotype and reveal the critical functions of the encoded pili during pathogenesis [142, 157].

Acknowledgements

I would like to thank Lisa Runco for starting this work and constructing the single usher deletions in the KIM6+ strains, and Celine Pujol for converting the KIM6+ usher deletion strains into the fully virulent KIM5+ strains. I would also like to thank Susan van Horn for help with the electron microscopy, Steven Park at PHRI in New Jersey for performing the mouse infections, Indra Jayatilaka for obtaining huMDM, and Galina Romanov for providing the muBMDM.

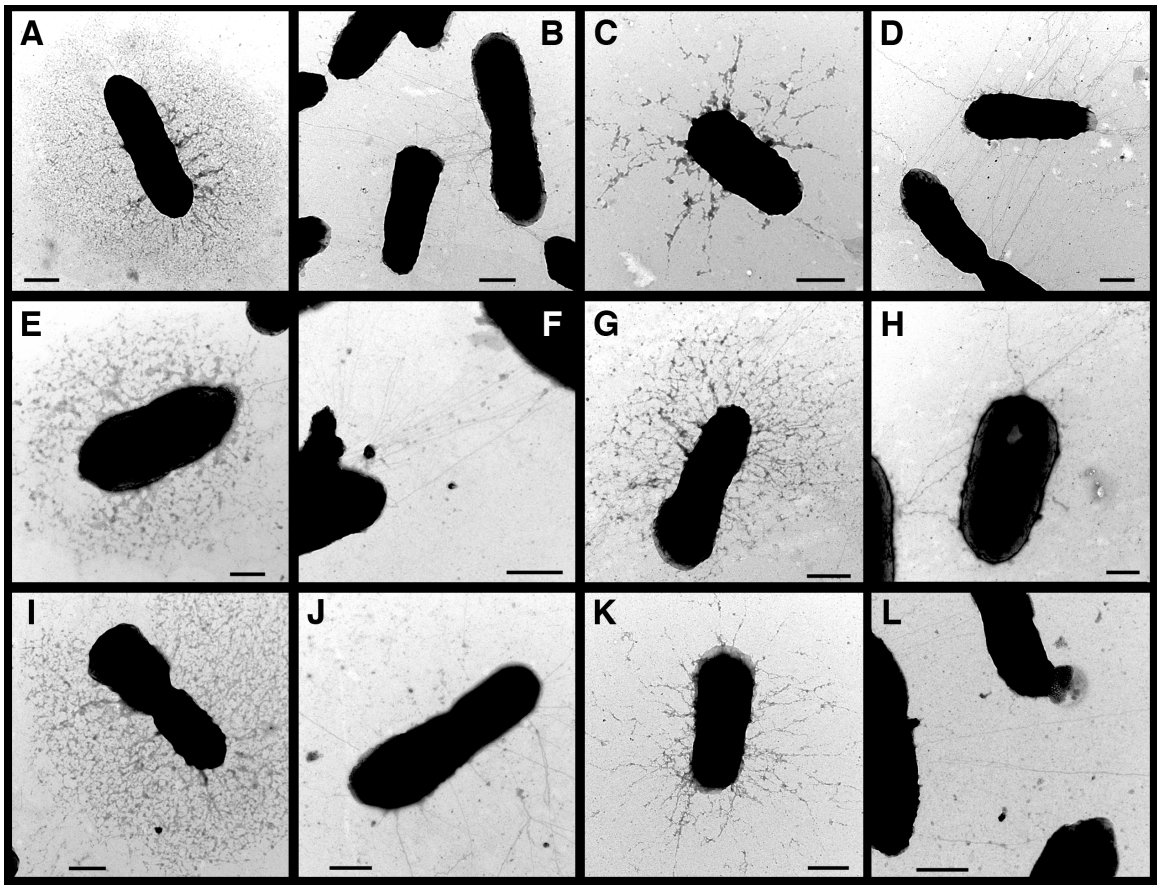

Figure 3.1: Whole bacteria negative stain transmission electron microscopy of *Y. pestis* usher deletion mutants. Whole bacteria, negative-stain TEM of *Y. pestis* usher deletion mutants in chaperone/usher pathways (Runco and Thanassi, unpublished data). (A and B) KIM6+ Δ*y0350*; (C and D); KIM6+ Δ*y0562*; (E and F) KIM6+ Δ*y1858*; (G and H) KIM6+ Δ*y1871*; (I and J) KIM6+ Δ*y2390*; (K and L) KIM6+ Δ*y3480*. Bar equals 500 nm.

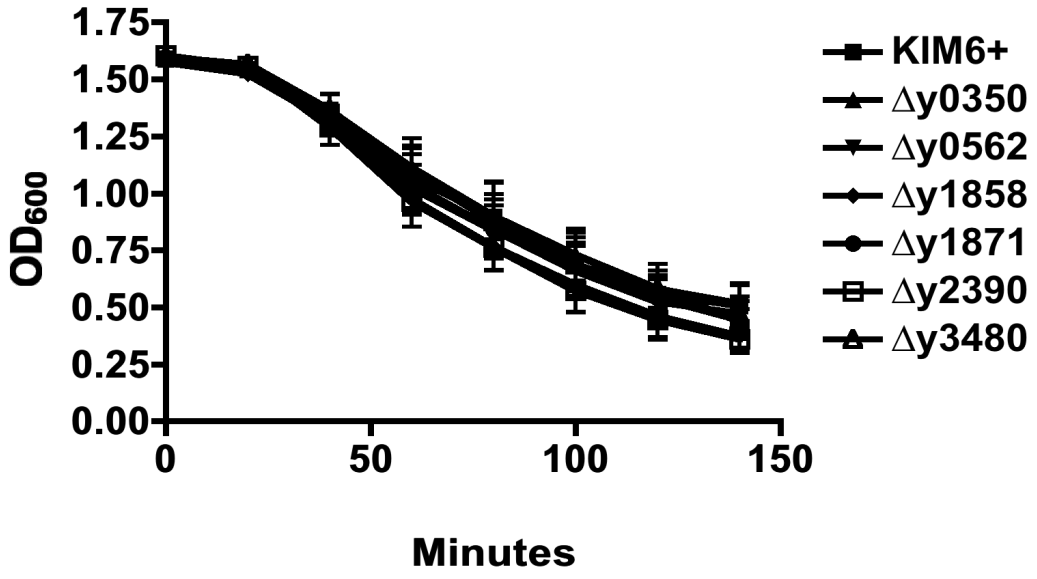

Figure 3.2: Autoaggregation of *Y. pestis* usher deletion mutants at 28°C. *Y. pestis* strain KIM6+ or usher deletion mutants were grown in HIB and incubated statically at 28°C in 1.5 mL plastic cuvettes for 140 minutes. The OD_{600} of the cultures were then read every 20 minutes. No significant difference was seen between the wild type KIM6+ and any usher deletion mutant. Three independent experiments were done in triplicate and analyzed by ANOVA using GraphPad Prism. Bars represent means ± SEM.

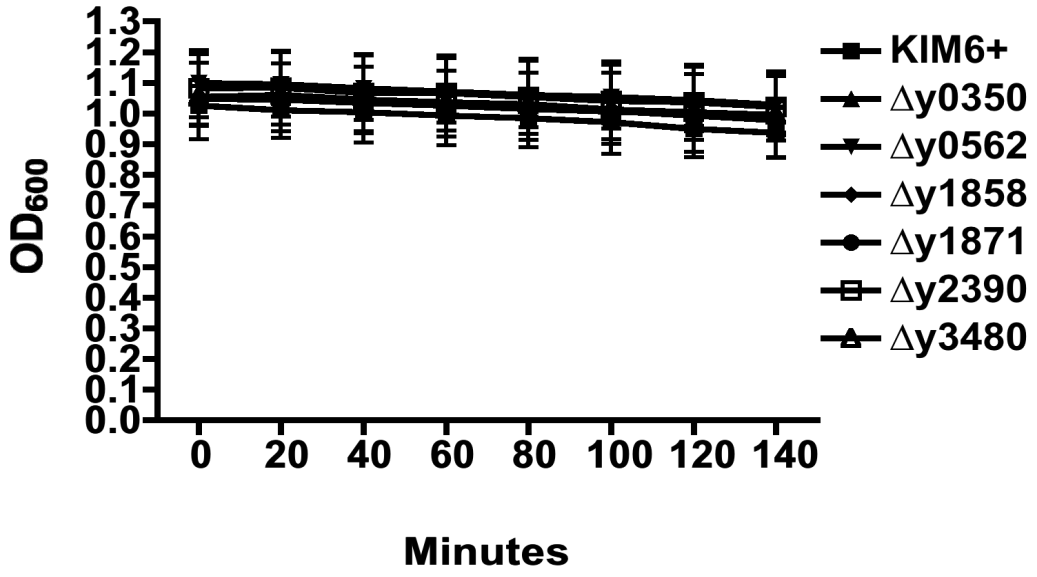

Figure 3.3: Autoaggregation of *Y. pestis* usher deletion mutants at 37°C. *Y. pestis* strain KIM6+ or usher deletion mutants were grown in HIB and incubated statically at 37°C in 1.5 mL plastic cuvettes for 140 minutes. The OD_{600} of the cultures were then read every 20 minutes. No significant difference was seen between the wild type KIM6+ and any usher deletion mutant. Three independent experiments were done in triplicate and analyzed by ANOVA using GraphPad Prism. Bars represent means ± SEM.

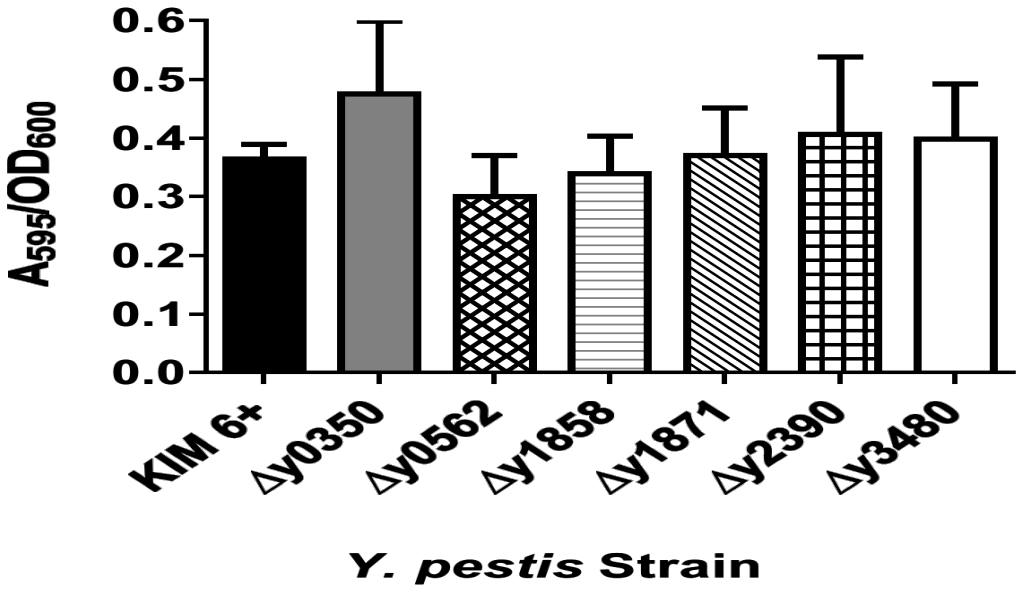

Figure 3.4: Biofilm formation by *Y. pestis* usher deletion mutants at 28°C. *Y. pestis* strain KIM6+ or usher deletion mutants were grown in HIB and then incubated statically at 28°C in 96-well flat bottom plates for 24 hours. Biofilm formation was determined by crystal violet staining. No significant difference was seen between the wild type KIM6+ and any usher deletion mutant. Three independent experiments were done in triplicate and analyzed by ANOVA using GraphPad Prism. Bars represent means ± SEM.

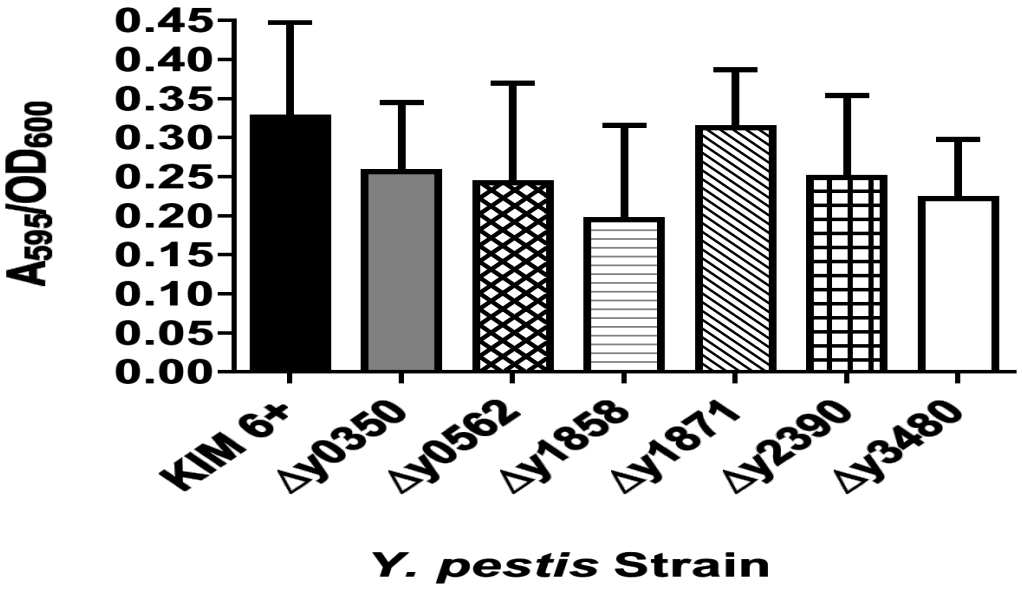

Figure 3.5: Biofilm formation by *Y. pestis* usher deletion mutants at 37°C. *Y. pestis* strain KIM6+ or usher deletion mutants were grown in HIB and then incubated statically at 37°C in 96-well flat bottom plates for 24 hours. Biofilm formation was determined by crystal violet staining. No significant difference was seen between the wild type KIM6+ and any usher deletion mutant. Three independent experiments were done in triplicate and analyzed by ANOVA using GraphPad Prism. Bars represent means ± SEM.

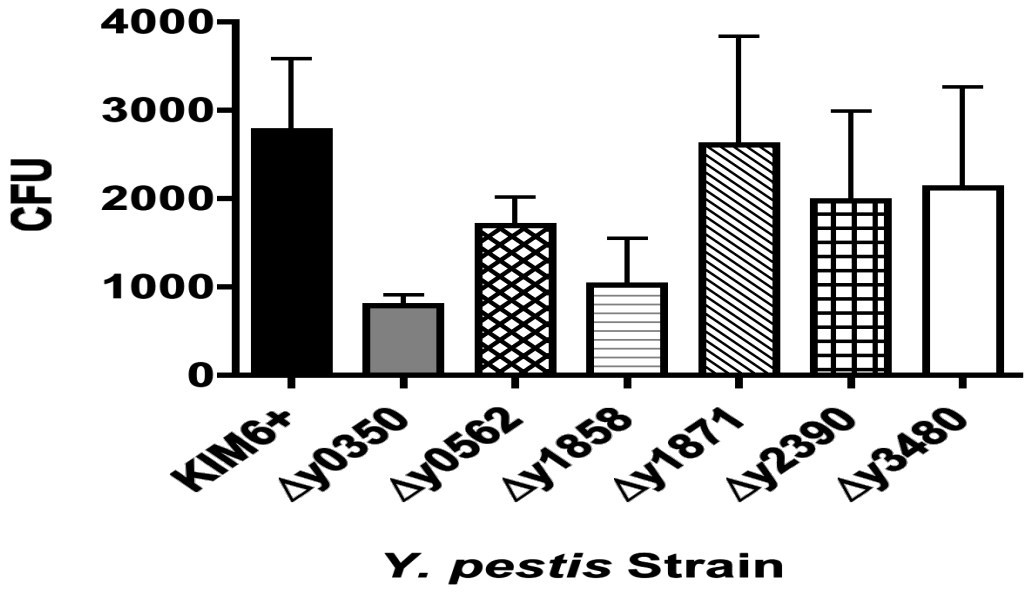

Figure 3.6: Binding of KIM6+ usher deletion mutants to A549 cells determined by colony forming unit assay. A549 cells were infected with *Y. pestis* wild type or single usher deletion mutants grown at 37^{o}C at an MOI of 50 for 2 hours. At that time point the cells were lysed, and bacteria were plated for CFU. No significant difference was seen between the wild type KIM6+ and any usher deletion mutant. Three independent experiments were done in triplicate and analyzed by ANOVA using GraphPad Prism. Bars represent means ± SEM.

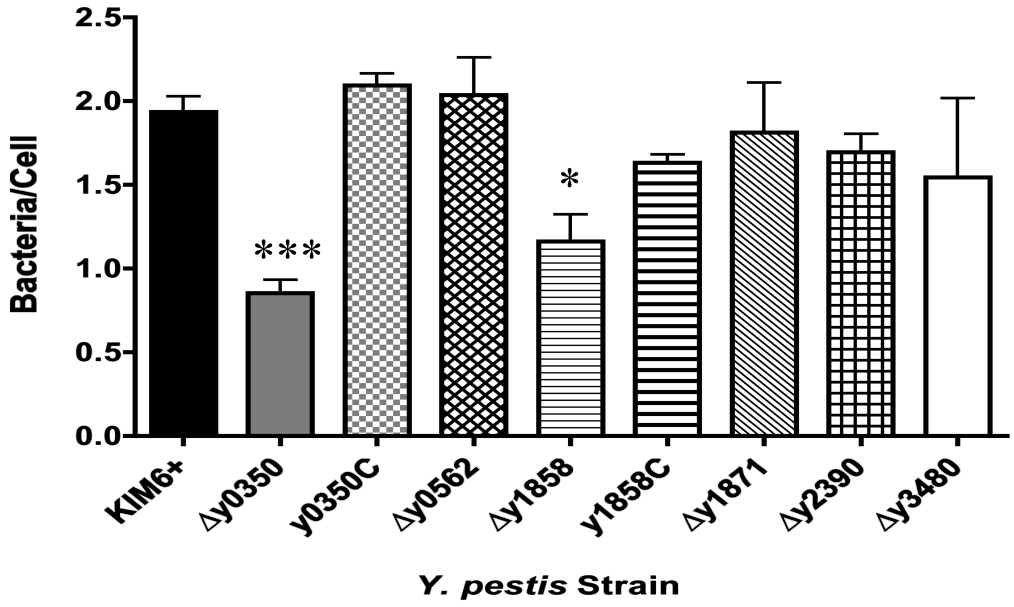

Figure 3.7: Binding of *Y. pestis* usher deletion mutants to A549 cells. A549 cells were infected with KIM6+ wild type, usher deletion mutants, or complemented strains (denoted with a "C") at an MOI of 50 for 2 h. Cells were then fixed and stained with a rabbit anti-*Yersinia* primary antibody and a goat anti-rabbit secondary antibody conjugated to AlexaFluor594 (red). For each infection, phase-contrast and epifluorescence images from 10 random fields with approximately 150-200 cells per field were captured using a 40X objective, and the average number of bacteria/cell was calculated. Results (bacteria/cell) were calculated from three independent experiments with three replicates per experiment analyzed by ANOVA using GraphPad Prism. Bars represent means ± standard errors of the mean (SEM); *P < 0.05 and ***P < 0.001 for comparison of each strain with wild type.

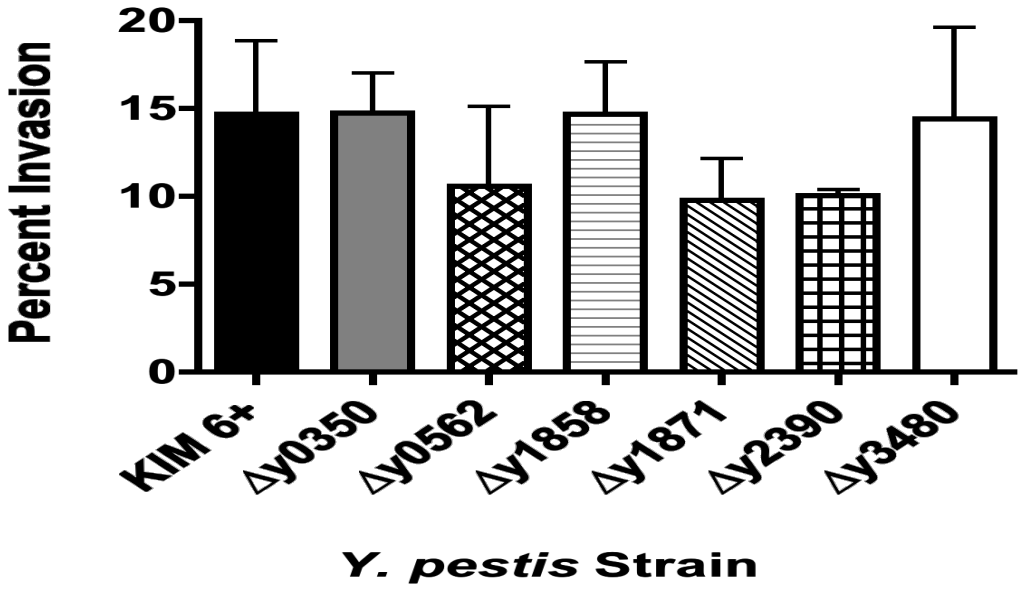

Figure 3.8: Invasion of *Y. pestis* usher deletion mutants to HEp-2 cells. HEp-2 cells were infected with *Y. pestis* wild type or usher deletion mutants expressing GFP at an MOI of 50 for 2 hours. Cells were then fixed and stained. Rabbit anti-*Yersinia* primary antibody and goat anti-rabbit secondary antibody conjugated to AlexaFluor594 (red) were used for staining. Results (percent invasion) were calculated by percent of green (internal) bacteria divided by both green and red (total) bacteria from three independent experiments with triplicate wells per experiment and analyzed by ANOVA using GraphPad Prism. Bars represent means ± SEM. No significant difference was seen between the wild type KIM6+ and any usher deletion mutant.

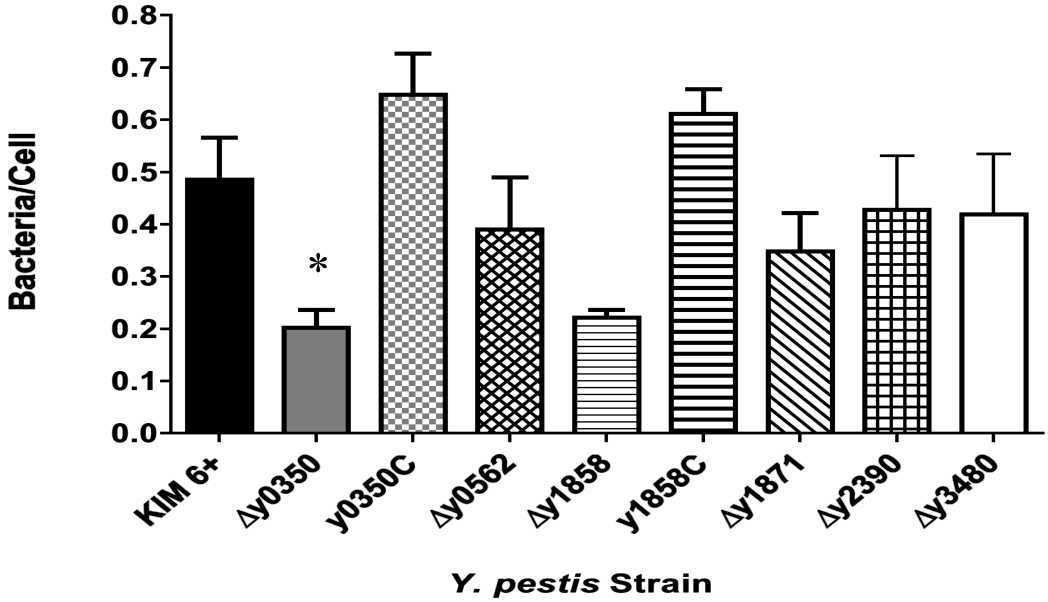

Figure 3.9: Binding of *Y. pestis* usher deletion mutants to HEp-2 cells. HEp-2 cells were infected with KIM6+ wild type, usher deletion mutants, or complemented strains as described in Figure 3.7. Results (bacteria/cell) were calculated from three independent experiments with three replicates per experiment and analyzed by ANOVA using GraphPad Prism. Bars represent means ± SEM; *P < 0.05 for comparison of each strain with wild type.

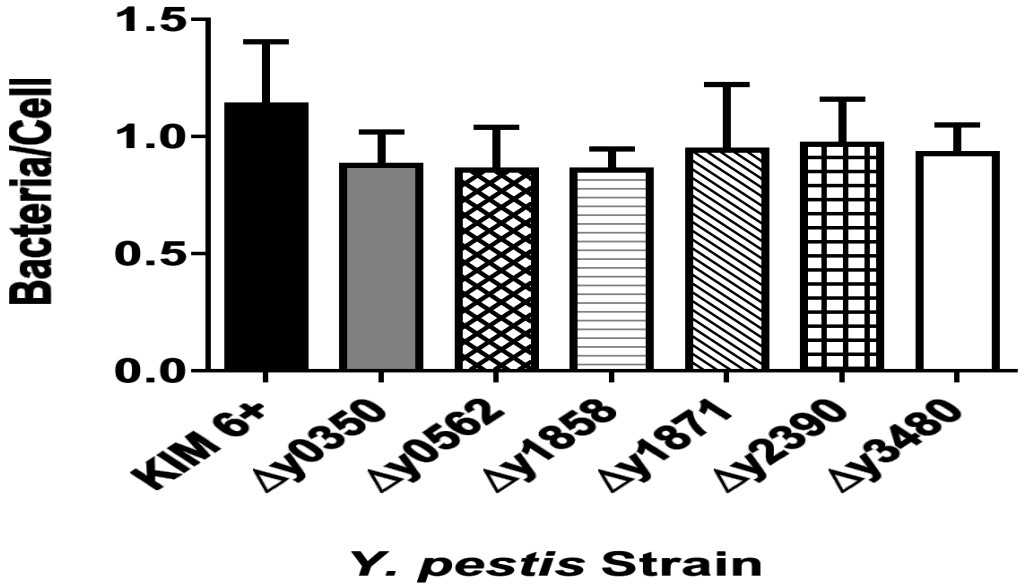

Figure 3.10: Association of *Y. pestis* usher deletion mutants with murine bone marrow derived macrophages. MuBMDM were infected with KIM6+ wild type or usher deletion mutants as described in Figure 3.7. Results (bacteria/cell) were calculated from three independent experiments with three replicates per experiment and analyzed by ANOVA using GraphPad Prism. Bars represent means ± SEM. No significant difference was seen between the wild type KIM6+ and any usher deletion mutant

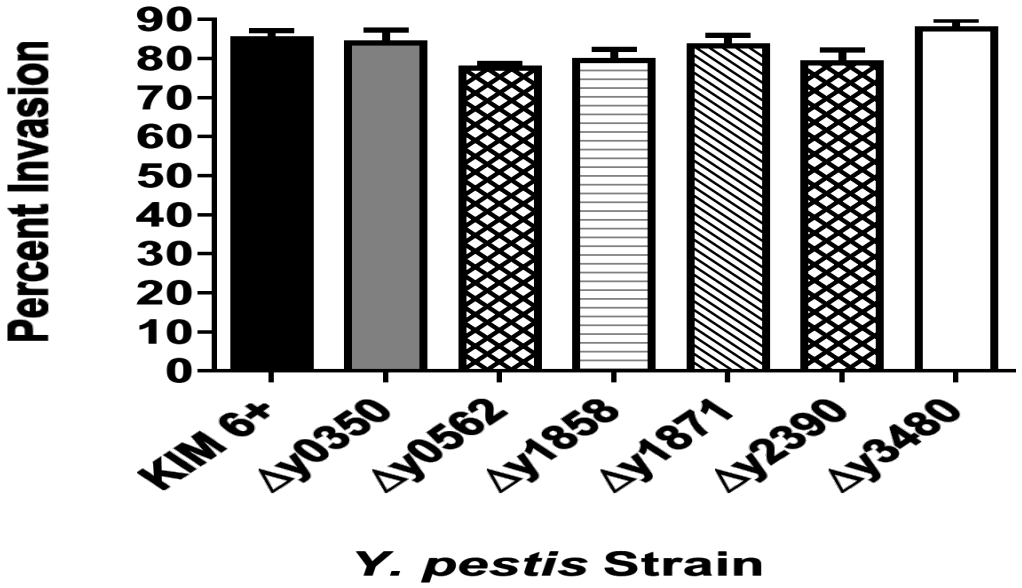

Figure 3.11: Invasion of *Y. pestis* usher deletion mutants into murine bone marrow derived macrophages. MuBMDM were infected with *Y. pestis* wild type or usher deletion mutants expressing GFP at an MOI of 10 for 20 minutes. Cells were then fixed and stained. Rabbit anti-*Yersinia* primary antibody and goat anti-rabbit secondary antibody conjugated to AlexaFluor594 (red) were used for staining. Results (percent invasion) were calculated by percent of green (internal) bacteria divided by both green and red (total) bacteria from three independent experiments with triplicate wells per experiment and analyzed by ANOVA using GraphPad Prism. Bars represent means ± SEM. No significant difference was seen between the wild type KIM6+ and any usher deletion mutant

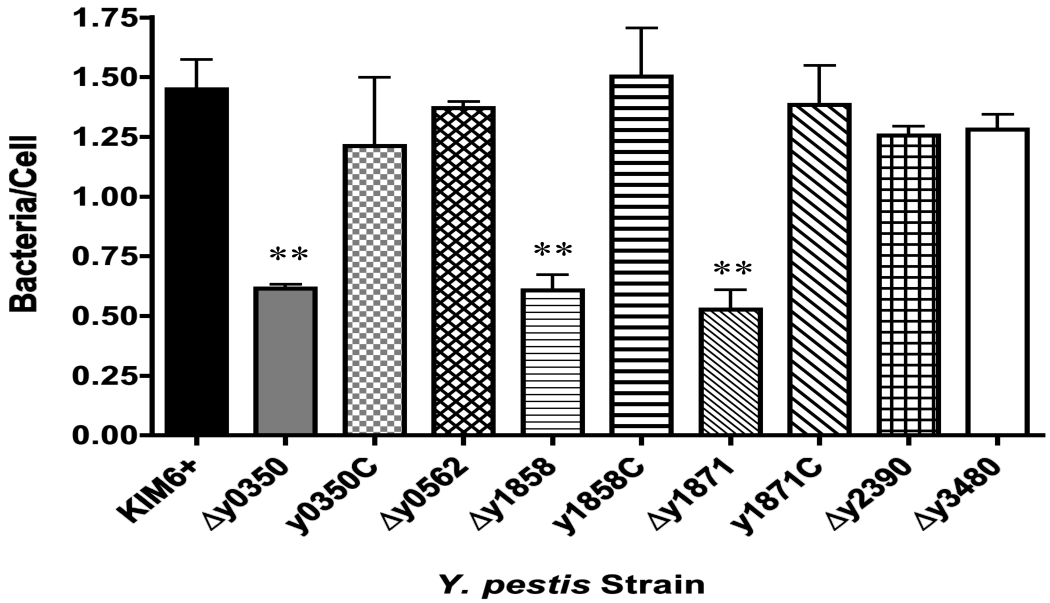

Figure 3.12: Binding of *Y. pestis* usher deletion mutants to murine bone marrow-derived macrophages. MuBMDM were treated with 5 µg/mL Cytochalasin D for 1 hour, then infected with KIM6+ wild type, usher deletion mutants, or complemented strains as described in Figure 3.7. Results (bacteria/cell) were calculated from three independent experiments with three replicates per experiment and analyzed by ANOVA using GraphPad Prism. Bars represent means ± SEM; **P < 0.01 for comparison of each strain with wild type.

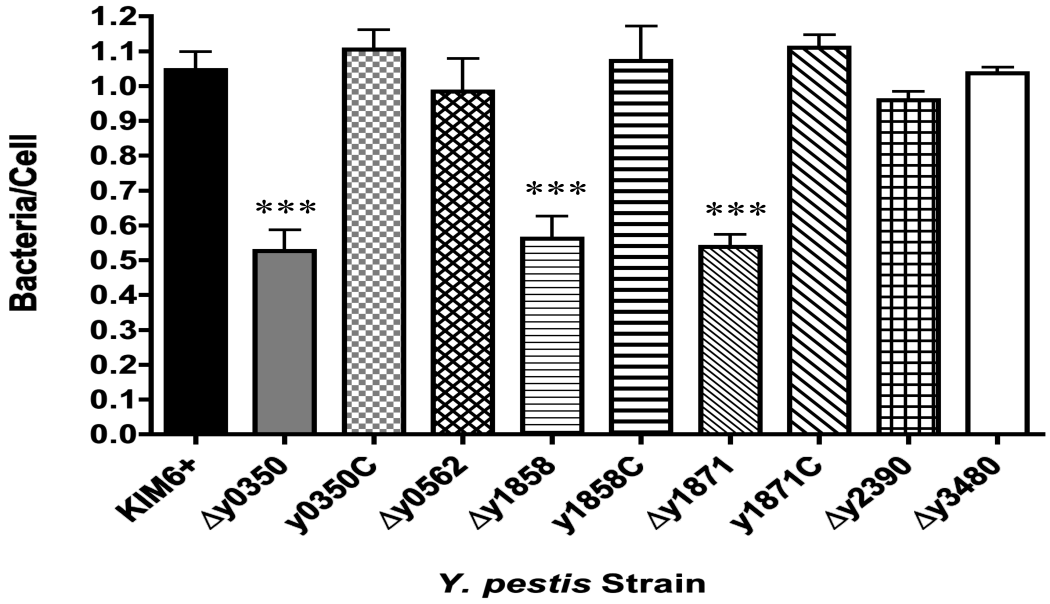

Figure 3.13: Binding of *Y. pestis* usher deletion mutants to human monocyte derived macrophages. HuMDM were treated with 5 μg/mL Cytochalasin D for 1 hour, then infected with KIM6+ wild type, usher deletion mutants, or complemented strains as described in Figure 3.7. Results (bacteria/cell) were calculated from three independent experiments with three replicates per experiment and analyzed by ANOVA using GraphPad Prism. Bars represent means ± SEM; ***P < 0.001 for comparison of each strain with wild type.

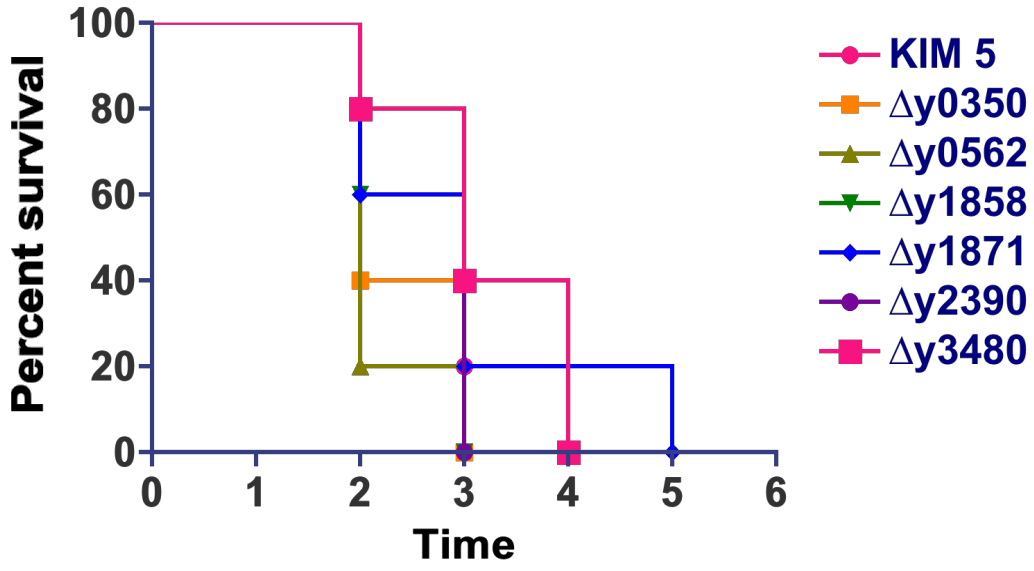

Figure 3.14: Subcutaneous infection of C57BL/6 mice with a high dose of *Y. pestis* usher deletion mutants. Mice were infected with wild type KIM5+ or usher deletion mutants via the subcutaneous route with 10 LD_{50} (500 CFU), and time to death was recorded. Mice were monitored for signs of illness or death for 21 days or until death. This graph represents the data from one experiment with 5 mice per group. There were no significant differences for any of the deletion mutants compared to the wild type strain.

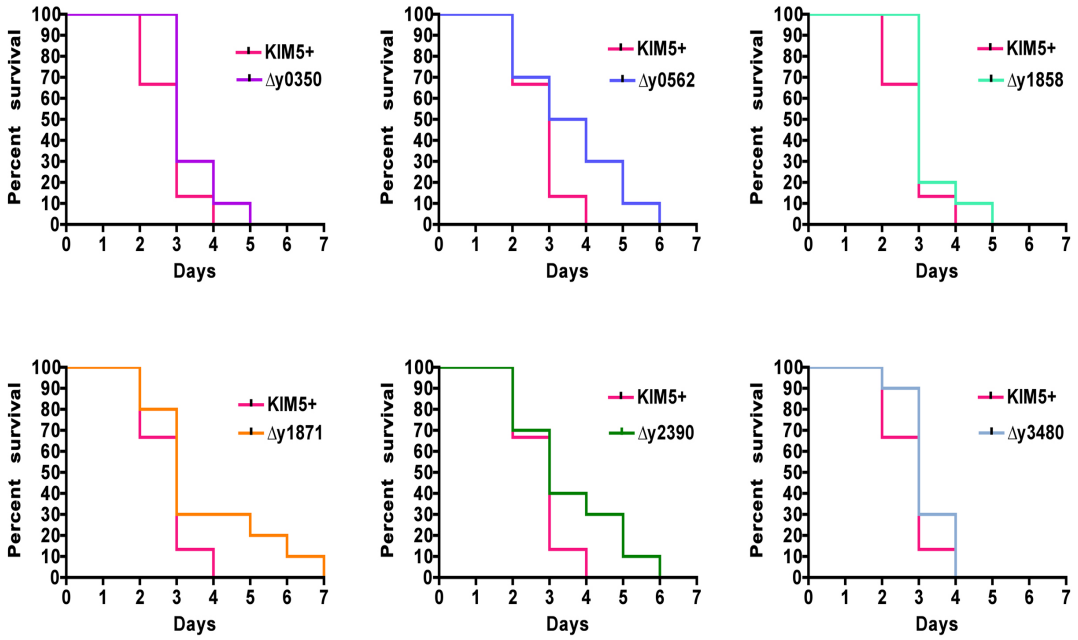

Figure 3.15: Subcutaneous infection of C57BL/6 mice with a low dose of *Y. pestis* usher deletion mutants. Mice were infected with wild type KIM5+ or usher deletion mutants via the subcutaneous route with 4-5 LD_{50} (200-250 CFU), and time to death was recorded. Mice were monitored for signs of illness or death for 21 days or until death. Each graph represents the combined data from three separate experiments with 5 mice each for a total of 15 mice per strain. There were no significant differences for any of the deletion mutants compared to the wild type strain.

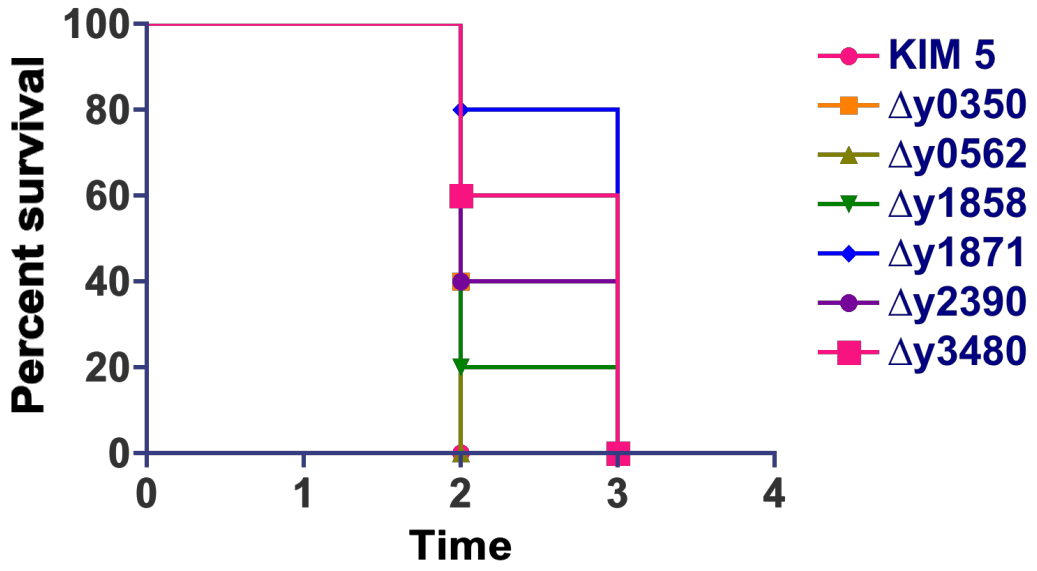

Figure 3.16: Intranasal infection of C57BL/6 mice with a high dose of *Y. pestis* usher deletion mutants. Mice were infected with wild type KIM5+ or usher deletion mutants via the intranasal route with 10 LD_{50} (5,000 CFU) and time to death was recorded. Mice were monitored for signs of illness or death for 21 days or until death. This graph represents the data from one experiment with 5 mice per group. There were no significant differences for any of the deletion mutants compared to the wild type strain.

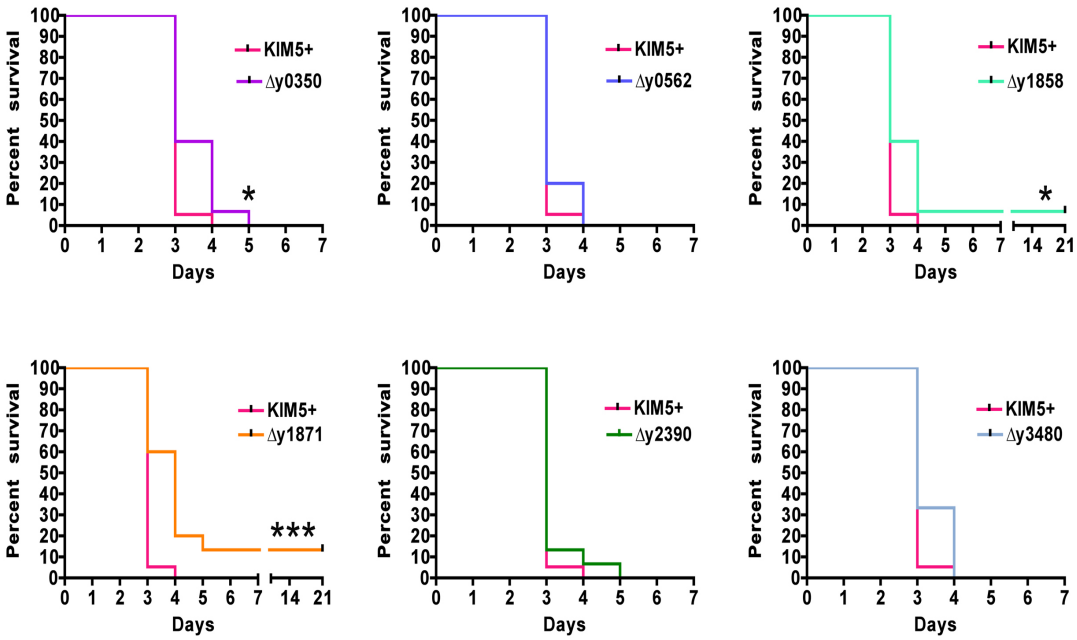

Figure 3.17. Intranasal infection of C57BL/6 mice with a low dose of *Y. pestis* usher deletion mutants. Mice were infected with wild type KIM5+ or usher deletion mutants via the intranasal route with 4-5 LD_{50} (2000-2500 CFU), and time to death was recorded. Mice were monitored for signs of illness or death for 21 days or until death. Each graph represents the combined data from three separate experiments with 5 mice each for a total of 15 mice per strain. Mice infected with deletion mutants Δ*y0350*, Δ*y1858*, or Δ*y1871* were significantly attenuated (*P < 0.05; ***P < 0.001) compared to mice infected with the wild type strain.

Chapter 4: Construction and *in vitro* Analysis of a Complete Knockout Library of the Chaperone/Usher Pathways of *Yersinia pestis*

Abstract

All previous studies done by myself and others on the novel chaperone/usher pathways of *Y. pestis* have focused either on a subset of the pathways or deletion mutants that did not encompass an entire pathway [10, 83, 116]. Therefore, I constructed a complete library of full chaperone/usher pathway deletion mutants of all nine novel pathways. These mutants were examined for the ability to form pili on the bacterial surface, biofilm formation, autoaggregation, and binding to multiple host cell types. These studies recapitulated findings with the single usher deletion mutants, and identified an additional, previously unstudied pathway that plays a role in adhesion to host cells. I also began experiments to determine the nature of the virulence attenuation of the chaperone/usher deletion mutants. Finally, I began creating multiple-pathway deletion mutants by sequentially deleting chaperone/usher pathways in a single *Y. pestis* strain.

Introduction

Upon an initial examination of the genome of *Y. pestis* there appeared to be eight total and six functional chaperone/usher pathways, not including the *caf* or *psa* pathways [9, 10]. The usher genes of two of the *Y. pestis* CU pathways (*y1539-1544* and *y4060-y4063*) are disrupted by an insertion sequence or premature stop codon, and thus these pathways were not expected to be functional (Figure 1.3). However, it was found through expression and microarray analysis that those two pathways might in fact be active and producing proteins [158, 159]. In addition, *Y. pestis* also contains a ninth chaperone/usher pathway, *y0429-y0433*, that belongs to the alternative chaperone/usher subfamily, which was originally thought to be a distinct system [160]. Therefore, to obtain a complete picture of the *Y. pestis* chaperone/usher pathways, I created a library of nine full pathway chaperone/usher mutants using a suicide vector system [122]. Studies on the functions of multiple chaperone/usher pathways present in the genomes of other bacterial pathogens have also found redundancy and have documented cross-talk among the various pathways, such that loss of one pathway may be compensated for by expression of another [115, 142, 157]. By creating full pathway unmarked deletions I not only eliminated the concern of cross-talk or cross-regulation between pathways, but it allowed me to make multiple pathway deletions in a single strain. Using this set of mutants, I also wanted to explore the possibility that deletion of a chaperone/usher pathway could affect the ability of *Y. pestis* to deliver Yops into host cells or trigger an altered cytokine response from macrophages. Either an impaired ability to deliver Yops or an altered cytokine response could hint at a possible mechanism of attenuation that was observed when mice were infected intranasally with usher deletions Δ*y0350,* Δ*y1858,* or Δ*y1871*.

Results

Construction, growth analysis, and assessment of pilus formation of full pathway deletion mutants

A new library of chaperone/usher mutants was constructed using a well established suicide vector system [122]. By using allelic exchange, entire pilus operons were deleted as described in Chapter 2 (Figure 2.1). The new panel of mutants was first checked for growth at both 28^{o}C and 37^{o}C in HIB to ensure that there were no secondary growth defects when these chaperone/usher pathway mutants were constructed. All mutants had growth kinetics similar to the wild type KIM6+ strain at both temperatures (data not shown). I next examined the panel of complete deletion mutants for expression of pili on the bacterial surface using transmission electron microscopy. All of the deletion mutants still expressed pili on their surface (Figure 4.1). Thus, as for the single usher deletion strains, no single chaperone/usher pathway is responsible for the expression of the *Y. pestis* pilus-like fibers.

The chaperone/usher pathways of Y. pestis do not contribute to biofilm formation or autoaggregation

Biofilms, as discussed before, are biologically important structures that help *Y. pestis* disseminate from the flea and can protect subpopulations of bacteria from antibiotics and antimicrobial peptides [146, 150, 151]. In *Y. pestis,* the exopolysaccharide controlled by the *hms* gene cluster and possibly regulated by *hfq* is important for biofilm formation [147, 156, 161]. This does not rule out the possibility that one of the nine

chaperone/usher pathways may play a small role in biofilm formation, as when they are expressed in *E. coli* they confer the ability to form biofilms [83]. Biofilm formation at both 28°C and 37°C for the wild type KIM6+ and all nine full pathway deletion mutants was assayed. The levels of biofilm formation at 28°C between the wild type and all the mutants were statistically similar, indicating that at this temperature none of the nine pathways plays an important role this process (Figure 4.2). This trend continued at 37°C, where each full pathway deletion mutant had statistically similar levels of biofilm formation as the KIM6+ parental strain (Figure 4.3).

Next, I assessed the ability of the full pathway deletion mutants to autoaggregate at both 28°C and 37°C. As for the single usher deletion mutants, at 28°C I found that all the full pathway mutants aggregated at a similar rate compared to the KIM6+ parental strain (Figure 4.4), and at 37°C there was much less aggregation compared to 28°C (Figure 4.5). Taken together, these studies confirm that none of the *Y. pestis* chaperone/usher pathways are required for biofilm formation or autoaggregation, at least under the conditions tested.

Four chaperone/usher pathways contribute to adherence to multiple cell types

The ability to adhere to host cells is critical for bacteria to gain a hold within the host and then cause disease [152]. Therefore, I was most interested in confirming my previous findings and determining whether any of the additional chaperone/usher pathways aided in cell adherence. With these questions in mind, I went on to repeat the cell culture work that was done with the single usher deletion mutants to determine the complete role of the pili of chaperone/usher pathways with respect to host cell adhesion.

I first examined binding to A549 human lung epithelial cells. Surprisingly, there were no statistically significant differences in adherence between any of the nine full pathway mutants and the parental KIM6+ strain (Figure 4.6). However, there was still a trend towards reduced binding, by about one-third, when pathways *y0348-y0352* or *y1858-y1862* were deleted compared to the parental strain. These are the same two pathways that had decreased binding for the single usher deletion mutants (Figure 3.7). Both mutants had approximately 1 bacterium per cell, whereas the wild type and all other seven strains had slightly more than 1.5 bacteria per cell on average. This difference lies just out of the range of statistical significance, with P values around 0.055.

Using HEp-2 cells, I found that not only were there significantly fewer bacteria bound when pathway *y0348-y0352* or *y1858-y1862* was knocked out, but when the previously unstudied pathway *y4060-y4063* was deleted, there were also fewer bacteria per cell (Figure 4.7). When pathways *y0348-y0352* or *y1858-y1862* were knocked out, there was a 2-fold reduction in binding that was highly significant with a P value of less than 0.001. These results closely mimicked the results with the single usher deletion mutants. The *y0348-y0352* and *y1858-y1862* mutants had approximately 0.5 bacteria per cell as compared to 1 bacterium per cell with the parental strain. Most interestingly, when pathway *y4060-y4063* was deleted, there was approximately 25% reduction in bacterial adherence equating to about 0.75 bacteria per cell. This defect in binding was very significant with a P value of under 0.01. This was a fascinating result, since pathway *y4060-y4063* has a premature stop codon within the usher gene (Figure 1.3). All six other full pathway deletion mutants bound to HEp-2 cells to similar levels as the wild type KIM6+.

Finally, I measured adhesion of the full pathway mutants to muBMDM pretreated with cytochalasin D to block phagocytosis. Under these conditions I saw that, as with the single usher deletion mutants, when pathways *y0348-y0352*, *y1858-y1862*, or *y1869-y1873* were deleted significantly fewer bacteria adhered to the macrophages (Figure 4.8). I also found that significantly fewer bacteria adhered when pathway *y4060-y4063* was knocked out, which recapitulated the effect that was seen in the HEp-2 cells. All four pathways had approximately 0.75-1 bacteria per cell compared to 1.5 bacteria per cell for the parental KIM6+ strain and other five full pathway deletion mutants. This was highly significant for all strains, with a P value under 0.01 for *y0348-y0352* and a P value under 0.001 for pathways *y1858-y1862*, *y1869-y1873*, and *y4060-y4063*.

The lack of any single chaperone/usher pathway does not affect the cytokine response of macrophages in vitro

The innate immune response is critical to protecting the host from a *Y. pestis* infection, because the disease is often fatal before an effective adaptive immune response can be mounted [17, 28]. An effective cytokine response and interactions between bacteria and macrophages are critical in the early stage of disease [17, 162]. I therefore tested if there was any alternation in the host response to *Y. pestis* lacking one of the chaperone/usher pathways.

To first assess the ability of any single pathway to modulate a wide variety of chemokines and cytokines, I used conditioned supernatants from muBMDM infected with either the KIM6+ wild type or one of the following chaperone/usher full pathway deletion mutants: *y0348-y0352*, *y1858-y1862*, or *y1869-1873*. The conditioned

supernatants were analyzed by a membrane-based cytokine array assay that can detect 23 different cytokines. Various differences were seen between the KIM6+ wild type and the mutants, most notably between KIM6+ and the *y1869-y1873* mutant in the ability to elicit IL-9 and IFN-γ secretion (data not shown). To further assess and quantify the possible differences observed on the membrane, I ran ELISAs for IL-9, TNF-α, and IFN-γ.

IL-9 was an intriguing place to start, since it has been implicated in the autoimmune response and as a contributor to asthma and allergic airway inflammation, and the strongest attenuation seen for the chaperone/usher mutants was via the intranasal route [163, 164]. When running the ELISA using conditioned supernatants from the infected muBMDM, I saw very little IL-9 produced by macrophages infected with the wild type KIM6+ or any of the chaperone/usher mutants (Figure 4.9). The levels of this cytokine never exceeded background levels secreted by uninfected cells. Unfortunately, this called into question the results from the membrane assay, since there was a fairly robust response when I used that system.

Both TNF-α and IFN-γ have been shown to be important for host protection against *Y. pestis* infections [165-167]. I ran ELISAs to determine if there was an altered production of either TNF-α or IFN-γ during infection of muBMDM with the wild type KIM6+ compared to the chaperone/usher pathway deletion mutants. Using the same conditioned supernatants that were used in previous experiments, very high levels of TNF-α from all samples were detected, with no differences between the wild type bacteria and any chaperone/usher mutant (Figure 4.10). Macrophages infected with the wild type organism or any of the three full pathway deletion mutants secreted approximately 1,700 pg/mL of TNF-α, which was significantly higher than the

uninfected controls. I saw very low levels of IFN-γ under all conditions despite the fact it was robustly detected in the membrane array, indicating that these muBMDM were either not producing this cytokine, or all strains had the ability to dampen the production of this molecule (Figure 4.11). Taken together, these results did not provide evidence that loss of a chaperone/usher pathway resulted in an altered immune response.

Delivery of Yops is decreased in the absence of pathways y0348-y0352, y1858-y1862 or *y4060-y4063*

Other groups have shown that adhesins such as Ail, Pla, and Psa contribute to the delivery of Yops to host cells, including HEp-2 cells [75, 79, 144]. The inability to efficiently deliver Yops to host cells has been implicated as a mechanism for the attenuation of adhesin mutants *in vivo* [75, 79]. I therefore investigated if any of the chaperone/usher pathways, specifically those that had a defect in binding to host cells, were important for the delivery of Yops to host cells. To do this, the KIM6+ strains of the full pathway deletion mutants were converted into KIM5- strains. First, strains were screened for the naturally occurring excision of the *pgm* locus, and then I added in the pCD1 plasmid for expression of the T3SS and Yops.

I infected HEp-2 cells with the KIM5- strain, a *yopB* deletion mutant which prevents the delivery of Yops to host cells and serves as a control, or mutants in pathways *y0348-y0352*, *y1858-y1862*, *y1869-y1873*, or *y4060-y4063*. Yop delivery was measured by the cytopathic effect on the host cells, defined as a shrinking of the cytoplasm with cell rounding and a darker nuclear staining with Giemsa stain. Using these criteria, after a two hour infection approximately 27% of the cells infected with the wild type KIM5-

showed a cytopathic effect, whereas the *yopB* deletion mutant caused approximately 4% of the cells to show a cytopathic effect above background levels (Figure 4.12). Deletion mutant *y1869-y1873*, which had wild type binding levels to HEp-2 cells, also had levels of Yop delivery similar to the wild type KIM5- strain. Deletion mutant *y4060-y4063*, which had a slight adhesin defect to HEp-2 cells, caused about 22% of the cells to show a cytopathic effect, which is significantly less than the KIM5- strain with a P value less than 0.05. Mutants *y0348-y0352* and *y1858-y1862*, which showed the largest adhesion defect, caused the least cytopathic effects, with only 11% of the cells affected (Figure 4.12). This reduction from wild type delivery levels was highly significant with a P value less than 0.001. These results indicate that the inability to bind efficiently to host cells decreases the ability of *Y. pestis* to deliver Yops effectively into the host cells and may contribute to the attenuation observed for the corresponding usher deletion mutants *in vivo.*

Construction of a multiple pathway deletion mutant

In order to determine whether bacteria that have multiple pathways deleted would bind less efficiently to host cells, and possibly be even further attenuated *in vivo*, I began creating multiple pathway deletion mutants. Starting with pathways that have been implicated in ability to bind to host cells, I iteratively knocked out pathways *y0348-y0352, y1858-y1862* and *y1869-y1873.* Currently, I am creating a quadruple knockout strain which will also have pathway *y4060-y4063* deleted.

Discussion

To obtain a more complete understanding of the functions of the chaperone/usher pathways of *Y. pestis*, I constructed a set of complete pathway deletion mutants for each of the nine chaperone/usher pathways other than the well-studied *caf* and *psa* gene clusters. The ability to make this series of mutants unmarked allowed me to begin constructing multiple pathway deletion mutants, targeting the pathways found to contribute to cell adhesion. Each of the nine chaperone/usher pathway deletion mutants was tested for contribution to a number of virulence associated characteristics. I also wanted to begin to try to determine if a mechanism beyond an inability to adhere contributed to the attenuation observed when mice were infected with the usher deletion mutants.

Biofilm formation, as mentioned before, can allow for efficient transmission from the flea vector by blocking the feeding tract, stimulating repeated feeding [146]. Within the host, bacteria within a biofilm are also protected from antimicrobial peptides and antibiotics [150, 151]. In *Y. pestis,* the mechanism of biofilm formation has been studied extensively, with the *hms* system and associated regulatory factors contributing heavily to biofilm formation [5, 147, 156, 161, 168]. However, it has been shown that when select chaperone/usher pathways are expressed in *E. coli* they can lead to biofilm formation [83]. Unlike what was found in *E. coli*, I observed no role for any of the nine chaperone/usher pathways in biofilm formation by *Y. pestis* at either 28^{o}C or 37^{o}C. This is most likely due to the fact that the KIM6+ strain used for these studies contains the *hms* system, which can dominate over any small effect the chaperone/usher pathways may have in biofilm formation.

The same trend emerged with regards to autoaggregation. This phenotype was important to study because the ability to efficiently autoaggregate is a virulence marker in *Yersinia spp.* [148, 169]. Mirroring what was seen with the previous usher deletion mutant studies, no single chaperone/usher pathway contributed to the ability of the bacteria to aggregate in rich media at either temperature. I found that the bacteria autoaggregated with a much lower efficiency at 37^{o}C compared to 28^{o}C, most likely due to the expression of an anti-adhesive factor such as the F1 capsule or the pH 6 antigen [7, 149]. The lack of an autoaggregation phenotype for the chaperone/usher pathway mutants can be explained by the role of the *pgmA* gene, which is critical for autoaggregation of *Y. pestis* [149].

The ability for a bacterium to adhere to host cells and establish a niche is a critical first step during infection of a new host [152, 170]. To understand what role the nine different chaperone/usher pathways predicted to form adhesive pili played in infection, I studied adherence of the full pathway deletion mutants to A549 cells, HEp-2 cells, and muBMDM. Most of the results recapitulated what was found with the single usher deletion mutants. When pathways *y0348-y0352* or *y1858-y1862* were deleted there was a 2-to-3-fold reduction in bacteria adhered to all cell types studied. This difference wasn't significant for A549 cells, but the trend was still present. As expected, when pathway *y1869-y1873* was knocked out, there was a 50% reduction in the number of bacteria adhered to the muBMDM, in keeping with the hypothesis that pili produced via this pathway bind to a macrophage specific moiety. What was most interesting from these studies was that a previously unstudied pathway, *y4060-y4063,* which contains a premature stop codon in the usher gene, had a 25-50% reduction in binding to HEp-2

cells and muBMDM. This finding was not unprecedented, as other groups have begun to show, mostly through microarray data, that genes of this pathway are differentially regulated when in contact with host cells, specifically macrophages [158, 159]. Also, *Salmonella* and *E. coli* both have chaperone/usher pathways that contain premature stop codons in the usher genes but still can produce functional pili [143, 171]. It is possible that these genes are still functional due to a read-through of the stop codon in the usher gene. Overall, these adhesion results are in line with a fairly modest reduction in host cell binding that other groups have seen when a single *Y. pestis* adhesin is deleted [31, 48, 74, 75, 77-79]. The findings from these cell culture infections reaffirmed and extended the findings with the single usher deletion mutants, showing specifically that pathways *y0348-y0352, y1858-y1862, y1869-y1873,* and *y4060-y4063* are important for host cell binding.

In addition to host cell binding, I examined chaperone/usher pathway deletion mutants for effects on cytokine production and Yop delivery to investigate mechanisms of chaperone/usher pathways in interactions with host cells. Using a membrane based approach that could detect 23 cytokines, I assayed to see if one of the full pathway deletion mutants, whose cognate usher deletion was attenuated *in vivo*, led to different immune responses by infected primary macrophages. Altered cytokine responses have been shown to protect mice infected with virulent *Y. pestis,* thus any change in cytokines produced could be highly significant [167]. Unfortunately, the results from the membrane-based assay were inconclusive. Further experiments were performed, using ELISAs for IL-9, which was one of the cytokines that appeared to have a differential

regulation, as well as TNF-α and IFN-γ, which are known important cytokines in response to *Y. pestis*.

I first examined IL-9, an interesting cytokine candidate as it has been implicated in lung immunity, mostly in the context of inflammation and asthma. However, it is classically thought of as a CD4+ T cell produced cytokine [163, 164]. Since IL-9 was detected by the membrane-based approach in conditioned supernatants of muBMDM, I decided to explore its differential secretion. Using ELISAs to assay levels of IL-9, I saw no more than background levels of this cytokine, barely above the limit of detection. There was no difference among the uninfected controls, the wild type KIM6+, or full pathway deletion mutants. This finding called into question the accuracy of the membrane system. Similar results were obtained with IFN-γ, which is also thought of as a T cell cytokine; there was little to no expression of the cytokine above background level for any of the infected cells [172]. Again, these results differed greatly from what was seen on the membrane assay.

The final cytokine I decided to explore was TNF-α, because along with IFN-γ it has been shown to be important in *Y. pestis* infection [60, 165-167]. High levels of this cytokine were produced by muBMDM infected with the parental strain and all three full pathway deletion strains, while very little cytokine was produced in the uninfected control. The levels of this cytokine were statistically similar for all infections, so again there appeared to be no role for these chaperone/usher pathways in affecting cytokine production, at least under conditions tested. This likely may be very different *in vivo* where the bacteria would interact with a vast number of cytokine producing cells including macrophages, neutrophils, T cells, and endothelial cells.

The presence of the pCD1 plasmid that encodes the T3SS and Yops is critical for the virulence of *Y. pestis* [75]. Yops have a wide range of function on host cells, from immune modulation to preventing phagocytosis. Therefore, I hypothesized that the inability to deliver Yops efficiently to host cells could be a mechanism by which the chaperone/usher mutants are attenuated [11, 13, 19, 43]. Other groups have shown that defects in delivery of Yops correlated with attenuation in the mouse model of infection, at least via the IV route [75, 79]. I found that when pathway *y0348-y0352, y1858-y1862,* or *y4060-y4063* was knocked out, there was a significant decrease in Yop delivery into host cells measured by the number of cells exhibiting cytopathic effects. This inability to deliver Yops correlates perfectly with the bacteria's reduced ability to bind to these host cells. This is a possible mechanism for the attenuation *in vivo* of the single usher deletion mutants. Although when pathway *y1869-y1873* was deleted there was no decrease in Yop delivery, this mutant binds to HEp-2 cells similarly to wild type KIM6+ and is only defective for binding to macrophages. This may indicate that this chaperone/usher pathway may only aid in delivering Yops to cells with which it specifically interacts, i.e., macrophages. It is also a possibility that there are two distinct mechanisms of attenuation, an inability to deliver Yops and/or an inability to effectively bind host cells.

Acknowledgements

I would like to thank Susan van Horn for help with the electron microscopy (Stony Brook University). I would also like to thank Maya Ivanov for technical help when constructing the KIM5- strains of the full pathway deletions, and Galina Romanov for providing the muBMDM for all the experiments

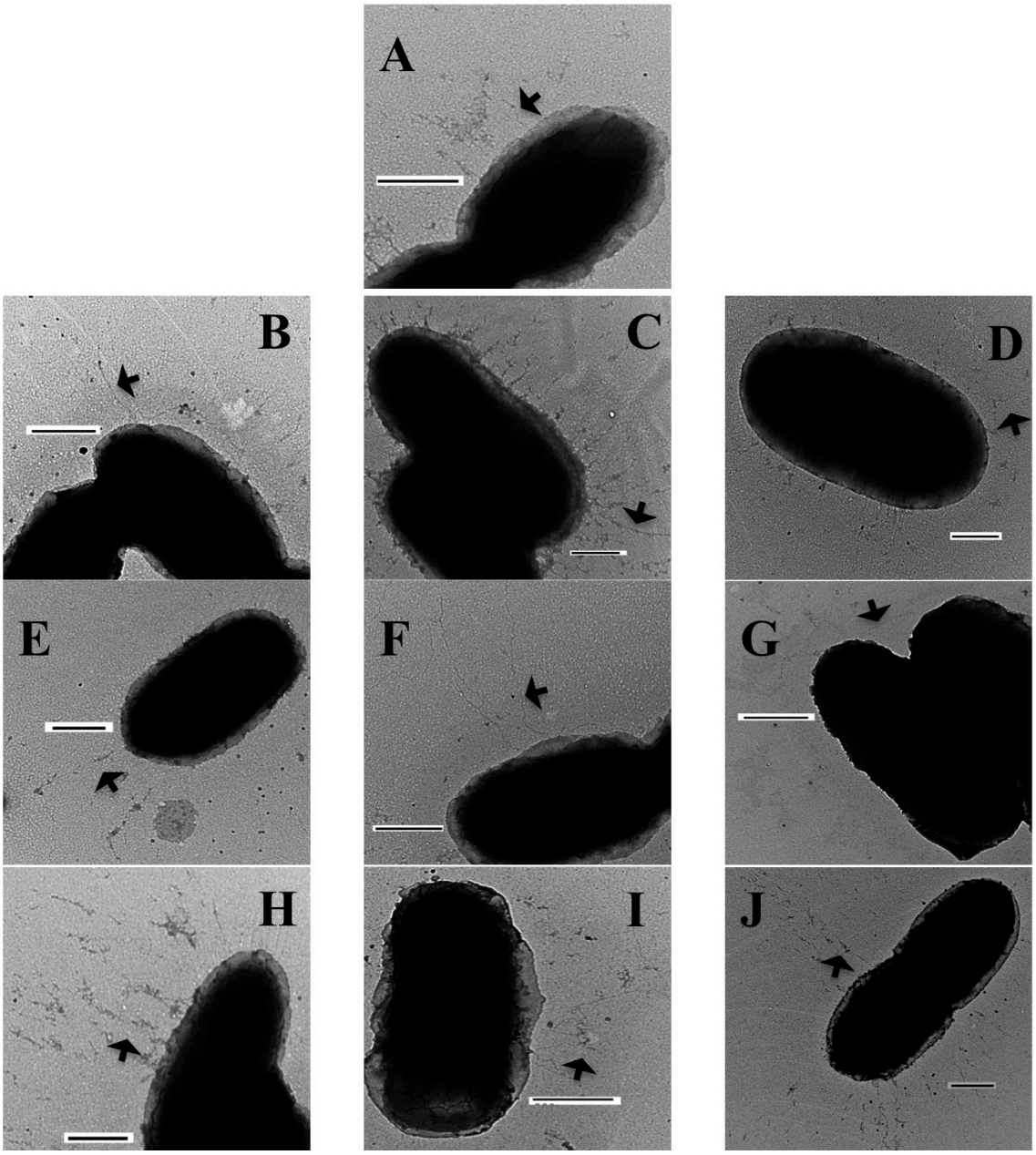

Figure 4.1: Whole bacteria negative stain transmission electron microscopy of *Y. pestis* full pathway deletion mutants. *Y. pestis* chaperone/usher pathway deletion mutants were negatively stained and examined by TEM for the presence of pili on the surface. KIM6+ (A); KIM6+ Δ*y0348-y0352* (B); KIM6+ Δ*y0429-y0433* (C); KIM6+ Δ*y0561-y0563* (D); KIM6+ Δ*y1539-y1544* (E); KIM6+ Δ*y1858-y1862* (F); KIM6+ Δ*y1869-y1873* (G); KIM6+ Δ*y23888-y2392* (H); KIM6+ Δ*y3478-y3480* (I); KIM6+ Δ*y4060-y4063* (J). All mutants still created pili on their surface. Scale bars = 500 nm.

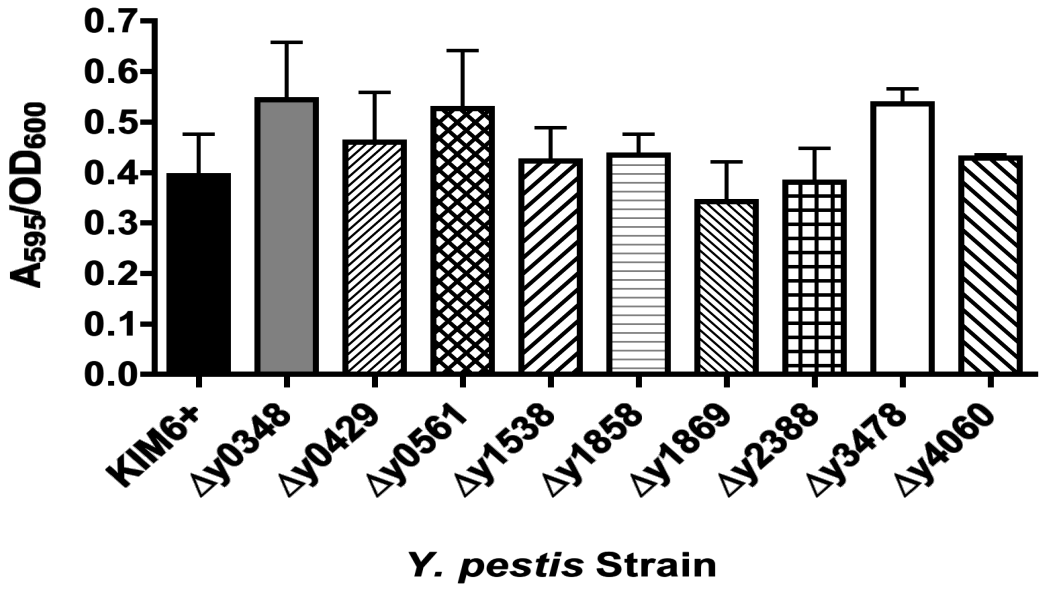

Figure 4.2: Biofilm formation by *Y. pestis* full pathway deletion mutants at 28°C. *Y. pestis* strain KIM6+ or full pathway deletion mutants were grown in HIB and then incubated statically at 28°C in 96-well flat bottom plates for 24 hours. Biofilm formation was determined by crystal violet staining. No significant difference was seen between the wild type KIM6+ and any full pathway deletion mutant. Three independent experiments were done in triplicate and analyzed by ANOVA using GraphPad Prism. Bars represent means ± SEM.

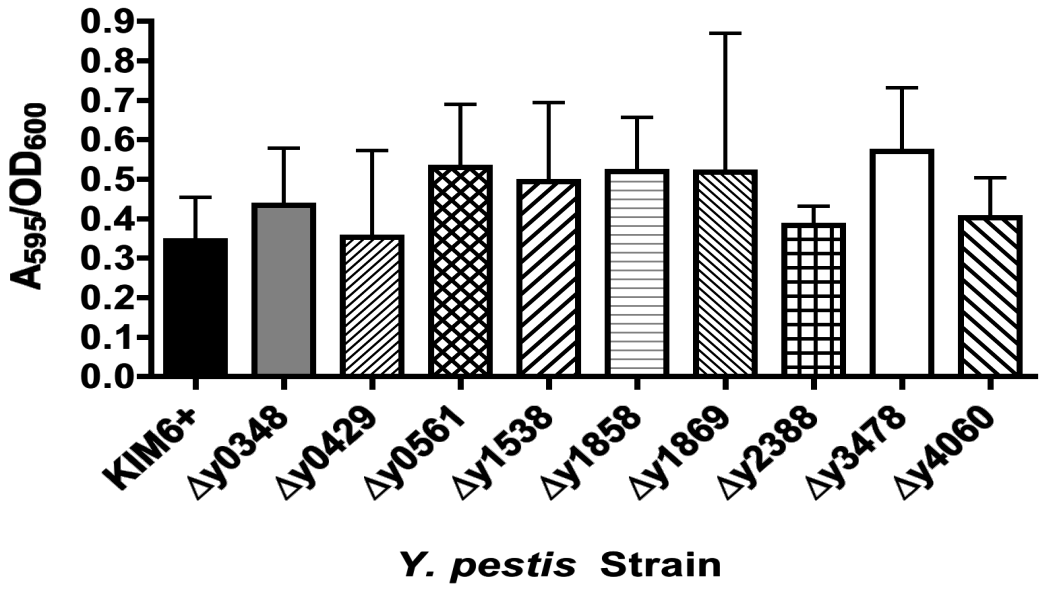

Figure 4.3: Biofilm formation by *Y. pestis* full pathway deletion mutants at 37°C. *Y. pestis* strain KIM6+ or full pathway deletion mutants were grown in HIB and then incubated statically at 37°C in 96-well flat bottom plates for 24 hours. Biofilm formation was determined by crystal violet staining. No significant difference was seen between the wild type KIM6+ and any full pathway deletion mutant. Three independent experiments were done in triplicate and analyzed by ANOVA using GraphPad Prism. Bars represent means ± SEM.

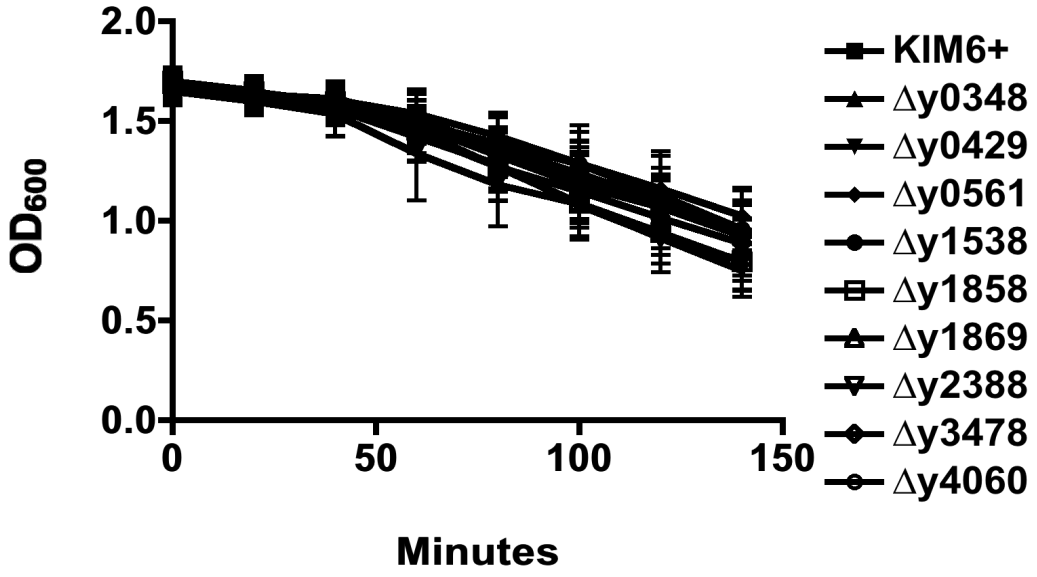

Figure 4.4: Autoaggregation of *Y. pestis* full pathway deletion mutants at 28°C. *Y. pestis* strain KIM6+ or full pathway deletion mutants were grown in HIB and then were incubated statically at 28°C in 1.5 mL plastic cuvettes for 140 minutes. The OD_{600} of the cultures were then read every 20 minutes. No significant difference was seen between the wild type KIM 6+ and any full pathway deletion mutant. Three independent experiments were done in triplicate and analyzed by ANOVA using GraphPad Prism. Bars represent means ± SEM.

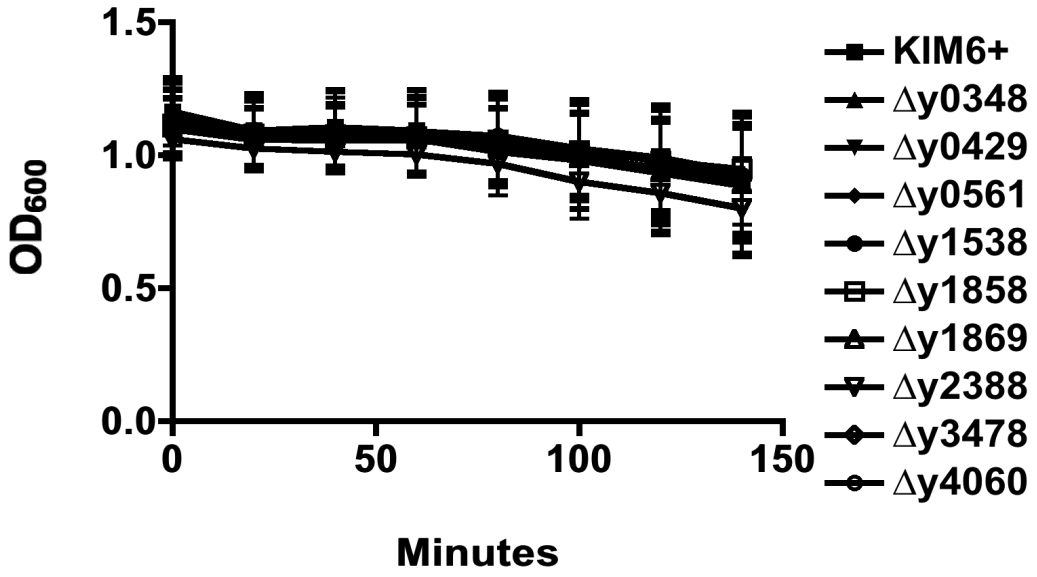

Figure 4.5: Autoaggregation of *Y. pestis* full pathway deletion mutants at 37°C. *Y. pestis* strain KIM6+ or full pathway deletion mutants were grown in HIB and then were incubated statically at 37°C in 1.5 mL plastic cuvettes for 140 minutes. The OD_{600} of the cultures were then read every 20 minutes. No significant difference was seen between the wild type KIM 6+ and any full pathway deletion mutant. Three independent experiments were done in triplicate and analyzed by ANOVA using GraphPad Prism. Bars represent means ± SEM.

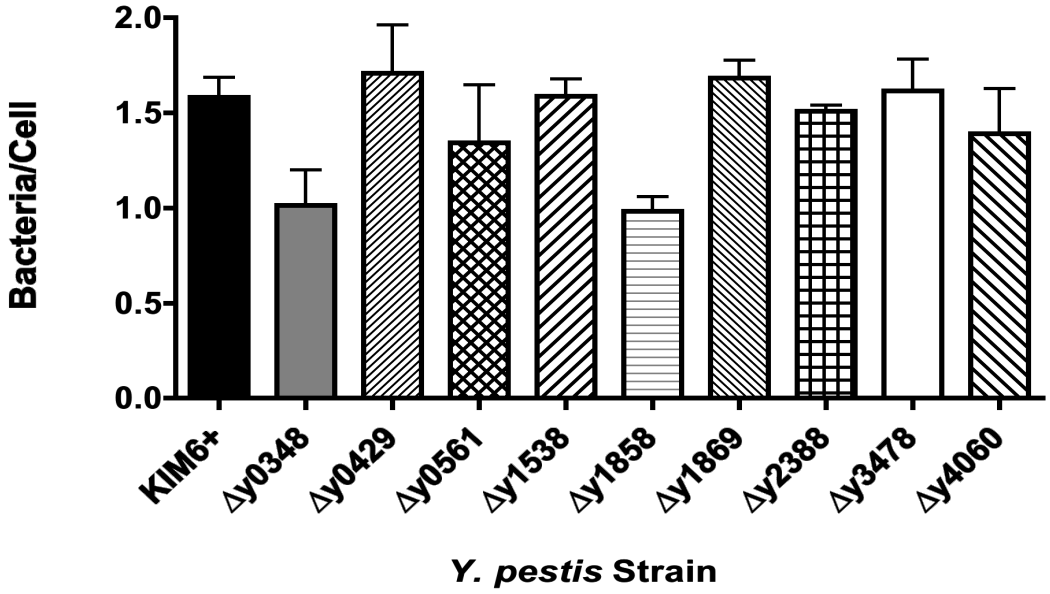

Figure 4.6: Binding of *Y. pestis* full pathway deletion mutants to A549 cells. A549 cells were infected with *Y. pestis* wild type or deletion mutants at an MOI of 50 for 2 hours. Cells were then fixed and stained. Rabbit anti-*Yersinia* primary antibody and goat anti-rabbit secondary antibody conjugated to AlexaFluor594 (red) were used for staining. No significant difference was seen between the wild type KIM 6+ and any full pathway deletion mutant. Results (bacteria/cell) were calculated from three independent experiments with triplicate wells per experiment and analyzed by ANOVA using GraphPad Prism. Bars represent means ± SEM.

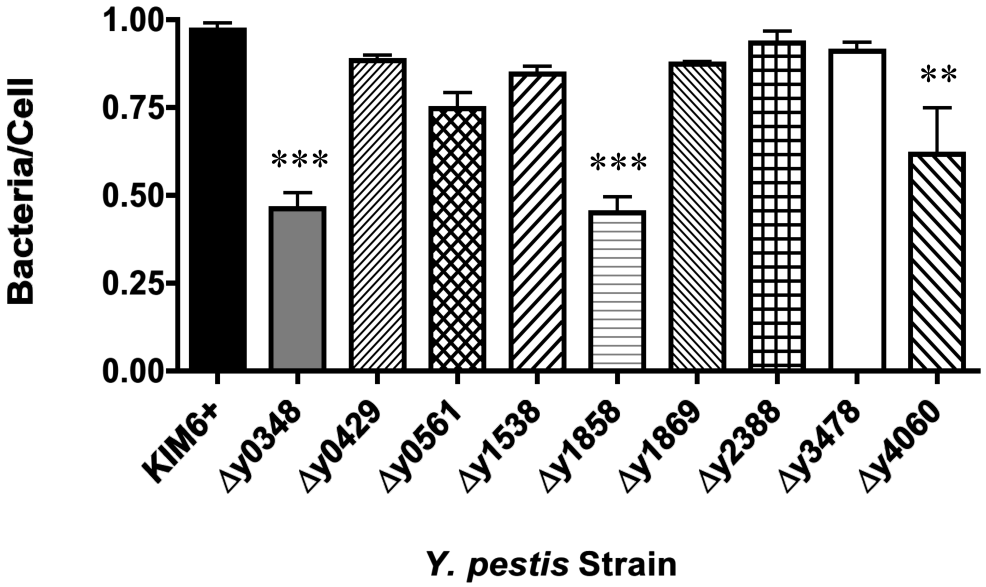

Figure 4.7: Binding of *Y. pestis* full pathway deletion mutants to HEp-2 cells. HEp-2 cells were infected as described in Figure 4.6. Results (bacteria/cell) were calculated from three independent experiments with triplicate wells per experiment and analyzed by ANOVA using GraphPad Prism (**, $P < 0.01$; ***, $P < 0.001$). Bars represent means ± SEM.

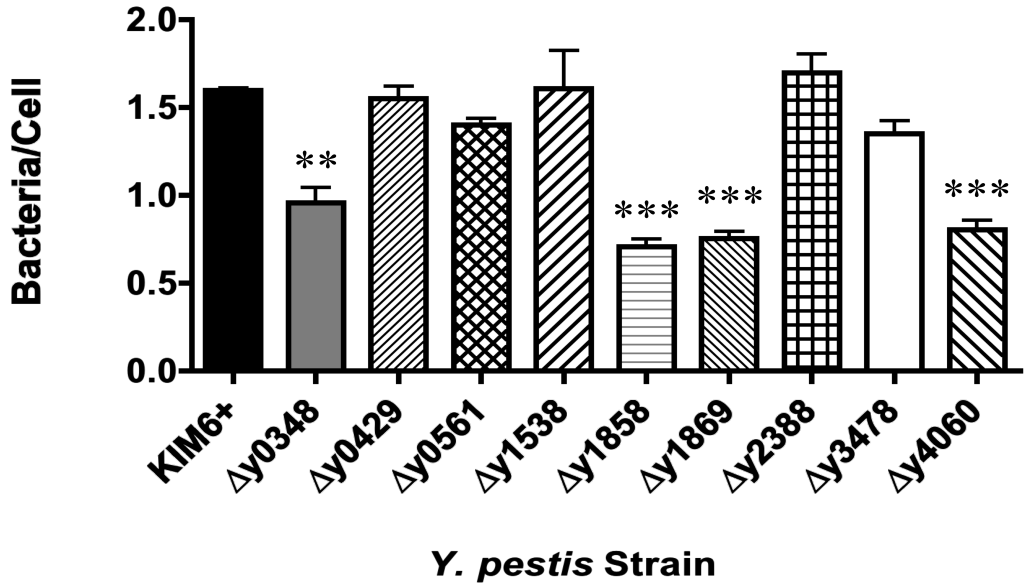

Figure 4.8: Binding of *Y. pestis* full pathway deletion mutants to murine bone marrow-derived macrophages. MuBMDM were treated with 5 µg/mL Cytochalasin D for 1 hour then infected as described in Figure 4.6. Results (bacteria/cell) were calculated from three independent experiments with triplicate wells per experiment and analyzed by ANOVA using GraphPad Prism (**, $P < 0.01$; ***, $P < 0.001$). Bars represent means ± SEM.

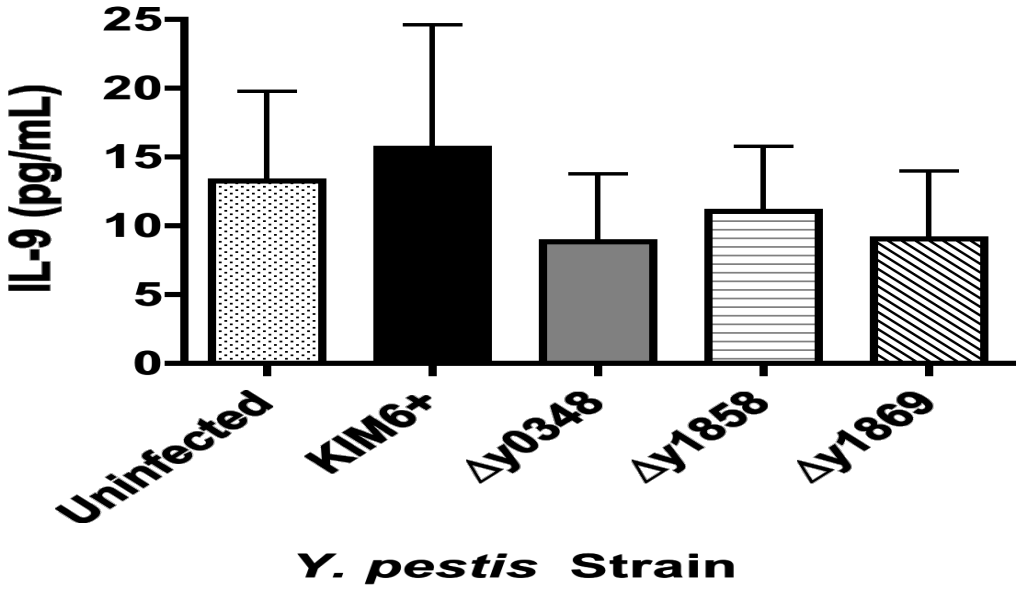

Figure 4.9: Quantification of IL-9 levels released by murine bone marrow-derived macrophages. MuBMDM were infected with KIM6+ or the indicated full pathway deletion mutants for 24 hours at an MOI of 20. Conditioned supernatant from infections was collected and used to run the ELISA for IL-9. No significant difference was seen between the wild type KIM 6+ and any full pathway deletion mutant. Results were calculated from three independent experiments with triplicate wells per experiment and analyzed by ANOVA using GraphPad Prism. Bars represent means ± SEM.

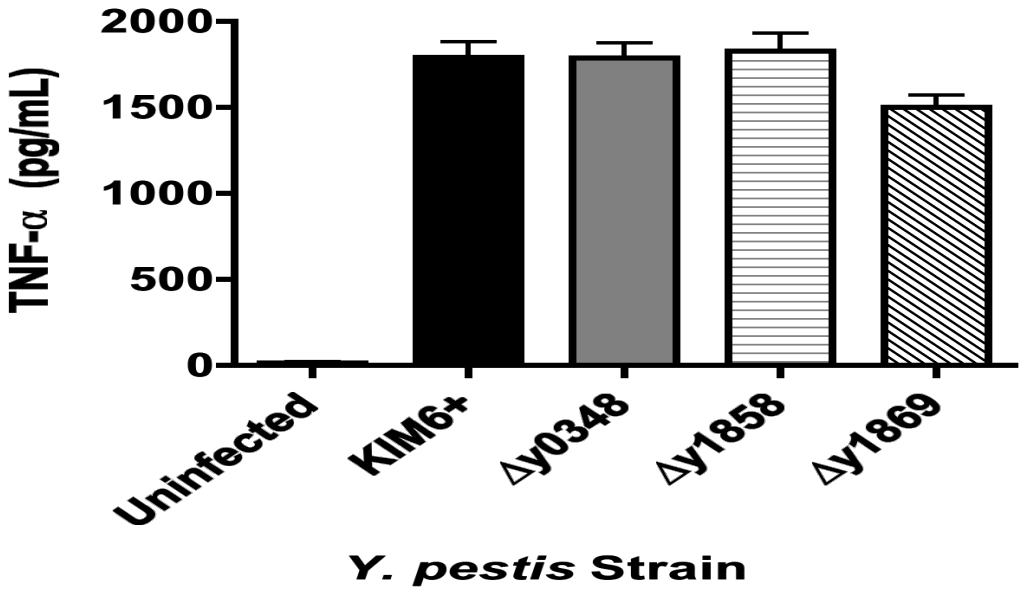

Figure 4.10: Quantification of TNF-α levels released by murine bone marrow-derived macrophages. MuBMDM were infected with KIM6+ or the indicated full pathway deletion mutants for 24 hours at an MOI of 20. Conditioned supernatant from infections was collected and used to run the ELISA for TNF-α. No significant difference was seen between the wild type KIM 6+ and any full pathway deletion mutant. Results were calculated from three independent experiments with triplicate wells per experiment and analyzed by ANOVA using GraphPad Prism. Bars represent means ± SEM.

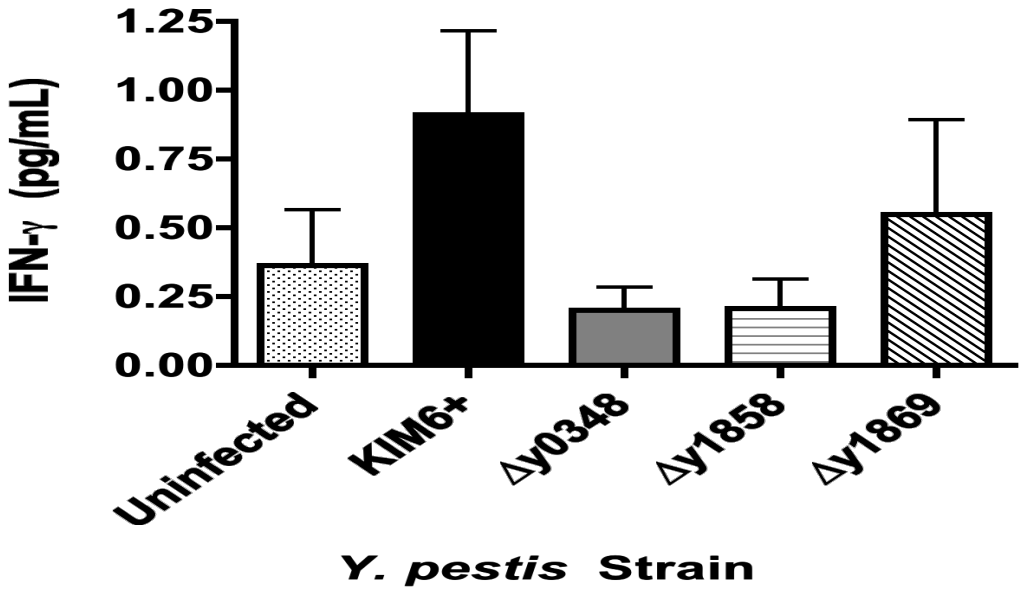

Figure 4.11: Quantification of IFN-γ levels released by murine bone marrow-derived macrophages. MuBMDM were infected with KIM6+ or the indicated full pathway deletion mutants for 24 hours at an MOI of 20. Conditioned supernatant from infections was collected and used to run the ELISA for IFN-γ. No significant difference was seen between the wild type KIM 6+ and any full pathway deletion mutant. Results were calculated from three independent experiments with triplicate wells per experiment and analyzed by ANOVA using GraphPad Prism. Bars represent means ± SEM.

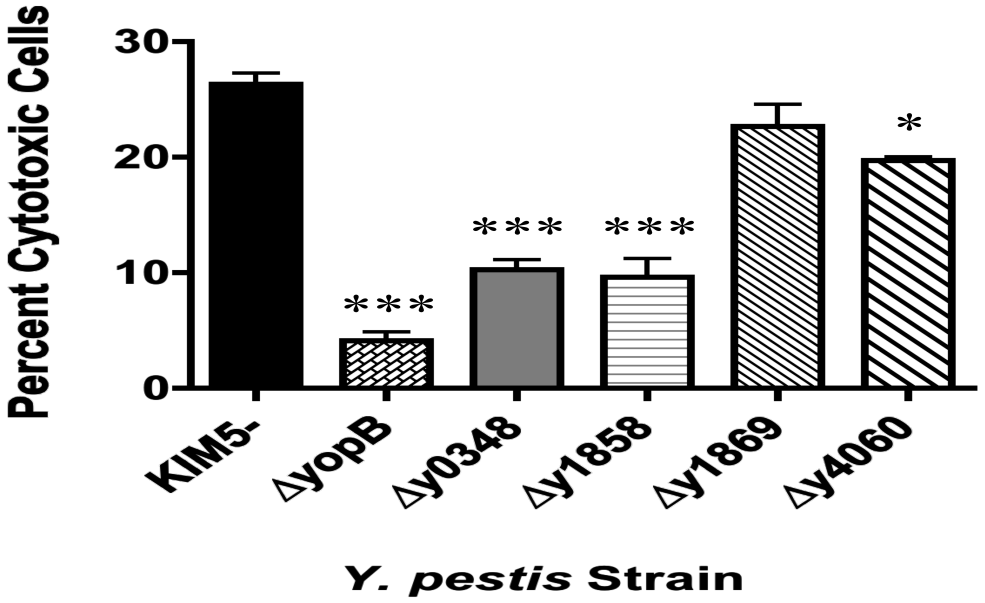

Figure 4.12: Delivery of Yops by *Y. pestis* full pathway deletion mutants to HEp-2 cells. HEp-2 cells were infected at an MOI of 10 for 2 hours with the KIM5- strain or the indicated full pathway deletion mutant. Cells were then stained with Giemsa stain. Percent cytotoxicity was calculated by dividing the number of rounded cells by the total cell number. Results (percent cytotoxicity) were calculated from three independent experiments with triplicate wells per experiment and analyzed by ANOVA using GraphPad Prism (**, $P < 0.01$; ***, $P < 0.001$). Bars represent means ± SEM.

Chapter 5: Conclusions and Future Directions

Conclusions

This dissertation focused on studying the roles of nine of the eleven chaperone/usher pathways of *Y. pestis* and demonstrated that a subset of the pathways contribute to the virulence of the bacterium. *Y. pestis* lacks the main adhesin molecules, YadA and Inv, of its closely related family members, *Y. pseudotuberculosis* and *Y. enterocolitica* [7, 23, 65]. However, *Y. pestis* expresses an arsenal of other adhesins to make up for the lack of YadA and Inv. A number of groups have studied various adhesins of *Y. pestis* and found that many contribute to host cell adhesion, Yop delivery, invasion, and virulence in various mouse models. However, none of the adhesins studied to date, when eliminated alone or in combination, has created a completely attenuated bacterium [29, 31, 48, 74, 75, 78-83, 116, 144, 173]. Along these lines, *Salmonella* encodes 12 chaperone/usher pathways, some of which contribute to virulence [142]. Van der Velden *et al.* demonstrated that a number of pathways contribute to the virulence of *S. typhimurium in vivo*. They showed that deletion of a single chaperone/usher pathway mildly attenuated the bacteria; however, combined deletion of four pathways in a single bacterium increased the attenuation significantly [142]. This demonstrates the redundancy of multiple chaperone/usher pathways during infection. A number of the chaperone/usher pathways in *Salmonella* are not only important for binding to host cells *in vitro*, but have been shown to be differentially expressed *in vivo* [143, 174]. These studies suggest that signals in the host can cause differential expression of the pathways, allowing the bacteria not only to adhere to specific environments, but also for a change in

pilus composition to avoid the immune system. Similarly, I hypothesized that some of the nine chaperone/usher pathways predicted to form fibrillar surface structures aid in the ability of *Y. pestis* to bind to host cells and contribute to the progression of disease.

My initial studies into the roles of these pathways consisted of using a previously constructed library of mutants, where six of the nine usher genes were individually deleted, thereby preventing the assembly of pili on the surface of the bacteria [98] (Runco and Thanassi, unpublished data). Heterologous expression of some of these six chaperone/usher pathways in *E. coli* was shown to promote biofilm formation [83]. However, I found that none of these pathways was important for biofilm formation by *Y. pestis* under any condition tested. This is most likely due to the presence of the *hms* locus in the KIM6+ strain, which is the major determining factor in biofilm formation by *Y. pesits* [5, 156]. I also tested the *Y. pestis* mutants for the ability to autoaggregate in culture medium, which is considered to be an indicator of virulence [148, 169]. Again all mutants behaved the same as the parental strain, indicating that there was no critical role for the chaperone/usher pathways in autoaggregation of *Y. pestis*. The *pgmA* gene was shown to be the major determinant regulating autoaggregation, so the lack of an effect of the usher deletion mutants is not surprising [149].

Using the panel of usher deletion mutants, I analyzed the ability of these pili to bind to two cell lines, A549 and HEp-2, as well as two types of primary cells, muBMDM and huMDM. I found that when ushers *y0350* or *y1858* were deleted there was a 2-to-3-fold reduction in bacteria bound to all cell types. This indicated that these two pathways form pili that most likely bind to a general carbohydrate moiety or protein found on the surface of most cell types. When usher *y1871* was deleted, there was a 2-fold reduction in

bacteria adhered to the two primary macrophage cells lines. Pili formed via this pathway most likely bind to a moiety specific to both human and murine macrophages. Bacterial adhesion to host cells of the usher deletion mutants could be restored to wild type levels by expression of the usher in trans, thus proving that the defect in binding was specific to the lack of the usher and not a secondary effect of the gene deletion. The other three chaperone/usher pathways I studied did not appear to play a role in adhesion to host cells, at least not under laboratory conditions.

To understand the role of the pili formed by these six pathways in the progression of plague, the mutants were used to infect mice via both the bubonic and pneumonic routes. These two routes are important in the dissemination of the plague, the bubonic route being the most common form of transmission during natural infection, and the pneumonic route being the most likely route of transmission encountered in an intentional release [4, 46, 54]. To mimic these diseases, I infected mice with the fully virulent KIM5+ strain of the bacteria via the intranasal and subcutaneous routes. While I saw no attenuation of the usher deletion mutants when mice were infected via the subcutaneous route, mimicking bubonic plague, I saw a mild attenuation for three of the mutant strains when mice were infected via the intranasal route, mimicking pneumonic plague. The mutants that showed binding defects to host cells, usher deletions *y0350*, *y1858*, and *y1871*, also showed a significant attenuation via the intranasal route. Usher deletion *y1858* had a mild attenuation with 1 out of 15 mice (6.7%) surviving the entire course of infection; however, usher deletion *y1871* showed the strongest attenuation with 2 out of 15 mice (13.3%) surviving the entire course of the infection. It is unusual to see an attenuation via the intranasal route without a corresponding attenuation via the

subcutaneous or intravenous routes [153, 175]. It is possible that the pili formed by these pathways specifically interact with the epithelial cells or macrophages in the lung, as shown by the *in vitro* binding assays, and that other adhesins play a more important role by the subcutaneous route. Felek *et al.* found that via the IV route there is an attenuation when pathway *y1858-y1862* is deleted, indicating that pili formed by this pathway may be important during systemic infection [83].

While it was the goal of this dissertation to determine the roles of the chaperone/usher pathways of *Y. pestis* in infection and interactions with host cells, Felek *et al.* also studied the roles of these chaperone/usher pathways. There are a number of differences between the two studies, including the background of the bacteria (KIM 5- vs. KIM6+ or KIM5+), the methodology for *in vitro* experiments (CFU plating vs. direct microscopy), mouse background for infection studies (Swiss-Weber vs. C57BL/6), and which mutants were examined (a small subset vs. all nine pathways). Most data between this dissertation and the data from Felek *et al.* overlap in a complementary manner and help form a picture of the roles these chaperone/usher pathways may be playing.

While the study from Felek *et al.* and the work I did on the panel of single usher deletion mutants shed significant light onto the role of the pili of *Y. pestis* in relation to host cell adhesion and disease, there were still additional unexplored chaperone/usher pathways. Studies done in *E. coli* and *Salmonella* revealed that bacteria had the ability to read through premature stop codons in the usher genes of chaperone/usher pathways and form functional pili on the bacterial surface [143, 171]. In addition, studies in *E. coli* demonstrated that there can been regulatory cross talk between different pilus operons [115, 176]. To eliminate any concern that the chaperone/usher pathways with only the

usher deleted could affect each other, even if they were not capable of making pili on the surface, or that the other pathways were fully functional, I used a suicide vector system to make complete deletions of each of the nine *Y. pestis* chaperone/usher pathways [122]. By creating nine unmarked full pathway deletion mutants in the KIM6+ background, I could begin to analyze the full scope that each pathway had during infection with *Yersinia pestis.*

This complete library of mutants confirmed many of the results obtained using the panel of six usher deletion mutants. There were no differences in biofilm formation or autoaggregation at either 28^{o}C or 37^{o}C with any single full pathway mutant. With regards to host cell adhesion, when pathways *y0348-y0352* or *y1858-y1862* were deleted, there was a decrease in binding to A549 cells albeit not significant and a significant decrease in binding to HEp-2 cells and muBMDM. Also, when pathway *y1869-y1873* was deleted, significantly fewer bacteria bound to the muBMDM. Interestingly, upon deletion of pathway *y4060-y4063*, which has a stop codon in the middle of the usher gene, there were significantly fewer bacteria bound to both HEp-2 cells and muBMDM. This suggests that *Y. pestis* can read through this stop codon and produce a functional usher that allows for the assembly of pili from this pathway, as has been described in *E. coli* and *Salmonella* [143, 171].

Levels of TNF-α and IFN-γ are critical for maintaining a proper immune response during infection by *Y. pestis* and are needed for protection in the context of a subunit vaccine [60, 165-167]. On the other hand, it has been shown that *Y. pestis* infection tends to be biphasic with macrophage cell death moving from a non-inflammatory apoptotic cell death to a highly inflammatory pyroptotic cell death, and this high level of cytokine

release may cross the threshold from protective to damaging [17]. Since it has been shown that immune modulation is so critical during an infection, I wanted to see if the chaperone/usher pathways, at least those whose usher deletion mutants were attenuated *in vivo*, played any role in up or down regulating these responses. Using a membrane-based assay to measure 23 different cytokines, I compared muBMDM infected with wild type KIM6+ or deletion mutants in pathways *y0348-y0352, y1858-y1862,* or *y1869-y1873*. Seeing some interesting trends, I then explored the levels of TNF-α, IFN-γ, and IL-9 using ELISAs. IL-9 has been shown to be important in lung inflammation and asthma, which is interesting since the *Y. pestis* pilus mutants are attenuated via the intranasal route; however, the main cellular source of IL-9 is CD4+ T cells [163, 164]. Unfortunately, using ELISAs to these three cytokines, I saw little to no induction of either IFN-γ or IL-9, most likely due to the fact that both cytokines tend to be produced from CD4+ T cells, and no statistical differences were observed in the levels of TNF-α among the wild type and the full pathway deletion mutants [163, 172].

The type three secretion system of *Y. pestis* delivers Yops directly into host cells, not only altering their signaling but also preventing phagocytosis and robust early immune responses from cells such as macrophages [16, 43, 129, 177, 178]. Clearly, efficient Yop delivery is critical for *Y. pestis* to be able to modulate the immune system and cause disease. Conversely, inefficient Yop delivery would give the host a better chance at mounting an effective immune response. By converting the KIM6+ full pathway deletions strains into KIM5- strains, I was able to test the roles of the four chaperone/usher pathways that contributed to adhesion in the delivery of Yops into host cells. Pathways *y0348-y0352* and *y1858-y1862*, which had approximately 50% reduction

in binding to host cells, had a 2-to-3 fold decrease in the delivery of Yops as measured by host cell cytotoxicity. This difference was highly significant, decreasing the amount of cytopathic cells from 27% when infected with the KIM5- strain to approximately 11% with these mutants. The Yop delivery defect was not as impaired as a *yopB* mutant that is unable to deliver Yops at all, which only causes ~4% of cells to become cytopathic. However, there has yet to be an adhesin that when deleted decreases levels of Yop delivery to the null phenotype [75, 79]. The Yop delivery results correlated perfectly with ability to bind specific host cells, as deletion mutant *y1869-y1873,* which had a binding defect to macrophages but not epithelial cells, delivered Yops to wild type levels. Deletion mutant *y4060-y4063* had a milder binding defect to HEp-2 cells and also had only a slight but significant defect in Yop delivery, being able to cause ~21% of cells to become cytopathic. Along with the inability to adhere to host cells efficiently, this may be a main cause of attenuation of the bacteria that lack the pili formed by the chaperone/usher pathways. While there may be other pathways that can compensate for these defects in the host, it is important to understand that many of the chaperone/usher pathways of *Y. pestis* affect the virulence of this bacteria, and the redundancy of adhesins within the genome may be one of the *Yersinia's* strongest weapons.

Future Directions and Open Questions

Create a four-pathway knockout and complement existing knockouts

To take these studies to the next level, it is important to create a strain of *Y. pestis* that lacks all four chaperone/usher pathways that have been shown to contribute to either host cell adhesion or virulence in the mouse model of infection. Once this mutant has been created, it can be used to determine if these pathways work in a synergistic manner. It could also be determined if there is a further reduced ability for bacteria lacking all four pathways to bind host cells, and if when just a single chaperone/usher pathway is deleted, other adhesins can compensate. Ultimately, it will be important to create a *Y. pestis* mutant deleted for all nine chaperone/usher pathways to create a completely pilus null strain. Finally, in regards to cloning work, it would be important to complement all of the full pathway deletion mutants to confirm that the effects seen are specifically due to the lack of the pilus operon and not a secondary effect. Since there was difficulty with the *in vivo* mouse infection studies when ushers were complemented on a plasmid, using a Tn-7 chromosomal integration system and the operons under their natural promoters would be the best method to complement these mutants [179].

In vivo infections

The next step for the library of nine complete pathway chaperone/usher mutants, as well as the quadruple mutant, would be to repeat the mouse infections done with the usher deletion mutants. Most important would be converting the KIM6+ strains to fully virulent KIM5+ strains under BSL-3 conditions and then performing both the

subcutaneous and intranasal infections. This would broaden the field of knowledge since three of these pathways have yet to be tested in any *in vivo* models, and the quadruple mutant would be the first *Y. pestis* multi-pathway mutant tested. Using this mutant would again inform us whether knocking out multiple pathways could increase the attenuation of the bacteria.

Performing infections with the KIM5+ strains has the drawback of requiring ABSL-3 conditions, which are not currently available at Stony Brook. As an alternative, the KIM6+ strains can be converted into KIM5- strains by screening for the naturally occurring *pgm* deletion, and then electroporating in the pCD1 plasmid. Using these KIM5- strains, intravenous infections can then be done on site under BSL-2 conditions. Other groups have used the IV route of infection with *Y. pestis* chaperone/usher mutants and have gathered some intriguing data [83]. By using the quadruple and single pathway mutants, we can gain information on exactly what role each pathway is playing in the host. An added advantage of doing the infection on site under BSL-2 conditions is that organs could be harvested for histology and organ burden assays to determine if there is a colonization defect, and serum can be collected to determine if there is a difference in various cytokine levels. All of these experiments would be critical in taking the work on these pathways to the next level. Furthermore, if no attenuation is seen via the IV route, competitive infections could be done to determine if there is an advantage of one strain over another. However, in light of recent studies done, competitive infections may not be ideal when looking for attenuations in *Y. pestis* [21]. Lastly, mice surviving infection with any of the chaperone/usher mutants could be challenged with wild type *Y. pestis* to see if any of the mutants would be a good vaccine candidate.

Expression conditions, binding moieties, and antibody development

Three additional experiments would also be important to furthering work on these pathways. qRT-PCR experiments have been done by our group and others to determine when each pathway is expressed and have yielded inconclusive, but intriguing, results [83] (Runco and Thanassi, unpublished data). Another set of experiments could be done to determine when each pathway is induced. By putting a GFP reporter gene under the control of the promoters from the various chaperone/usher pathways, we can test a wide range of conditions that may induce these pathways that may not be detected using qRT-PCR. Most notably, I would be able to study whether some of the pathways are specifically induced by interactions with host cells, and whether in the extracellular or intracellular state. This system would also allow a quick transient expression to be detected due to the long half-life of GFP, where RNA may be degraded too quickly to detect [180].

Another important experiment would be to develop clean, specific, high affinity antibodies to all of the pathways that play a role in adhesion and virulence. To do this, it would be necessary to isolate the pili from each pathway, which has proven difficult. However, once these pili have been isolated, the proteins can be purified and used to develop antibodies against the subunit proteins. These antibodies could then be used in a variety of assays, such as immuno-gold transmission electron microscopy, testing for blocking adhesion to host cells, and passive protection during mouse infections.

Finally, it is important to determine exactly what moieties each pilus is binding to. Pili formed via the chaperone/usher pathways of Gram-negative bacteria have previously

shown to bind to sugar moieties on host cells. The P pili and Type 1 pilus systems of *E. coli* bind to Galα(1-4) Gal and mannose moieties, respectively [87]. The binding moieties of some of the pili formed by *S. typhimurium*, which contains numerous chaperone/usher pathways like *Y. pestis,* have also been determined and found to be sugar moieties such as the Lewis X antigen using glycomic studies [181]. For these studies, whole chaperone/usher operons can be cloned onto plasmids and expressed in non-fimbriated *E. coli* strains. These pili can be purified and then added to 384-well microtiter plates that have been pre-coated with various sugar ligands. Using these studies, specific binding moieties could be determined for each pathway, and it could be determined where these moieties are most highly concentrated *in vivo*. It would also be possible to develop small molecule inhibitors or competitors to block pili from binding to their intended target, thus preventing successful host colonization.

References

1. Bottone, E.J., *Yersinia enterocolitica: overview and epidemiologic correlates.* Microbes Infect, 1999. **1**(4): p. 323-33.

2. Hubbert, W.T., et al., *Yersinia pseudotuberculosis infection in the United States. Speticema, appendicitis, and mesenteric lymphadenitis.* Am J Trop Med Hyg, 1971. **20**(5): p. 679-84.

3. Hinnebusch, B.J., et al., *Role of Yersinia murine toxin in survival of Yersinia pestis in the midgut of the flea vector.* Science, 2002. **296**(5568): p. 733-5.

4. Perry, R.D. and J.D. Fetherston, *Yersinia pestis--etiologic agent of plague.* Clin Microbiol Rev, 1997. **10**(1): p. 35-66.

5. Hinnebusch, B.J., R.D. Perry, and T.G. Schwan, *Role of the Yersinia pestis hemin storage (hms) locus in the transmission of plague by fleas.* Science, 1996. **273**(5273): p. 367-70.

6. Achtman, M., et al., *Yersinia pestis, the cause of plague, is a recently emerged clone of Yersinia pseudotuberculosis.* Proc Natl Acad Sci U S A, 1999. **96**(24): p. 14043-8.

7. Brubaker, R.R., *Factors promoting acute and chronic diseases caused by yersiniae.* Clin Microbiol Rev, 1991. **4**(3): p. 309-24.

8. Bos, K.I., et al., *A draft genome of Yersinia pestis from victims of the Black Death.* Nature, 2011. **478**(7370): p. 506-10.

9. Parkhill, J., et al., *Genome sequence of Yersinia pestis, the causative agent of plague.* Nature, 2001. **413**(6855): p. 523-7.

10. Deng, W., et al., *Genome sequence of Yersinia pestis KIM.* J Bacteriol, 2002. **184**(16): p. 4601-11.

11. Cornelis, G.R., et al., *The virulence plasmid of Yersinia, an antihost genome.* Microbiol Mol Biol Rev, 1998. **62**(4): p. 1315-52.

12. Cornelis, G.R., *The Yersinia Ysc-Yop 'type III' weaponry.* Nat Rev Mol Cell Biol, 2002. **3**(10): p. 742-52.

13. Cornelis, G.R., *The Yersinia Ysc-Yop virulence apparatus.* Int J Med Microbiol, 2002. **291**(6-7): p. 455-62.

14. Straley, S.C. and W.S. Bowmer, *Virulence genes regulated at the transcriptional level by Ca2+ in Yersinia pestis include structural genes for outer membrane proteins.* Infect Immun, 1986. **51**(2): p. 445-54.

15. Straley, S.C., et al., *Regulation by Ca2+ in the Yersinia low-Ca2+ response.* Mol Microbiol, 1993. **8**(6): p. 1005-10.

16. Bliska, J.B., *Yop effectors of Yersinia spp. and actin rearrangements.* Trends Microbiol, 2000. **8**(5): p. 205-8.

17. Bergsbaken, T. and B.T. Cookson, *Innate immune response during Yersinia infection: critical modulation of cell death mechanisms through phagocyte activation.* J Leukoc Biol, 2009. **86**(5): p. 1153-8.

18. Forsberg, A., R. Rosqvist, and H. Wolf-Watz, *Regulation and polarized transfer of the Yersinia outer proteins (Yops) involved in antiphagocytosis.* Trends Microbiol, 1994. **2**(1): p. 14-9.

19. Straley, S.C., et al., *Yops of Yersinia spp. pathogenic for humans.* Infect Immun, 1993. **61**(8): p. 3105-10.

20. Lathem, W.W., et al., *Progression of primary pneumonic plague: a mouse model of infection, pathology, and bacterial transcriptional activity.* Proc Natl Acad Sci U S A, 2005. **102**(49): p. 17786-91.

21. Price, P.A., J. Jin, and W.E. Goldman, *Pulmonary infection by Yersinia pestis rapidly establishes a permissive environment for microbial proliferation.* Proc Natl Acad Sci U S A, 2012. **109**(8): p. 3083-8.

22. Sodeinde, O.A., et al., *Plasminogen activator/coagulase gene of Yersinia pestis is responsible for degradation of plasmid-encoded outer membrane proteins.* Infect Immun, 1988. **56**(10): p. 2749-52.

23. Cowan, C., et al., *Invasion of epithelial cells by Yersinia pestis: evidence for a Y. pestis-specific invasin.* Infect Immun, 2000. **68**(8): p. 4523-30.

24. Benedek, O., G. Nagy, and L. Emody, *Intracellular signalling and cytoskeletal rearrangement involved in Yersinia pestis plasminogen activator (Pla) mediated HeLa cell invasion.* Microb Pathog, 2004. **37**(1): p. 47-54.

25. Lathem, W.W., et al., *A plasminogen-activating protease specifically controls the development of primary pneumonic plague.* Science, 2007. **315**(5811): p. 509-13.

26. Lindler, L.E., et al., *Complete DNA sequence and detailed analysis of the Yersinia pestis KIM5 plasmid encoding murine toxin and capsular antigen.* Infect Immun, 1998. **66**(12): p. 5731-42.

27. Brubaker, R.R., *The genus Yersinia: biochemistry and genetics of virulence.* Curr Top Microbiol Immunol, 1972. **57**: p. 111-58.

28. Cornelius, C., et al., *Protective immunity against plague.* Adv Exp Med Biol, 2007. **603**: p. 415-24.

29. Runco, L.M., et al., *Biogenesis of the fraction 1 capsule and analysis of the ultrastructure of Yersinia pestis.* J Bacteriol, 2008. **190**(9): p. 3381-5.

30. Du, Y., R. Rosqvist, and A. Forsberg, *Role of fraction 1 antigen of Yersinia pestis in inhibition of phagocytosis.* Infect Immun, 2002. **70**(3): p. 1453-60.

31. Liu, F., et al., *Effects of Psa and F1 on the adhesive and invasive interactions of Yersinia pestis with human respiratory tract epithelial cells.* Infect Immun, 2006. **74**(10): p. 5636-44.

32. Williamson, E.D., et al., *Recombinant (F1+V) vaccine protects cynomolgus macaques against pneumonic plague.* Vaccine, 2011. **29**(29-30): p. 4771-7.

33. Chichester, J.A., et al., *A single component two-valent LcrV-F1 vaccine protects non-human primates against pneumonic plague.* Vaccine, 2009. **27**(25-26): p. 3471-4.

34. Cornelius, C.A., et al., *Yersinia pestis IS1541 transposition provides for escape from plague immunity.* Infect Immun, 2009.

35. Kiefer, D., et al., *Phenotypical Characterization of Mongolian Yersinia pestis Strains.* Vector Borne Zoonotic Dis, 2012. **12**(3): p. 183-8.

36. Sha, J., et al., *Characterization of an F1 deletion mutant of Yersinia pestis CO92, pathogenic role of F1 antigen in bubonic and pneumonic plague, and evaluation of sensitivity and specificity of F1 antigen capture-based dipsticks.* J Clin Microbiol, 2011. **49**(5): p. 1708-15.

37. Weening, E.H., et al., *The dependence of the Yersinia pestis capsule on pathogenesis is influenced by the mouse background.* Infect Immun, 2011. **79**(2): p. 644-52.

38. Pujol, C., et al., *Replication of Yersinia pestis in interferon gamma-activated macrophages requires ripA, a gene encoded in the pigmentation locus.* Proc Natl Acad Sci U S A, 2005. **102**(36): p. 12909-14.

39. Grabenstein, J.P., et al., *The response regulator PhoP of Yersinia pseudotuberculosis is important for replication in macrophages and for virulence.* Infect Immun, 2004. **72**(9): p. 4973-84.

40. Prior, J.L., et al., *The failure of different strains of Yersinia pestis to produce lipopolysaccharide O-antigen under different growth conditions is due to mutations in the O-antigen gene cluster.* FEMS Microbiol Lett, 2001. **197**(2): p. 229-33.

41. Prior, J.L., et al., *Characterization of the lipopolysaccharide of Yersinia pestis.* Microb Pathog, 2001. **30**(2): p. 49-57.

42. Rebeil, R., et al., *Variation in lipid A structure in the pathogenic yersiniae.* Mol Microbiol, 2004. **52**(5): p. 1363-73.

43. Pujol, C. and J.B. Bliska, *Turning Yersinia pathogenesis outside in: subversion of macrophage function by intracellular yersiniae.* Clin Immunol, 2005. **114**(3): p. 216-26.

44. Une, T. and R.R. Brubaker, *In vivo comparison of avirulent Vwa- and Pgm- or Pstr phenotypes of yersiniae.* Infect Immun, 1984. **43**(3): p. 895-900.

45. Wimsatt, J. and D.E. Biggins, *A review of plague persistence with special emphasis on fleas.* J Vector Borne Dis, 2009. **46**(2): p. 85-99.

46. Cole, S.T. and C. Buchrieser, *Bacterial genomics. A plague o' both your hosts.* Nature, 2001. **413**(6855): p. 467, 469-70.

47. Butler, T., *Plague into the 21st century.* Clin Infect Dis, 2009. **49**(5): p. 736-42.

48. Felek, S., M.B. Lawrenz, and E.S. Krukonis, *The Yersinia pestis autotransporter YapC mediates host cell binding, autoaggregation and biofilm formation.* Microbiology, 2008. **154**(Pt 6): p. 1802-12.

49. Lukaszewski, R.A., et al., *Pathogenesis of Yersinia pestis infection in BALB/c mice: effects on host macrophages and neutrophils.* Infect Immun, 2005. **73**(11): p. 7142-50.

50. Pujol, C., et al., *Yersinia pestis can reside in autophagosomes and avoid xenophagy in murine macrophages by preventing vacuole acidification.* Infect Immun, 2009. **77**(6): p. 2251-61.

51. Shailubhai, K., *Bioterrorism: a new frontier for drug discovery and development.* IDrugs, 2003. **6**(8): p. 773-80.

52. Dattwyler, R.J., *Community-acquired pneumonia in the age of bio-terrorism.* Allergy Asthma Proc, 2005. **26**(3): p. 191-4.

53. Galimand, M., et al., *Multidrug resistance in Yersinia pestis mediated by a transferable plasmid.* N Engl J Med, 1997. **337**(10): p. 677-80.

54. Inglesby, T.V., et al., *Plague as a biological weapon: medical and public health management. Working Group on Civilian Biodefense.* JAMA, 2000. **283**(17): p. 2281-90.

55. Duschet, P., *The threat of biological warfare.* Arch Dermatol, 1999. **135**(11): p. 1417-8.

56. Oyston, P.C. and K.E. Isherwood, *Yersinia: an update.* Trends Microbiol, 2002. **10**(12): p. 550-1.

57. Welkos, S., et al., *Determination of the virulence of the pigmentation-deficient and pigmentation-/plasminogen activator-deficient strains of Yersinia pestis in non-human primate and mouse models of pneumonic plague.* Vaccine, 2002. **20**(17-18): p. 2206-14.

58. Russell, P., et al., *A comparison of Plague vaccine, USP and EV76 vaccine induced protection against Yersinia pestis in a murine model.* Vaccine, 1995. **13**(16): p. 1551-6.

59. Titball, R.W. and E.D. Williamson, *Vaccination against bubonic and pneumonic plague.* Vaccine, 2001. **19**(30): p. 4175-84.

60. Smiley, S.T., *Immune defense against pneumonic plague.* Immunol Rev, 2008. **225**: p. 256-71.

61. Morton, M., et al., *A Salmonella enterica serovar Typhi vaccine expressing Yersinia pestis F1 antigen on its surface provides protection against plague in mice.* Vaccine, 2004. **22**(20): p. 2524-32.

62. Heath, D.G., et al., *Protection against experimental bubonic and pneumonic plague by a recombinant capsular F1-V antigen fusion protein vaccine.* Vaccine, 1998. **16**(11-12): p. 1131-7.

63. Eitel, J. and P. Dersch, *The YadA protein of Yersinia pseudotuberculosis mediates high-efficiency uptake into human cells under environmental conditions in which invasin is repressed.* Infect Immun, 2002. **70**(9): p. 4880-91.

64. Rosqvist, R., M. Skurnik, and H. Wolf-Watz, *Increased virulence of Yersinia pseudotuberculosis by two independent mutations.* Nature, 1988. **334**(6182): p. 522-4.

65. Simonet, M., et al., *Invasin production by Yersinia pestis is abolished by insertion of an IS200-like element within the inv gene.* Infect Immun, 1996. **64**(1): p. 375-9.

66. Isberg, R.R., D.L. Voorhis, and S. Falkow, *Identification of invasin: a protein that allows enteric bacteria to penetrate cultured mammalian cells.* Cell, 1987. **50**(5): p. 769-78.

67. Hudson, K.J., J.B. Bliska, and A.H. Bouton, *Distinct mechanisms of integrin binding by Yersinia pseudotuberculosis adhesins determine the phagocytic response of host macrophages.* Cell Microbiol, 2005. **7**(10): p. 1474-89.

68. Deuretzbacher, A., et al., *beta(1) integrin-dependent engulfment of Yersinia enterocolitica by macrophages is coupled to the activation of autophagy and suppressed by type III protein secretion.* J Immunol, 2009. **183**(9): p. 5847-60.

69. Schmid, Y., et al., *Yersinia enterocolitica adhesin A induces production of interleukin-8 in epithelial cells.* Infect Immun, 2004. **72**(12): p. 6780-9.

70. Miller, V.L., et al., *Identification of regions of Ail required for the invasion and serum resistance phenotypes.* Mol Microbiol, 2001. **41**(5): p. 1053-62.

71. Bliska, J.B. and S. Falkow, *Bacterial resistance to complement killing mediated by the Ail protein of Yersinia enterocolitica.* Proc Natl Acad Sci U S A, 1992. **89**(8): p. 3561-5.

72. Pierson, D.E. and S. Falkow, *The ail gene of Yersinia enterocolitica has a role in the ability of the organism to survive serum killing.* Infect Immun, 1993. **61**(5): p. 1846-52.

73. Miller, V.L. and S. Falkow, *Evidence for two genetic loci in Yersinia enterocolitica that can promote invasion of epithelial cells.* Infect Immun, 1988. **56**(5): p. 1242-8.

74. Kolodziejek, A.M., et al., *Phenotypic characterization of OmpX, an Ail homologue of Yersinia pestis KIM.* Microbiology, 2007. **153**(Pt 9): p. 2941-51.

75. Felek, S. and E.S. Krukonis, *The Yersinia pestis Ail protein mediates binding and Yop delivery to host cells required for plague virulence.* Infect Immun, 2009. **77**(2): p. 825-36.

76. Lenz, J.D., et al., *Expression during host infection and localization of Yersinia pestis autotransporter proteins.* J Bacteriol, 2011. **193**(21): p. 5936-49.

77. Lawrenz, M.B., J.D. Lenz, and V.L. Miller, *A novel autotransporter adhesin is required for efficient colonization during bubonic plague.* Infect Immun, 2009. **77**(1): p. 317-26.

78. Forman, S., et al., *yadBC of Yersinia pestis, a new virulence determinant for bubonic plague.* Infect Immun, 2008. **76**(2): p. 578-87.

79. Felek, S., T.M. Tsang, and E.S. Krukonis, *Three Yersinia pestis adhesins facilitate Yop delivery to eukaryotic cells and contribute to plague virulence.* Infect Immun, 2010. **78**(10): p. 4134-50.

80. Huang, X.Z. and L.E. Lindler, *The pH 6 antigen is an antiphagocytic factor produced by Yersinia pestis independent of Yersinia outer proteins and capsule antigen.* Infect Immun, 2004. **72**(12): p. 7212-9.

81. Lindler, L.E., M.S. Klempner, and S.C. Straley, *Yersinia pestis pH 6 antigen: genetic, biochemical, and virulence characterization of a protein involved in the pathogenesis of bubonic plague.* Infect Immun, 1990. **58**(8): p. 2569-77.

82. Anisimov, A.P., et al., *The subcutaneous inoculation of pH 6 antigen mutants of Yersinia pestis does not affect virulence and immune response in mice.* J Med Microbiol, 2009. **58**(Pt 1): p. 26-36.

83. Felek, S., et al., *Contributions of chaperone/usher systems to cell binding, biofilm formation and Yersinia pestis virulence.* Microbiology, 2011. **157**(Pt 3): p. 805-18.

84. Thanassi, D.G., E.T. Saulino, and S.J. Hultgren, *The chaperone/usher pathway: a major terminal branch of the general secretory pathway.* Curr Opin Microbiol, 1998. **1**(2): p. 223-31.

85. Stathopoulos, C., et al., *Secretion of virulence determinants by the general secretory pathway in gram-negative pathogens: an evolving story.* Microbes Infect, 2000. **2**(9): p. 1061-72.

86. Izard, J.W. and D.A. Kendall, *Signal peptides: exquisitely designed transport promoters.* Mol Microbiol, 1994. **13**(5): p. 765-73.

87. Thanassi, D.G. and S.J. Hultgren, *Assembly of complex organelles: pilus biogenesis in gram-negative bacteria as a model system.* Methods, 2000. **20**(1): p. 111-26.

88. Waksman, G. and S.J. Hultgren, *Structural biology of the chaperone-usher pathway of pilus biogenesis.* Nat Rev Microbiol, 2009. **7**(11): p. 765-74.

89. Choudhury, D., et al., *X-ray structure of the FimC-FimH chaperone-adhesin complex from uropathogenic Escherichia coli.* Science, 1999. **285**(5430): p. 1061-6.

90. Holmgren, A. and C.I. Branden, *Crystal structure of chaperone protein PapD reveals an immunoglobulin fold.* Nature, 1989. **342**(6247): p. 248-51.

91. Sauer, F.G., et al., *Structural basis of chaperone function and pilus biogenesis.* Science, 1999. **285**(5430): p. 1058-61.

92. Barnhart, M.M., et al., *Chaperone-subunit-usher interactions required for donor strand exchange during bacterial pilus assembly.* J Bacteriol, 2003. **185**(9): p. 2723-30.

93. Barnhart, M.M., et al., *PapD-like chaperones provide the missing information for folding of pilin proteins.* Proc Natl Acad Sci U S A, 2000. **97**(14): p. 7709-14.

94. Sauer, F.G., et al., *PapD-like chaperones and pilus biogenesis.* Semin Cell Dev Biol, 2000. **11**(1): p. 27-34.

95. Soto, G.E., et al., *Periplasmic chaperone recognition motif of subunits mediates quaternary interactions in the pilus.* EMBO J, 1998. **17**(21): p. 6155-67.

96. Slonim, L.N., et al., *Interactive surface in the PapD chaperone cleft is conserved in pilus chaperone superfamily and essential in subunit recognition and assembly.* EMBO J, 1992. **11**(13): p. 4747-56.

97. Dodson, K.W., et al., *Outer-membrane PapC molecular usher discriminately recognizes periplasmic chaperone-pilus subunit complexes.* Proc Natl Acad Sci U S A, 1993. **90**(8): p. 3670-4.

98. Sauer, F.G., et al., *Fiber assembly by the chaperone-usher pathway.* Biochim Biophys Acta, 2004. **1694**(1-3): p. 259-67.

99. Remaut, H., et al., *Donor-strand exchange in chaperone-assisted pilus assembly proceeds through a concerted beta strand displacement mechanism.* Mol Cell, 2006. **22**(6): p. 831-42.

100. Zavialov, A.V., et al., *Structure and biogenesis of the capsular F1 antigen from Yersinia pestis: preserved folding energy drives fiber formation.* Cell, 2003. **113**(5): p. 587-96.

101. Sauer, F.G., et al., *Chaperone priming of pilus subunits facilitates a topological transition that drives fiber formation.* Cell, 2002. **111**(4): p. 543-51.

102. Ng, T.W., et al., *The usher N terminus is the initial targeting site for chaperone-subunit complexes and participates in subsequent pilus biogenesis events.* J Bacteriol, 2004. **186**(16): p. 5321-31.

103. Thanassi, D.G., *Ushers and secretins: channels for the secretion of folded proteins across the bacterial outer membrane.* J Mol Microbiol Biotechnol, 2002. **4**(1): p. 11-20.

104. Mapingire, O.S., et al., *Modulating effects of the plug, helix, and N- and C-terminal domains on channel properties of the PapC usher.* J Biol Chem, 2009. **284**(52): p. 36324-33.

105. Thanassi, D.G., et al., *The PapC usher forms an oligomeric channel: implications for pilus biogenesis across the outer membrane.* Proc Natl Acad Sci U S A, 1998. **95**(6): p. 3146-51.

106. Henderson, N.S., et al., *Topology of the outer membrane usher PapC determined by site-directed fluorescence labeling.* J Biol Chem, 2004. **279**(51): p. 53747-54.

107. Li, H., et al., *The outer membrane usher forms a twin-pore secretion complex.* J Mol Biol, 2004. **344**(5): p. 1397-407.

108. So, S.S. and D.G. Thanassi, *Analysis of the requirements for pilus biogenesis at the outer membrane usher and the function of the usher C-terminus.* Mol Microbiol, 2006. **60**(2): p. 364-75.

109. Thanassi, D.G., et al., *Bacterial outer membrane ushers contain distinct targeting and assembly domains for pilus biogenesis.* J Bacteriol, 2002. **184**(22): p. 6260-9.

110. Phan, G., et al., *Crystal structure of the FimD usher bound to its cognate FimC-FimH substrate.* Nature, 2011. **474**(7349): p. 49-53.

111. Li, Q., et al., *The differential affinity of the usher for chaperone-subunit complexes is required for assembly of complete pili.* Mol Microbiol, 2010.

112. Jacob-Dubuisson, F., R. Striker, and S.J. Hultgren, *Chaperone-assisted self-assembly of pili independent of cellular energy.* J Biol Chem, 1994. **269**(17): p. 12447-55.

113. Hung, D.L., et al., *Molecular basis of two subfamilies of immunoglobulin-like chaperones.* EMBO J, 1996. **15**(15): p. 3792-805.

114. Wiles, T.J., R.R. Kulesus, and M.A. Mulvey, *Origins and virulence mechanisms of uropathogenic Escherichia coli.* Exp Mol Pathol, 2008. **85**(1): p. 11-9.

115. Xia, Y., et al., *Regulatory cross-talk between adhesin operons in Escherichia coli: inhibition of type 1 fimbriae expression by the PapB protein.* EMBO J, 2000. **19**(7): p. 1450-7.

116. Felek, S., et al., *Characterization of six novel chaperone/usher systems in Yersinia pestis.* Adv Exp Med Biol, 2007. **603**: p. 97-105.

117. Thanassi, D.G., J.B. Bliska, and P.J. Christie, *Surface Organelles Assembled by Secretion Systems of Gram-Negative Bacteria: Diversity in Structure and Function.* FEMS Microbiol Rev, 2012.

118. Achtman, M., et al., *Microevolution and history of the plague bacillus, Yersinia pestis.* Proc Natl Acad Sci U S A, 2004. **101**(51): p. 17837-42.

119. Gong, S., et al., *Characterization of the Yersinia pestis Yfu ABC inorganic iron transport system.* Infect Immun, 2001. **69**(5): p. 2829-37.

120. Kaniga, K., J.C. Bossio, and J.E. Galan, *The Salmonella typhimurium invasion genes invF and invG encode homologues of the AraC and PulD family of proteins.* Mol Microbiol, 1994. **13**(4): p. 555-68.

121. Kaniga, K., I. Delor, and G.R. Cornelis, *A wide-host-range suicide vector for improving reverse genetics in gram-negative bacteria: inactivation of the blaA gene of Yersinia enterocolitica.* Gene, 1991. **109**(1): p. 137-41.

122. Skrzypek, E., et al., *New suicide vector for gene replacement in yersiniae and other gram-negative bacteria.* Plasmid, 1993. **29**(2): p. 160-3.

123. Cha-aim, K., et al., *Reliable fusion PCR mediated by GC-rich overlap sequences.* Gene, 2009. **434**(1-2): p. 43-9.

124. Quigley, B.R., et al., *A foreign protein incorporated on the Tip of T3 pili in Lactococcus lactis elicits systemic and mucosal immunity.* Infect Immun, 2010. **78**(3): p. 1294-303.

125. Quigley, B.R., et al., *Linkage of T3 and Cpa pilins in the Streptococcus pyogenes M3 pilus.* Mol Microbiol, 2009. **72**(6): p. 1379-94.

126. O'Toole, G.A., et al., *Genetic approaches to study of biofilms.* Methods Enzymol, 1999. **310**: p. 91-109.

127. Pujol, C. and J.B. Bliska, *The ability to replicate in macrophages is conserved between Yersinia pestis and Yersinia pseudotuberculosis.* Infect Immun, 2003. **71**(10): p. 5892-9.

128. Forestal, C.A., et al., *A conserved and immunodominant lipoprotein of Francisella tularensis is proinflammatory but not essential for virulence.* Microb Pathog, 2008. **44**(6): p. 512-23.

129. Black, D.S. and J.B. Bliska, *The RhoGAP activity of the Yersinia pseudotuberculosis cytotoxin YopE is required for antiphagocytic function and virulence.* Mol Microbiol, 2000. **37**(3): p. 515-27.

130. Surgalla, M.J. and E.D. Beesley, *Congo red-agar plating medium for detecting pigmentation in Pasteurella pestis.* Appl Microbiol, 1969. **18**(5): p. 834-7.

131. Hare, J.M. and K.A. McDonough, *High-frequency RecA-dependent and -independent mechanisms of Congo red binding mutations in Yersinia pestis.* J Bacteriol, 1999. **181**(16): p. 4896-904.

132. Grant, S.G., et al., *Differential plasmid rescue from transgenic mouse DNAs into Escherichia coli methylation-restriction mutants.* Proc Natl Acad Sci U S A, 1990. **87**(12): p. 4645-9.

133. Datsenko, K.A. and B.L. Wanner, *One-step inactivation of chromosomal genes in Escherichia coli K-12 using PCR products.* Proc Natl Acad Sci U S A, 2000. **97**(12): p. 6640-5.

134. Simon, R., *High frequency mobilization of gram-negative bacterial replicons by the in vitro constructed Tn5-Mob transposon.* Mol Gen Genet, 1984. **196**(3): p. 413-20.

135. Zhang, Y., G. Romanov, and J.B. Bliska, *Type III secretion system-dependent translocation of ectopically expressed Yop effectors into macrophages by intracellular Yersinia pseudotuberculosis.* Infect Immun, 2011. **79**(11): p. 4322-31.

136. Chaveroche, M.K., J.M. Ghigo, and C. d'Enfert, *A rapid method for efficient gene replacement in the filamentous fungus Aspergillus nidulans.* Nucleic Acids Res, 2000. **28**(22): p. E97.

137. Murphy, K.C., *Use of bacteriophage lambda recombination functions to promote gene replacement in Escherichia coli.* J Bacteriol, 1998. **180**(8): p. 2063-71.

138. Hoang, T.T., et al., *A broad-host-range Flp-FRT recombination system for site-specific excision of chromosomally-located DNA sequences: application for isolation of unmarked Pseudomonas aeruginosa mutants.* Gene, 1998. **212**(1): p. 77-86.

139. Grabenstein, J.P., et al., *Characterization of phagosome trafficking and identification of PhoP-regulated genes important for survival of Yersinia pestis in macrophages.* Infect Immun, 2006. **74**(7): p. 3727-41.

140. Palmer, L.E., et al., *YopJ of Yersinia pseudotuberculosis is required for the inhibition of macrophage TNF-alpha production and downregulation of the MAP kinases p38 and JNK.* Mol Microbiol, 1998. **27**(5): p. 953-65.

141. Marx, C.J., *Development of a broad-host-range sacB-based vector for unmarked allelic exchange.* BMC Res Notes, 2008. **1**: p. 1.

142. van der Velden, A.W., et al., *Multiple fimbrial adhesins are required for full virulence of Salmonella typhimurium in mice.* Infect Immun, 1998. **66**(6): p. 2803-8.

143. Forest, C., et al., *Contribution of the stg fimbrial operon of Salmonella enterica serovar Typhi during interaction with human cells.* Infect Immun, 2007. **75**(11): p. 5264-71.

144. Tsang, T.M., S. Felek, and E.S. Krukonis, *Ail binding to fibronectin facilitates Yersinia pestis binding to host cells and Yop delivery.* Infect Immun, 2010. **78**(8): p. 3358-68.

145. Lindler, L.E. and B.D. Tall, *Yersinia pestis pH 6 antigen forms fimbriae and is induced by intracellular association with macrophages.* Mol Microbiol, 1993. **8**(2): p. 311-24.

146. Darby, C., *Uniquely insidious: Yersinia pestis biofilms.* Trends Microbiol, 2008. **16**(4): p. 158-64.

147. Rempe, K.A., A.K. Hinz, and V. Vadyvaloo, *Hfq regulates biofilm gut blockage that facilitates flea-borne transmission of Yersinia pestis.* J Bacteriol, 2012.

148. Laird, W.J. and D.C. Cavanaugh, *Correlation of autoagglutination and virulence of yersiniae.* J Clin Microbiol, 1980. **11**(4): p. 430-2.

149. Felek, S., et al., *Phosphoglucomutase of Yersinia pestis is required for autoaggregation and polymyxin B resistance.* Infect Immun, 2010. **78**(3): p. 1163-75.

150. Stewart, P.S. and J.W. Costerton, *Antibiotic resistance of bacteria in biofilms.* Lancet, 2001. **358**(9276): p. 135-8.

151. Fux, C.A., et al., *Survival strategies of infectious biofilms.* Trends Microbiol, 2005. **13**(1): p. 34-40.

152. Kline, K.A., et al., *Bacterial Adhesins in Host-Microbe Interactions.* Cell Host & Microbe, 2009. **5**(6): p. 580-592.

153. Bubeck, S.S. and P.H. Dube, *Yersinia pestis CO92 delta yopH is a potent live, attenuated plague vaccine.* Clin Vaccine Immunol, 2007. **14**(9): p. 1235-8.

154. Agar, S.L., et al., *Characterization of a mouse model of plague after aerosolization of Yersinia pestis CO92.* Microbiology, 2008. **154**(Pt 7): p. 1939-48.

155. Remaut, H. and G. Waksman, *Structural biology of bacterial pathogenesis.* Curr Opin Struct Biol, 2004. **14**(2): p. 161-70.

156. Bobrov, A.G., et al., *Insights into Yersinia pestis biofilm development: topology and co-interaction of Hms inner membrane proteins involved in exopolysaccharide production.* Environ Microbiol, 2008. **10**(6): p. 1419-32.

157. Spurbeck, R.R., et al., *Fimbrial profiles predict virulence of uropathogenic Escherichia coli strains: contribution of ygi and yad fimbriae.* Infect Immun, 2011. **79**(12): p. 4753-63.

158. Li, B., et al., *Use of protein microarray to identify gene expression changes of Yersinia pestis at different temperatures.* Can J Microbiol, 2011. **57**(4): p. 287-94.

159. Fukuto, H.S., et al., *Global gene expression profiling of Yersinia pestis replicating inside macrophages reveals the roles of a putative stress-induced operon in regulating type III secretion and intracellular cell division.* Infect Immun, 2010. **78**(9): p. 3700-15.

160. Anantha, R.P., et al., *Evolutionary and functional relationships of colonization factor antigen i and other class 5 adhesive fimbriae of enterotoxigenic Escherichia coli.* Infect Immun, 2004. **72**(12): p. 7190-201.

161. Sun, Y.C., et al., *The Yersinia pestis Rcs phosphorelay inhibits biofilm formation by repressing transcription of the diguanylate cyclase gene hmsT.* J Bacteriol, 2012.

162. Clark, R.T., et al., *Bacterial particle endocytosis by epithelial cells is selective and enhanced by tumor necrosis factor receptor ligands.* Clin Vaccine Immunol, 2009. **16**(3): p. 397-407.

163. Noelle, R.J. and E.C. Nowak, *Cellular sources and immune functions of interleukin-9.* Nat Rev Immunol, 2010. **10**(10): p. 683-7.

164. Li, H. and A. Rostami, *IL-9: basic biology, signaling pathways in CD4+ T cells and implications for autoimmunity.* J Neuroimmune Pharmacol, 2010. **5**(2): p. 198-209.

165. Lin, J.S., et al., *TNFalpha and IFNgamma contribute to F1/LcrV-targeted immune defense in mouse models of fully virulent pneumonic plague.* Vaccine, 2010. **29**(2): p. 357-62.

166. Kummer, L.W., et al., *Antibodies and cytokines independently protect against pneumonic plague.* Vaccine, 2008. **26**(52): p. 6901-7.

167. Nakajima, R. and R.R. Brubaker, *Association between virulence of Yersinia pestis and suppression of gamma interferon and tumor necrosis factor alpha.* Infect Immun, 1993. **61**(1): p. 23-31.

168. Sun, Y.C., et al., *Differential control of Yersinia pestis biofilm formation in vitro and in the flea vector by two c-di-GMP diguanylate cyclases.* PLoS One, 2011. **6**(4): p. e19267.

169. Kapperud, G. and J. Lassen, *Relationship of virulence-associated autoagglutination to hemagglutinin production in Yersinia enterocolitica and Yersinia enterocolitica-like bacteria.* Infect Immun, 1983. **42**(1): p. 163-9.

170. Boyle, E.C. and B.B. Finlay, *Bacterial pathogenesis: exploiting cellular adherence.* Curr Opin Cell Biol, 2003. **15**(5): p. 633-9.

171. Torres, A.G., et al., *Identification and characterization of lpfABCC'DE, a fimbrial operon of enterohemorrhagic Escherichia coli O157:H7.* Infect Immun, 2002. **70**(10): p. 5416-27.

172. Magram, J., et al., *IL-12-deficient mice are defective in IFN gamma production and type 1 cytokine responses.* Immunity, 1996. **4**(5): p. 471-81.

173. Tsang, T.M., et al., *Ail binds 9FNIII within the central 120-kDa region of fibronectin to facilitate cell binding by Yersinia pestis.* J Biol Chem, 2012.

174. Humphries, A.D., et al., *The use of flow cytometry to detect expression of subunits encoded by 11 Salmonella enterica serotype Typhimurium fimbrial operons.* Mol Microbiol, 2003. **48**(5): p. 1357-76.

175. Okan, N.A., et al., *The smpB-ssrA mutant of Yersinia pestis functions as a live attenuated vaccine to protect mice against pulmonary plague infection.* Infect Immun, 2010. **78**(3): p. 1284-93.

176. Holden, N.J., B.E. Uhlin, and D.L. Gally, *PapB paralogues and their effect on the phase variation of type 1 fimbriae in Escherichia coli.* Mol Microbiol, 2001. **42**(2): p. 319-30.

177. Brodsky, I.E., et al., *A Yersinia effector protein promotes virulence by preventing inflammasome recognition of the type III secretion system.* Cell Host Microbe, 2010. **7**(5): p. 376-87.

178. Zhang, Y. and J.B. Bliska, *YopJ-promoted cytotoxicity and systemic colonization are associated with high levels of murine interleukin-18, gamma interferon, and neutrophils in a live vaccine model of Yersinia pseudotuberculosis infection.* Infect Immun, 2010. **78**(5): p. 2329-41.

179. Choi, K.H., et al., *A Tn7-based broad-range bacterial cloning and expression system.* Nat Methods, 2005. **2**(6): p. 443-8.

180. Corish, P. and C. Tyler-Smith, *Attenuation of green fluorescent protein half-life in mammalian cells.* Protein Eng, 1999. **12**(12): p. 1035-40.

181. Chessa, D., et al., *Binding specificity of Salmonella plasmid-encoded fimbriae assessed by glycomics.* J Biol Chem, 2008. **283**(13): p. 8118-24.